Photo-detectors

Peter Križan

Ljubljana and Nagoya

University of Ljubljana

“Jožef Stefan” Institute

Nagoya University

Contents

Why (fast) single photon detection?

Photo-detectors

Some applications

Vacuum

- *Photomultiplier tubes (PMT)*
- *Microchannel plate photomultiplier tubes*

Solid-state photon detectors

Hybrid detectors

- *HPDs and HAPDs*
- *Other hybrid photosensors*

Gaseous photon detectors

Examples of applications

- *RICH detectors*
- *TOF counters*
- *Calorimeters*
- *Fiber trackers*
- *Non-accelerator experiments*

Example: photon detection in Ring Imaging Cherenkov (RICH) counters

RICH counter: measure photon impact point on the photon detector surface

→ detection of single photons with

- sufficient spatial resolution
- high efficiency and good signal-to-noise ratio
- over a large area (square meters)

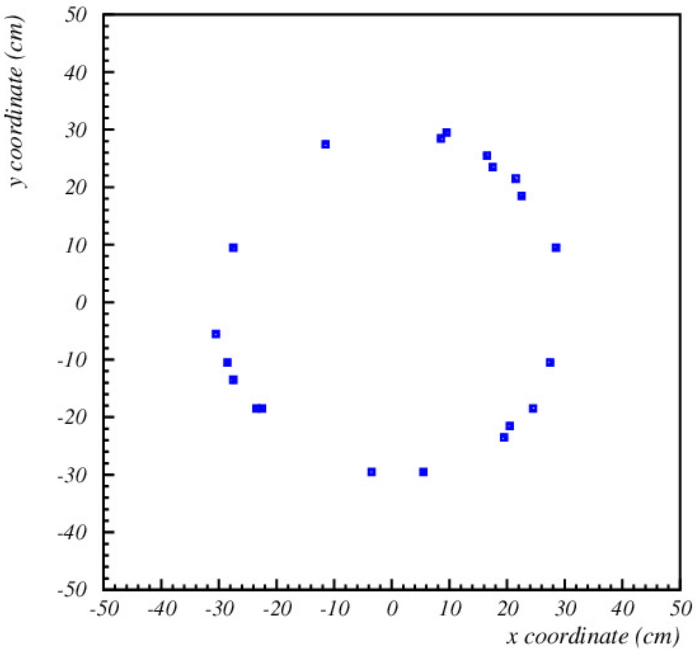

Special requirements:

- Operation in magnetic field
- High rate capability
- Very high spatial resolution
- Excellent timing (time-of-arrival information)

Parameters of photo-sensors

Photon detection efficiency (PDE)

- quantum efficiency
- collection efficiency / Geiger discharge probability

Granularity

Time resolution (transient time spread – TTS)

Long term stability

Operation in magnetic field

Dark count rate

+ …

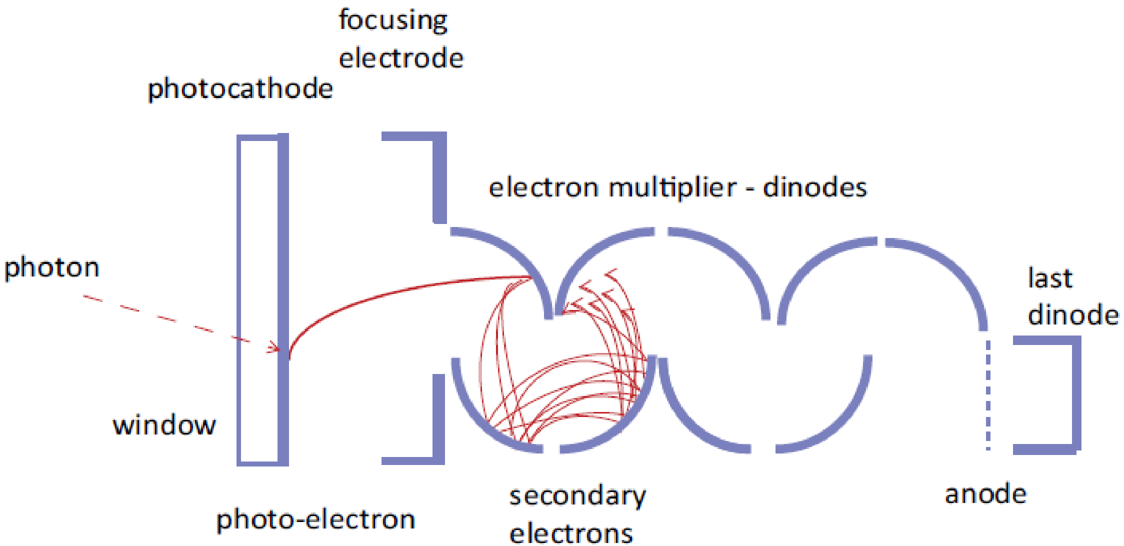

Detection of light

Vacuum

- *Photomultiplier tubes (PMT)*
- *Microchannel plate photomultiplier tubes*

Solid-state photon detectors

Hybrid detectors

- *HPDs and HAPDs*
- *Other hybrid photosensors*

Gaseous photon detectors

Photomultipler tube (PMT)

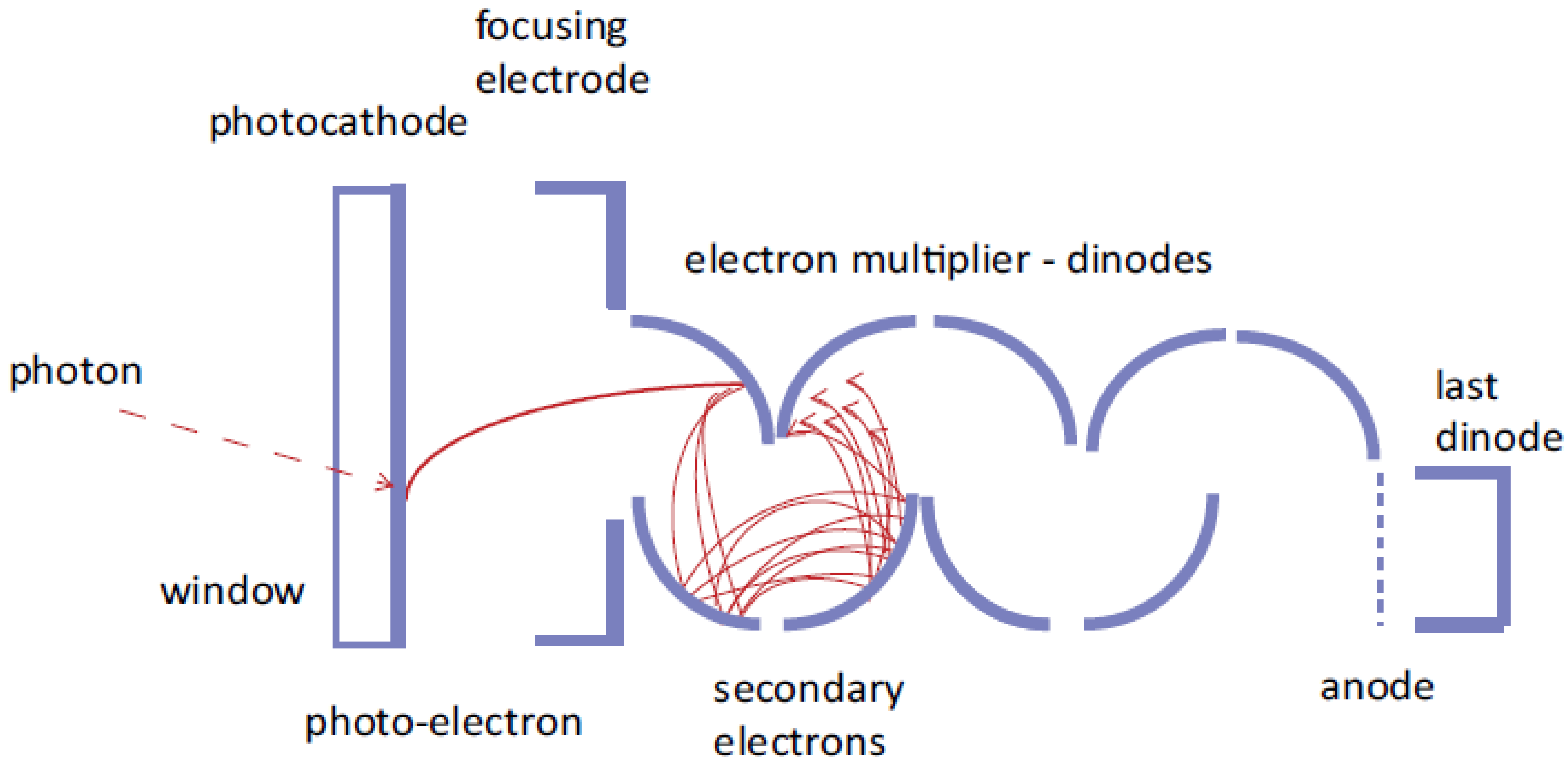

Photomultipler tube

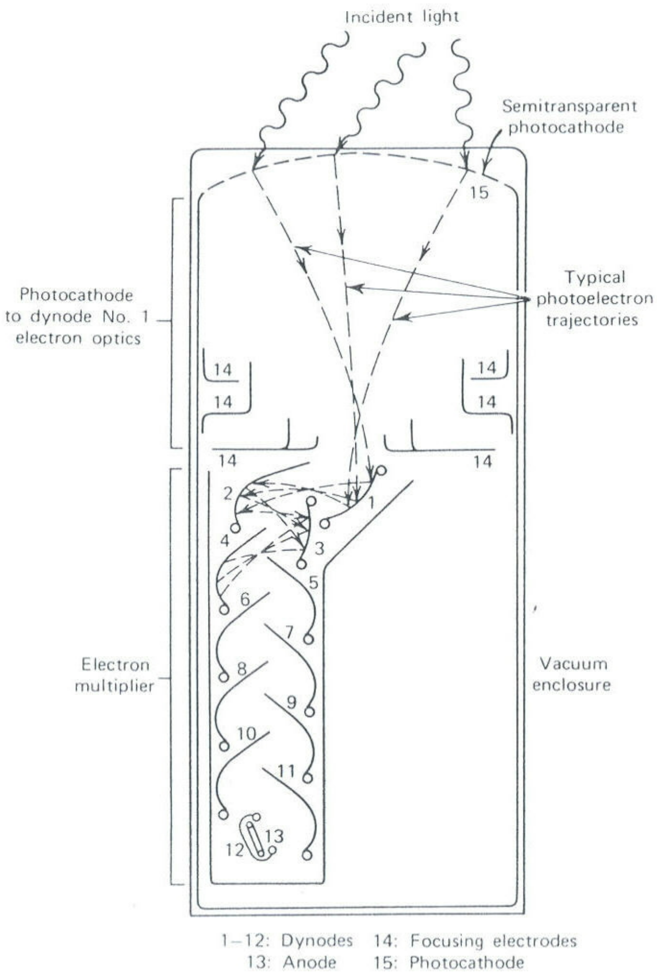

Figure 9-1 Basic elements of a PM tube. (From Ref. 1.)

+

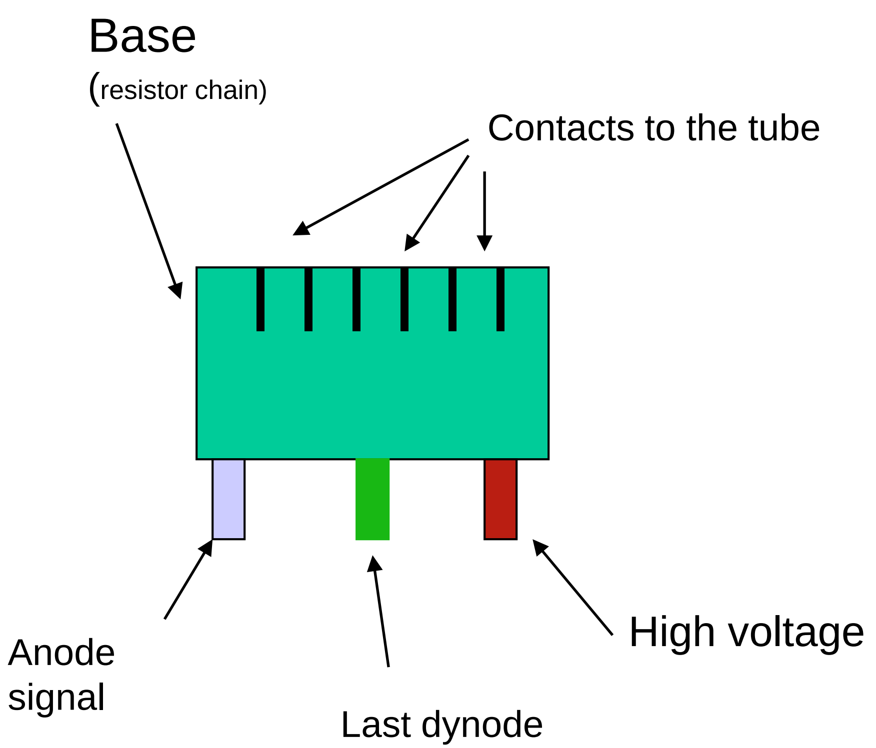

1) Measure pulses
2) Measure current

Photocathode

- Photoeffect : $E_e = h\nu - \Phi$

Max kinetic energy of the photo-electron → E_e

Energy of the photon → $h\nu$

Work function → Φ

- Quantum Efficiency

$$\eta(\lambda) = \frac{\text{Number of photoelectrons exiting the cathode}}{\text{Number of incoming photons}}$$

Spectral sensitivity

$$E(\lambda) = \frac{I_k}{P(\lambda)}$$

I_k: Photoelectron current (A)

$P(\lambda)$: Incoming light power (W)

$$\eta(\lambda) = \frac{I_k / e_o}{P(\lambda)/h\nu} = \frac{hc}{\lambda e_0} E(\lambda)$$

transmissive

photocathodes

reflective

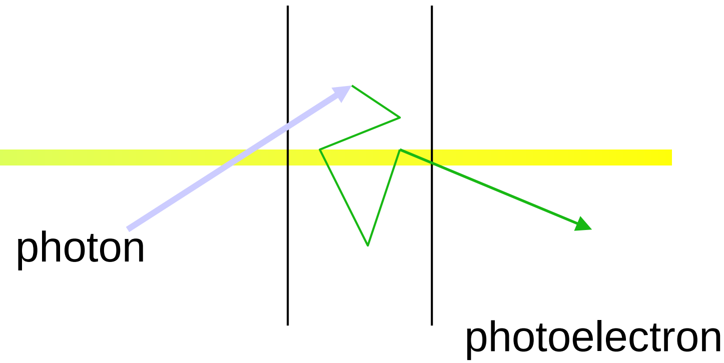

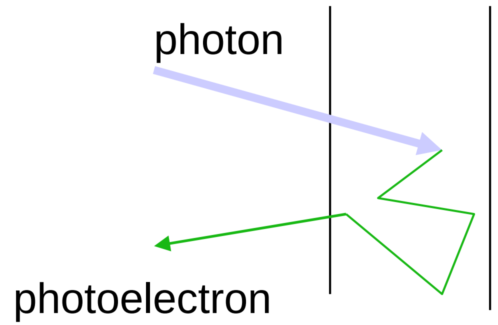

<u>Quatum efficiency is a product of</u>:

•Transmission probability (window)

• Probability for absorption and photoeffect

• Probability for the electron to exit the photocathode

$\Rightarrow$ Optimal photocathode thickness

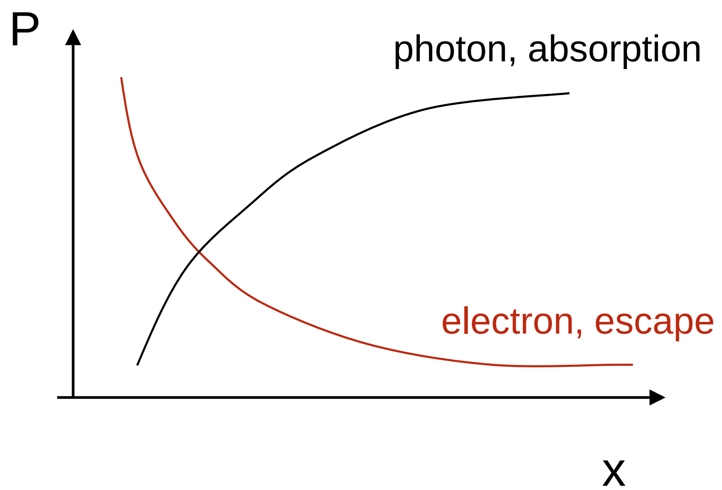

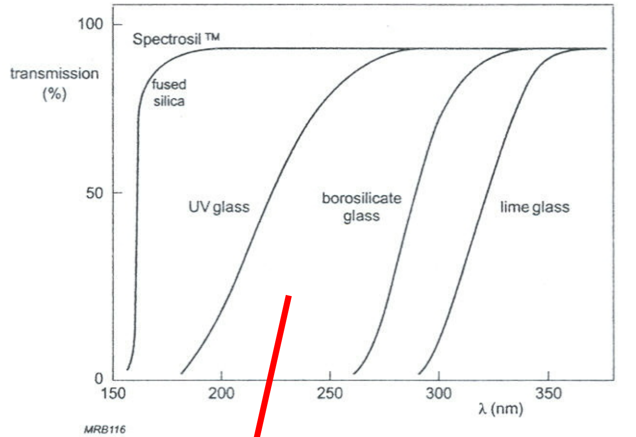

Fig.1.5 Transmission (%) as a function of wavelength λ for various glasses used in photomultiplier input windows (thickness 3 mm)

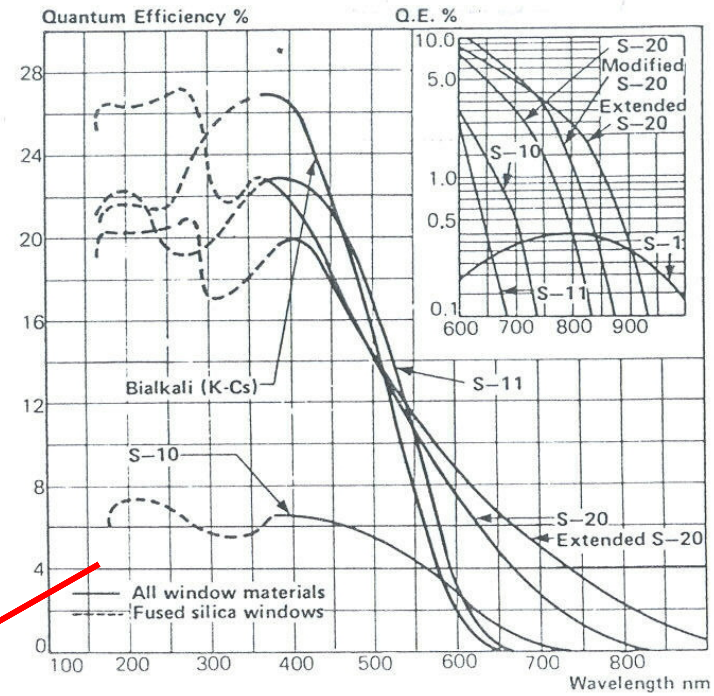

Fig. 8.2. Quantum efficiency of various photocathode materials (from *EMI Catalog* [8.2])

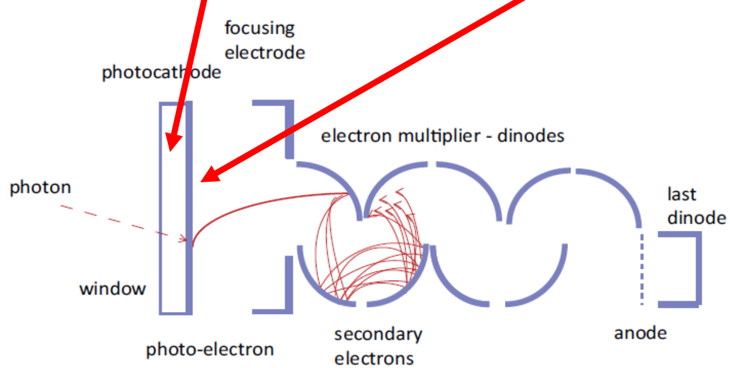

Table 8.1. Photocathode characteristics (from RTC catalog [8.3])

Cathode type	Composition	λ at peak response [nm]	Quantum efficiency at peak
S1 (C)	Ag – O – Cs	800	0.36
S4	SbCs	400	16
S11 (A)	SbCs	440	17
Super A	SbCs	440	22
S13 (U)	SbCs	440	17
S20 (T)	SbNa – KCs	420	20
S20R	SbNa – KCs	550	8
TU	SbNa – KCs	420	20
Bialkali	SbRb – Cs	420	26
Bialkali D	Sb – K – Cs	400	26
Bialkali DU	Sb – K – Cs	400	26
SB	Cs – Te	235	10

Photocathode material: usually semiconductors

e.g. antimony (Sb) + alkaline metals (K, Cs, Rb, Na ...)

• Photoelectron suffers energy losses in a metal because of many collisions with free electrons ($\eta \approx 0.1$ %)

• Semiconductors: conduction band has only a few free electrons → few collisions → smaller energy loss before reaching the surface, η = 10 – 30%.

• Materials with negative electron affinity (like GaP doped with Zn+Cs) for electrons in the conduction band, $\eta \approx 80$ %.

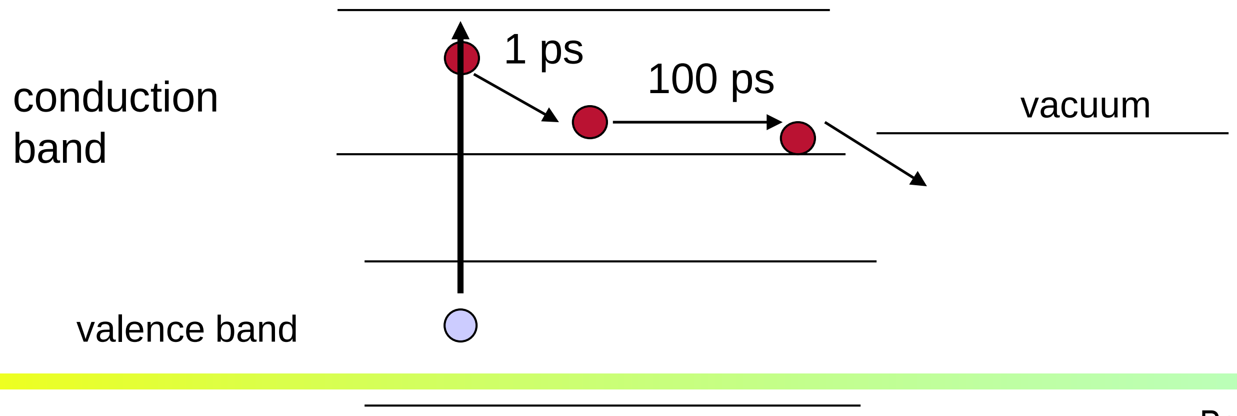

Quantum efficiency

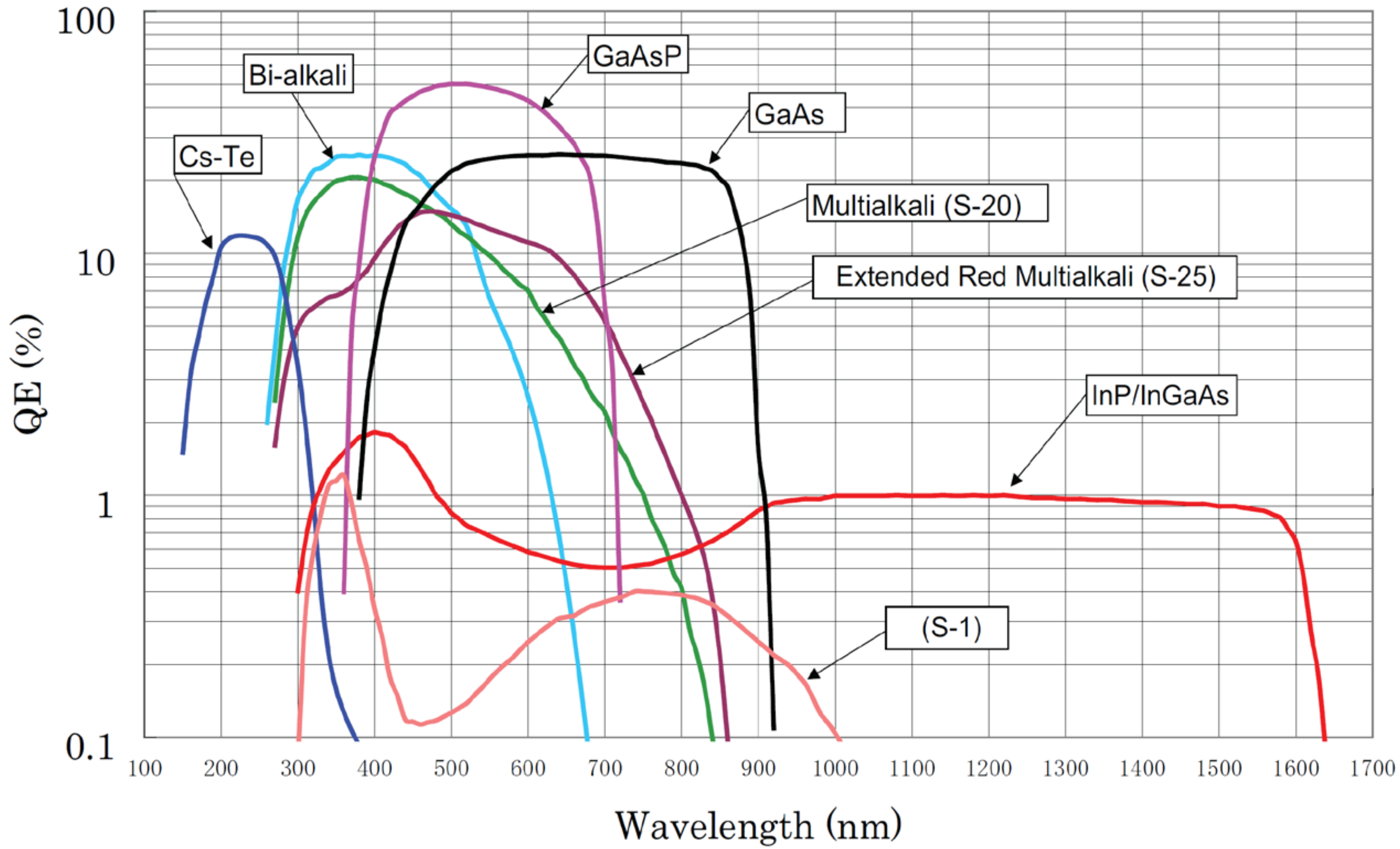

Extending PMT sensitivity to lower wavelengths

CBM RICH R+D: Wavelength-shifter coating of the PMT window

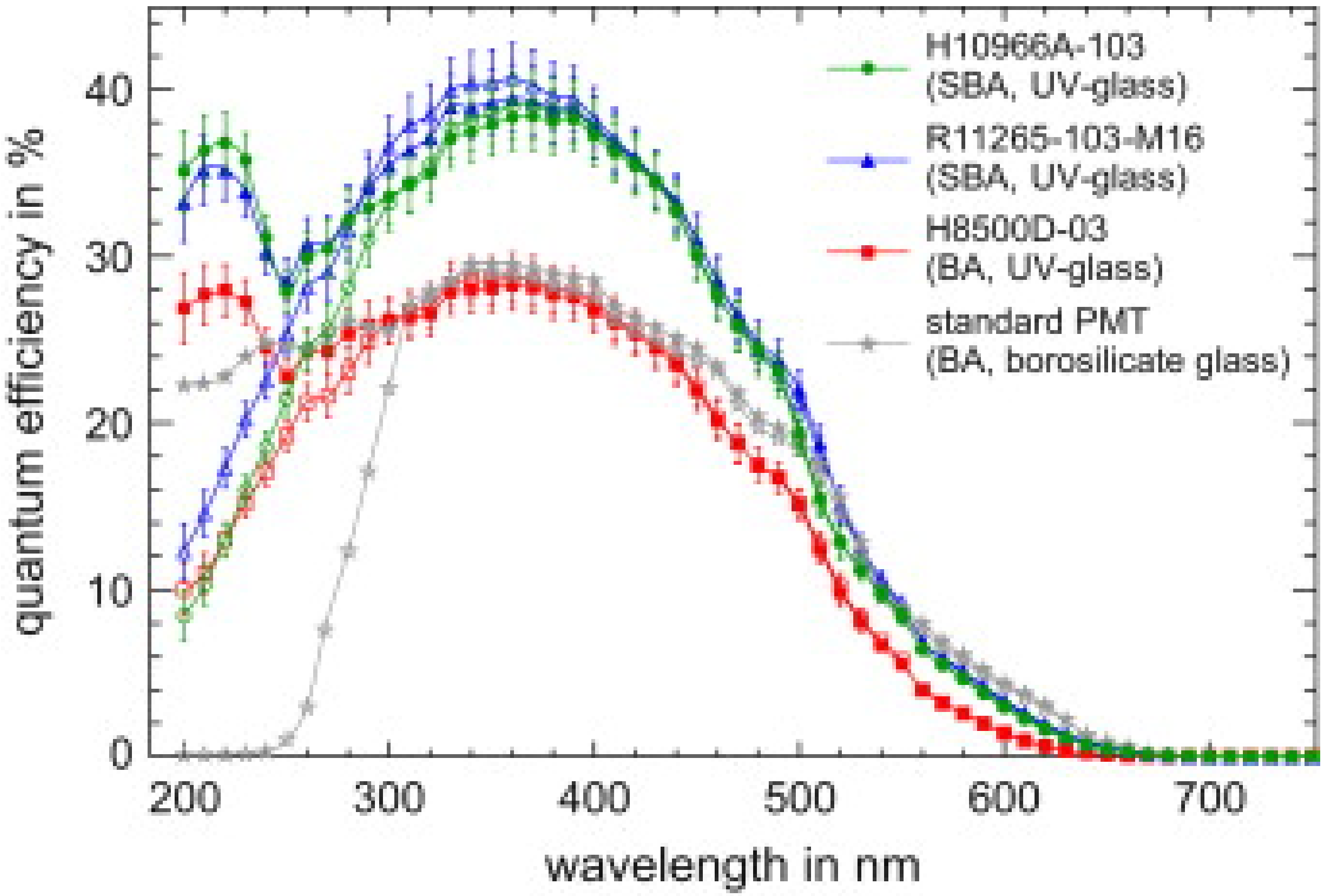

→NIM A766 (2014) 180

Collection of photoelectrons

Use a suitably formed electric filed between the photocathode and the first dynode

Requirements:

- high efficiency for the photo-electron collection (for different paths, exit energies, directions).

- the collection efficiency should not depend on the photoelectron exit point

- the time of flight to the first dynode should also not depend on the photoelectron exit point (impact on time resolution)

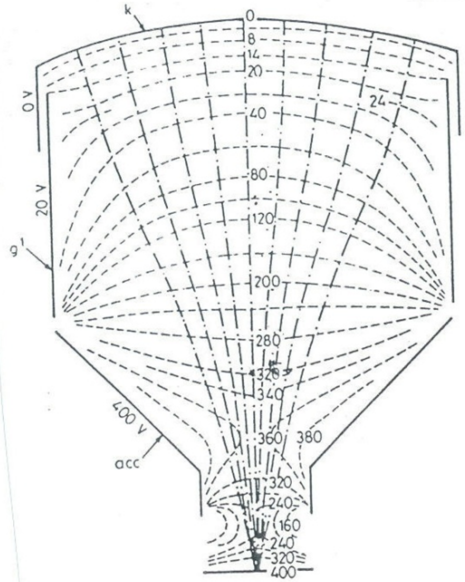

Fig. 8.15. Equipotential lines in the elec-tron-optical input system of a fast photo-multiplier (from *Hull* [8.9])

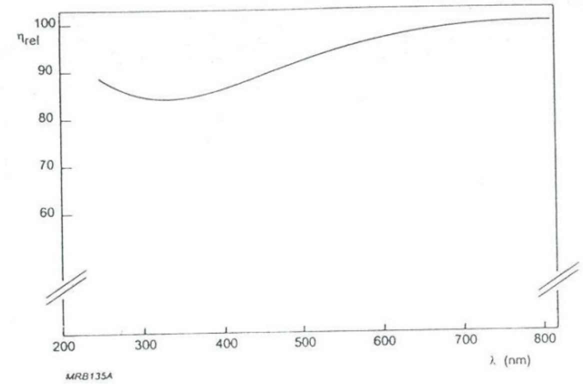

Fig.2.2 Example of relative input system collection efficiency as a function of wavelength

Fig. 4.2. Section through photomultiplier tube R 1449 with a spherical photocathode of 508 mm diameter [KU 83].

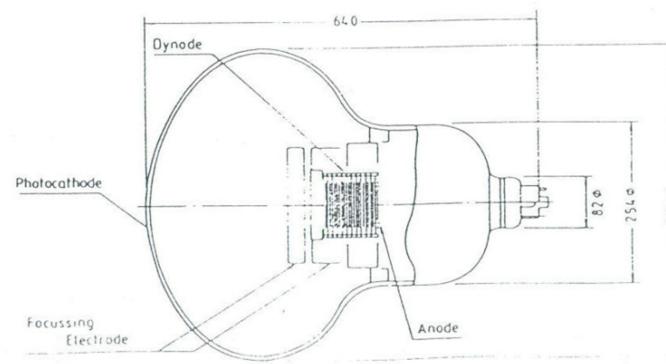

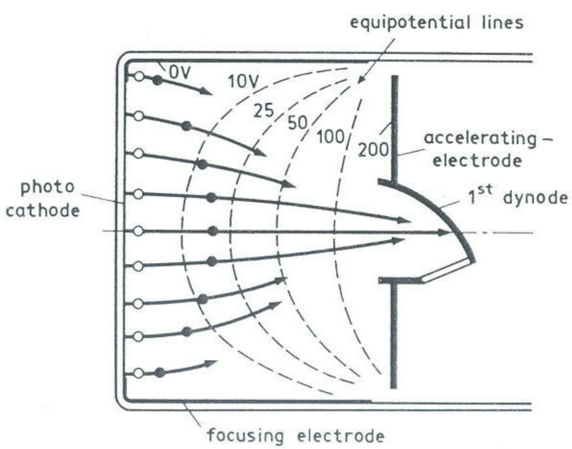

Fig. 8.14. Transit time difference (from *Schonkeren* [8.1])

Multiplication system (dynodes)

• secondary emission: number of secondary electrons per incoming electron $\delta \approx 3\text{-}5$

• dynode material: usually semiconductors or isolators (same reason as for the photocathode)

• semiconductor on a metal substrate (electric contact needed for E field for acceleration)

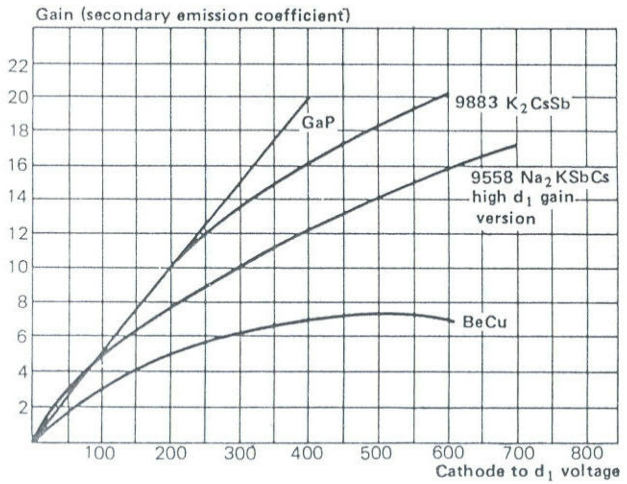

Fig. 8.9. Secondary emission factor for several dynode materials (from *EMI Catalog* [8.2])

• 10-14 dynodes ⟶ $G = 10^7\text{-}10^8$

• GaP dinode ⟶ 5 dynodes ⟶ same G

Dynode configuration

Linear focused

circular

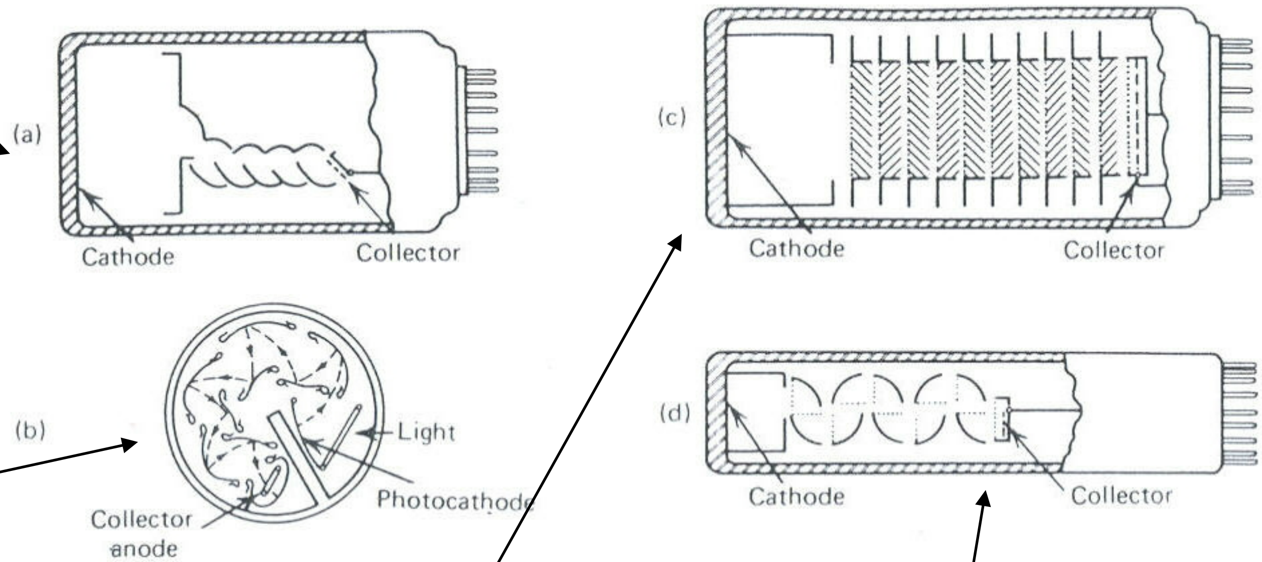

“venetian blind”

“box grid”

Figure 9-7 Configurations of some common types of PM tubes. (a) Focused linear structure. (b) Circular grid. (c) Venetian blind. (d) Box-and-grid. (Courtesy of EMI GENCOM Inc., Plainview, NY.)

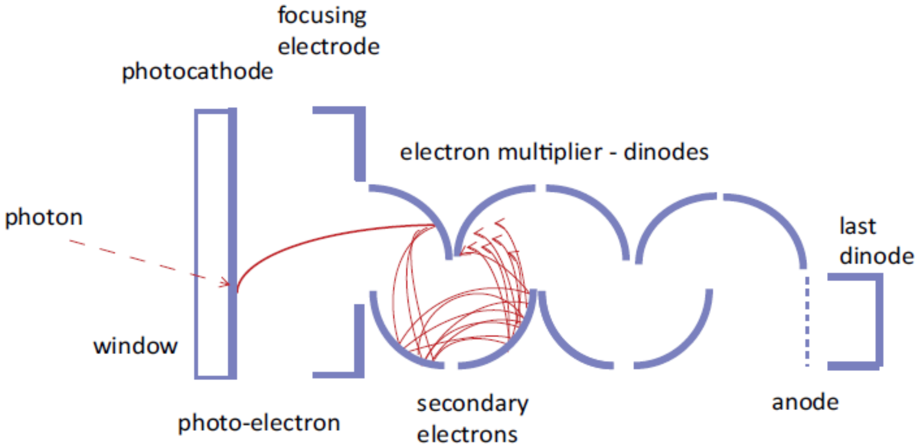

Voltage dividers

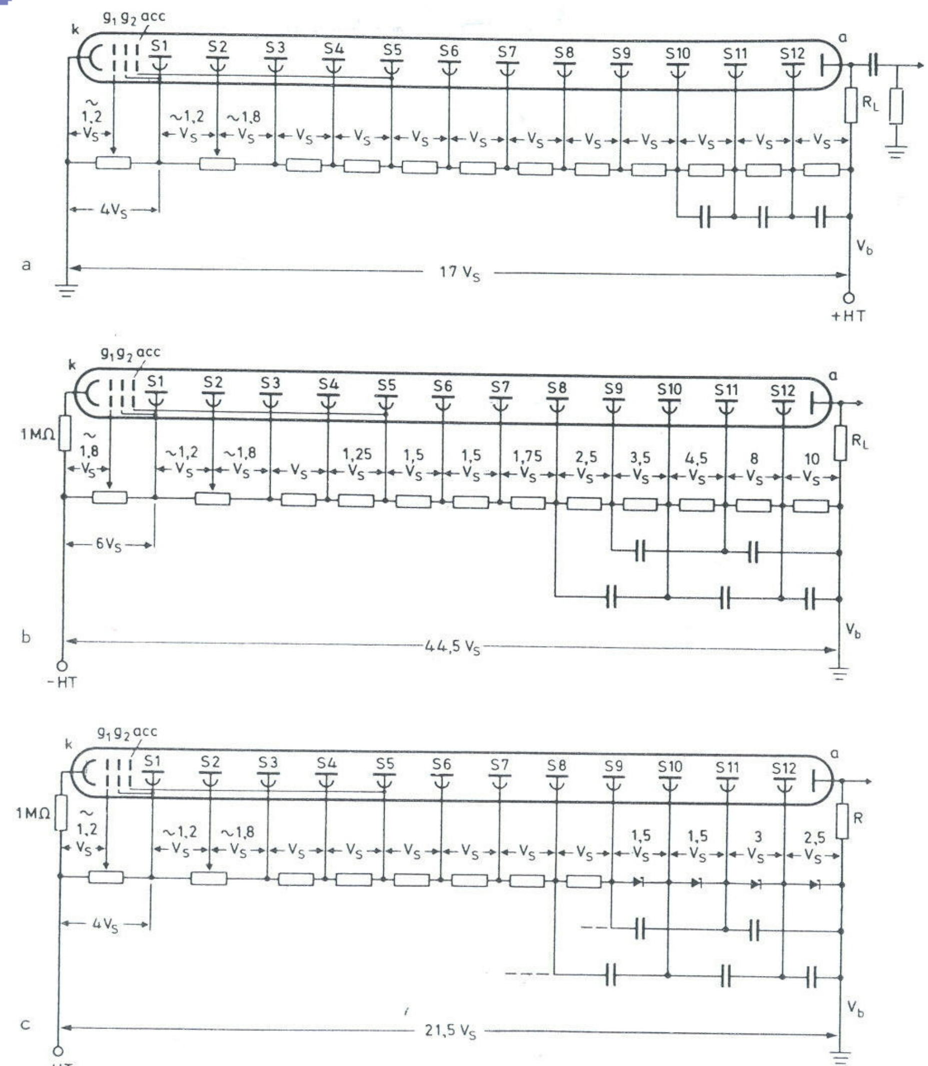

Pulse height distributions for single photoelectrons

(multiple photons: convolution)

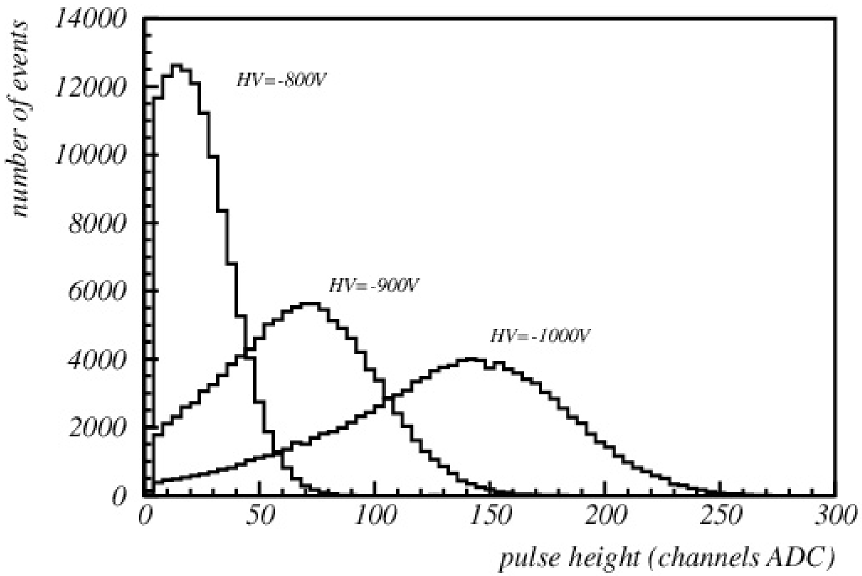

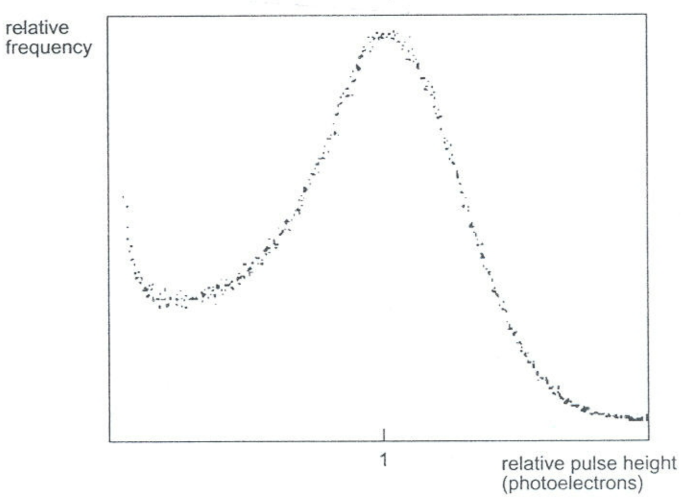

Fig.2.4 Typical single-electron spectrum. Resolution 67% FWHM. Peak-to-valley ratio 2.8:1

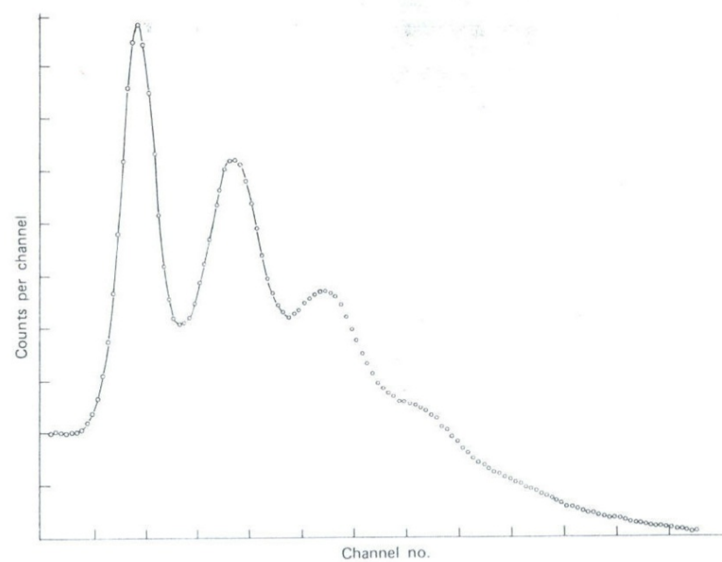

Figure 9-6 The measured pulse height spectrum for weak scintillation events obtained from a RCA 8850 photomultiplier tube. The high-gain first dynode results in distinguishable peaks in the spectrum corresponding to 1, 2, and 3 photoelectrons per pulse. (From Houtermans.[12])

Noise in a photomultiplier tube

1) thermionic emission from the photocathode and from the dynodes (most important contribution)

$I \propto T^2 \exp(-e\phi/kT)$, Richardson

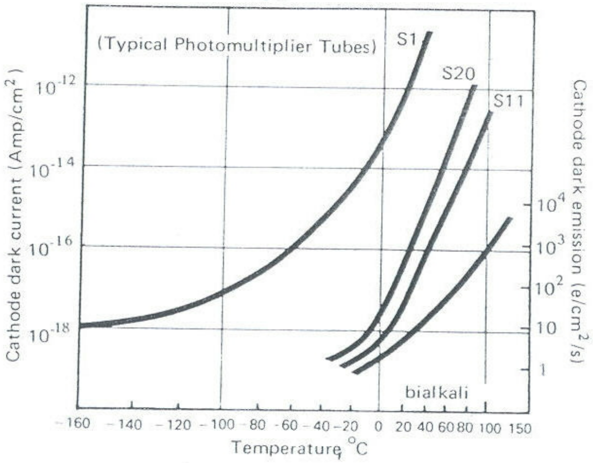

Fig. 8.19. Dark noise vs. temperature for various photocathodes (from *Wardle* [8.10])

2) Current from the base contacts (“leakage”)

3) Contamination of PMT materials with radio-active isotopes

<u>“afterpulsing”</u>

• Ionized molecules of the residual gas in the PMT volume hit the photocathode, kick out an electron → new pulse, $\Delta t \approx$ 100 ns – 1 μs

• “electrode glow”: the dynodes at the end of the dynode chain can emit light → hits the photocathode → new photoelectron; $\Delta t \approx$ 30-60 ns.

Enviromental effects

1) Exposure of the PMT to the ambient light
   - if PMT under HV, this can destroy the PMT, or at least increase the dark current / dark counts
   - no HV: šum level will increase, but will eventually decrease with time

2) B field (see next slide)
   - modifies the path of photoelectrons and of the secondary electrons
   - reduction of gain and of the photoelectron collection efficiency
   - most sensitive: path from the photocathode to the first dynode
   - partial mitigation with a μ-metal shield

3) Temperature
   - increase of the thermionic noise
   - QE depends on the T (typically -0.5%/K)

PMT in a B field: reduction of gain and of the photoelectron collection efficiency

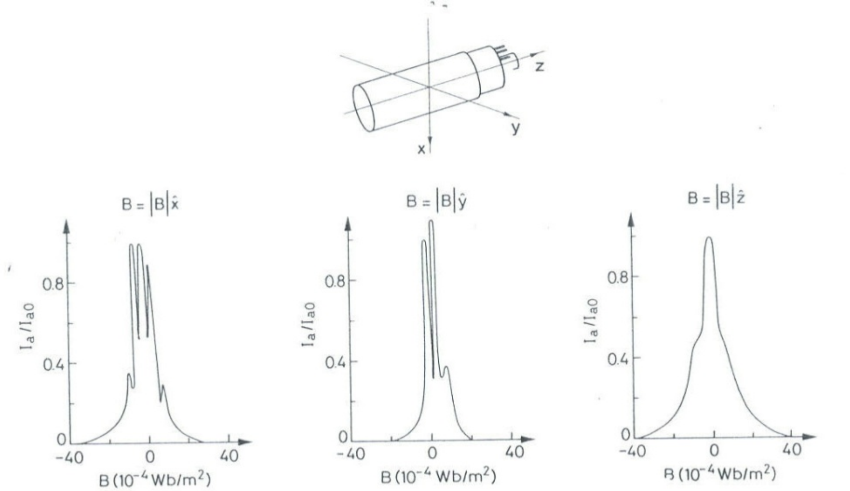

Fig. 8.17. Effect of magnetic fields on the anode current of an unscreened PM for different field orientations (from *Schonkeren* [8.1])

partial mitigation with a μ-metal shield

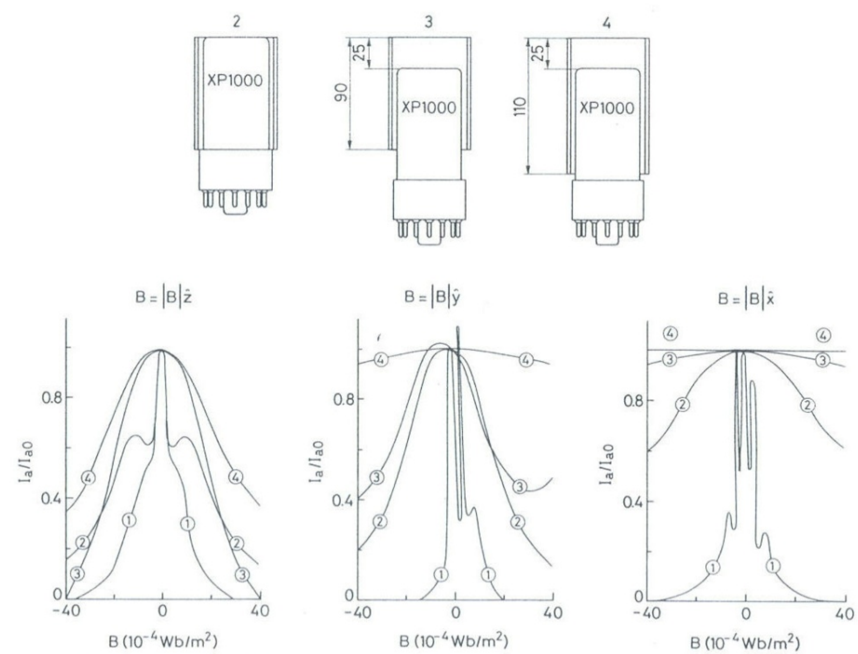

Fig. 8.18. Shielding effect of different mu-metal configurations (from *Schonkeren* [8.1])

Multianode PMTs

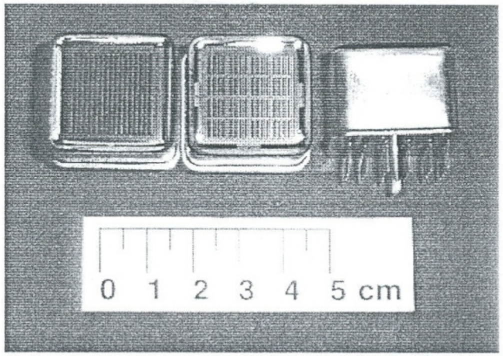

FIGURE 2. Hamamatsu multianode photomultipliers (L16, M16, M16 from left to right).

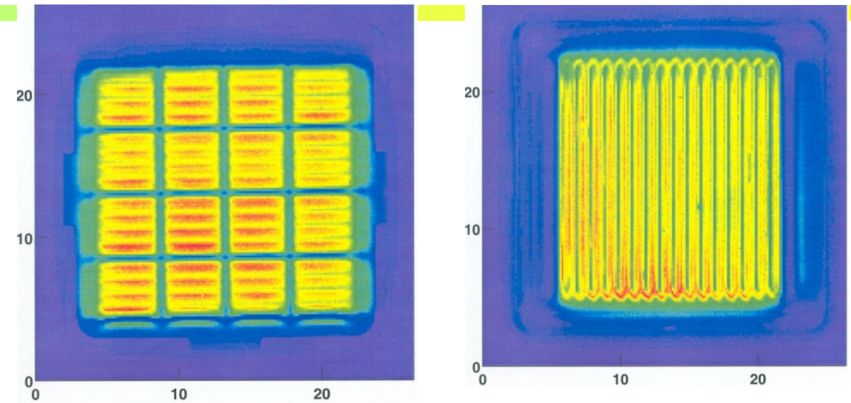

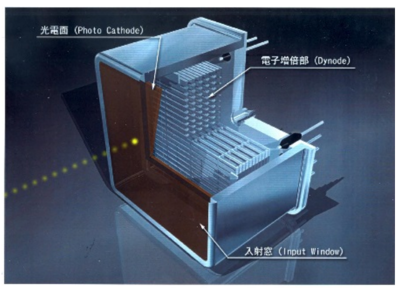

POSITION SENSITIVE PMT'S - EXAMPLES

Philips mesh
and foil types

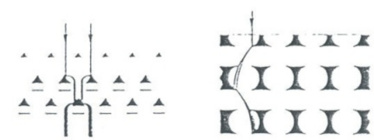

Hamamatsu
fine mesh

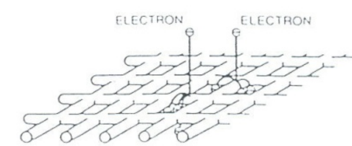

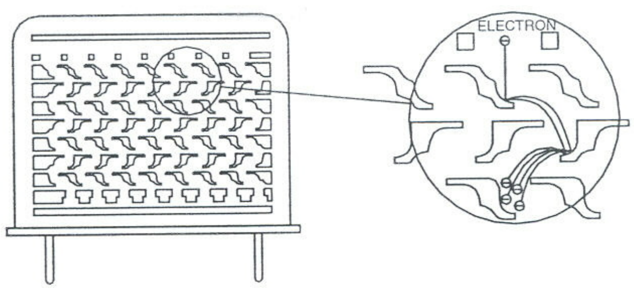

FIGURE 4. Metal channel type PMT [8].

First fast multianode sensor for single photons: MA PMT

Multianode PMT Hamamatsu R5900 with metal foil dynodes

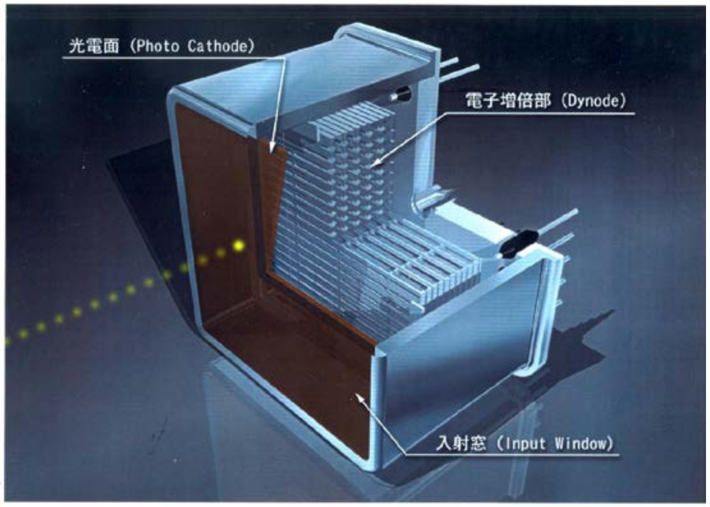

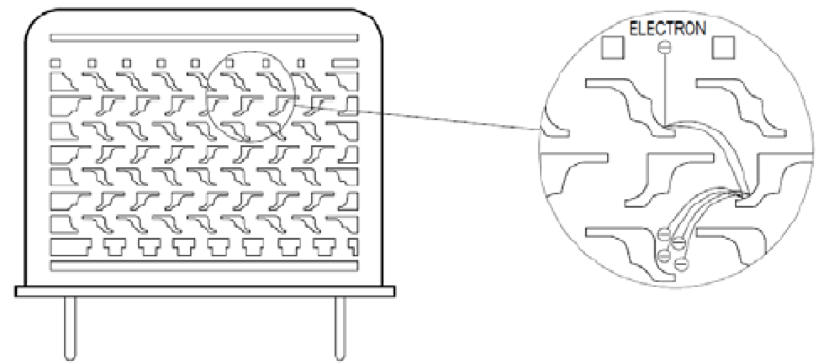

- Excellent single photon pulse height spectrum

- Low noise (few Hz/ch)

- Low cross-talk (<1%)

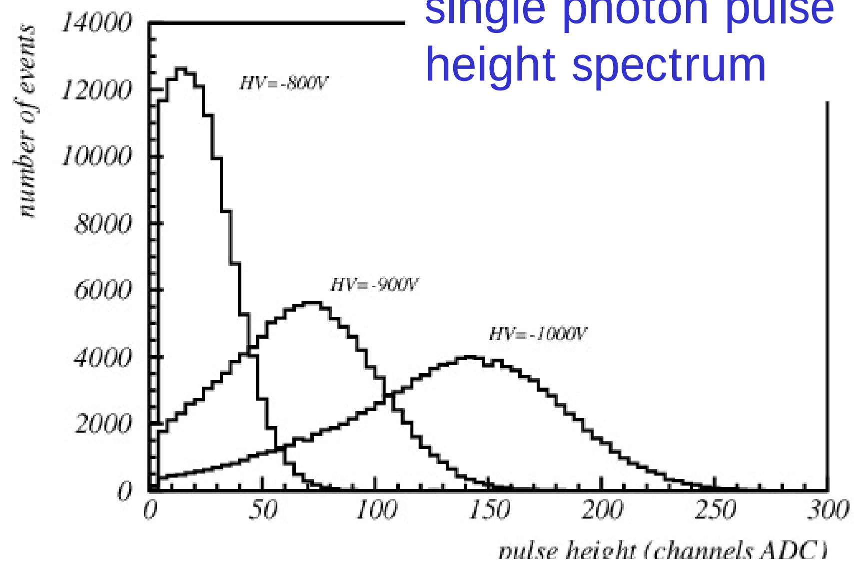

single photon pulse height spectrum

NIM A394 (1997) 27

Light collection for a multianode PMT

Light collection system (imaging!) to:

-Eliminate dead areas

-Adapt the pad size

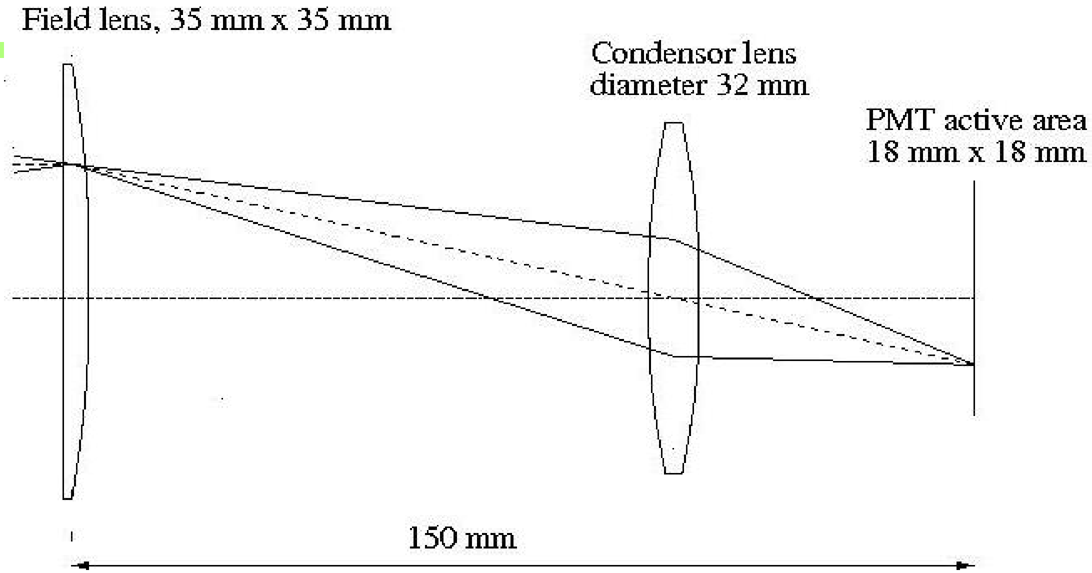

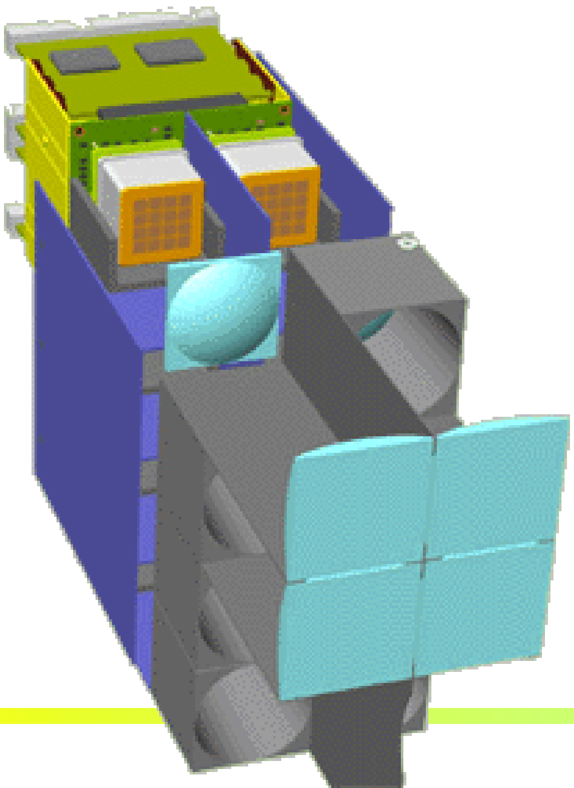

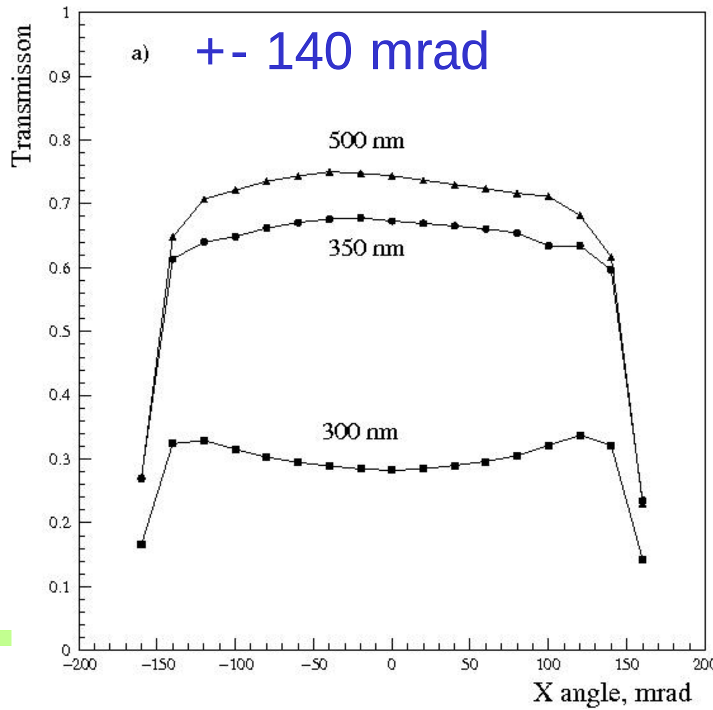

Flat pannel multianode PMTs

Problem of vacuum based sensors: active area fraction

One possible solution: make a larger sensor

Hamamatsu: flat pannel PMT H8500

- 52 x 52mm², 89% effective coverage
- 64 channels, pixel size 5.8 x 5.8 mm2
- 12 dynodes, metal foil type
- Bialkali cathode, max 25% quantum efficiency
- single photon pulse height distribution not as good as in the smaller R5900 (and related tubes like 7600)

Flat pannel MA PMTs

First used in a prototype RICH
for Belle II, with aerogel radiator.

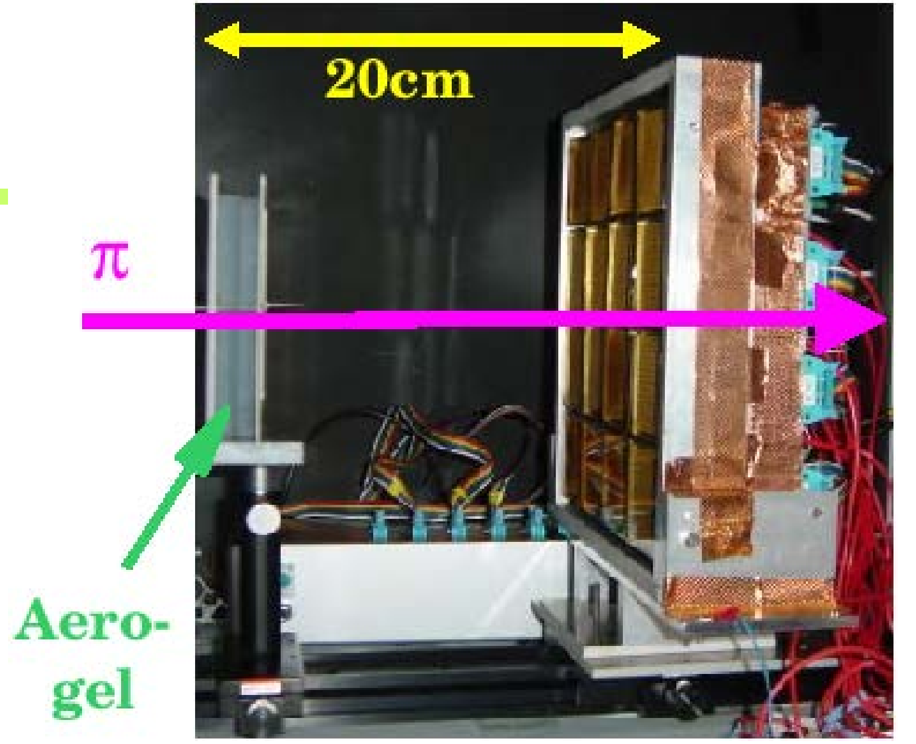

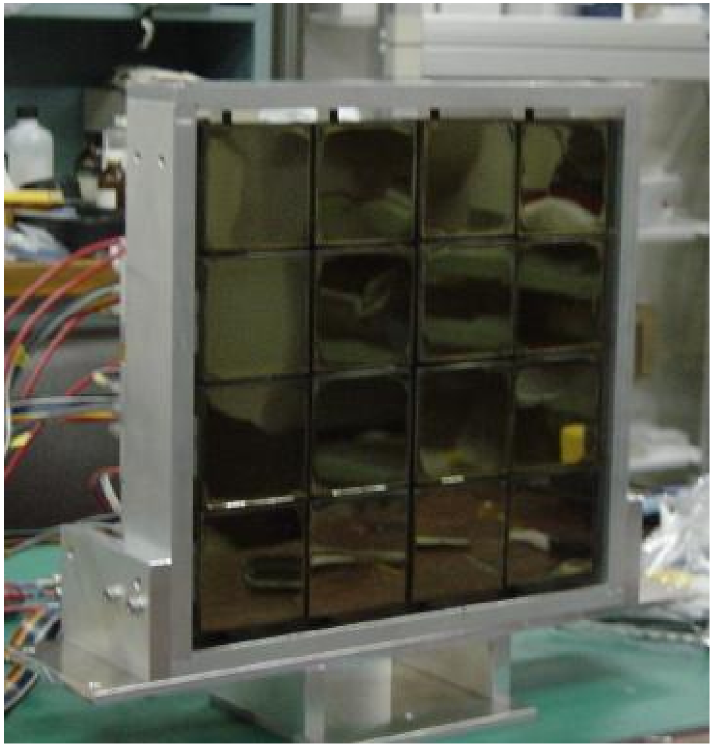

array of 16 H8500 PMTs

Clear rings, little background

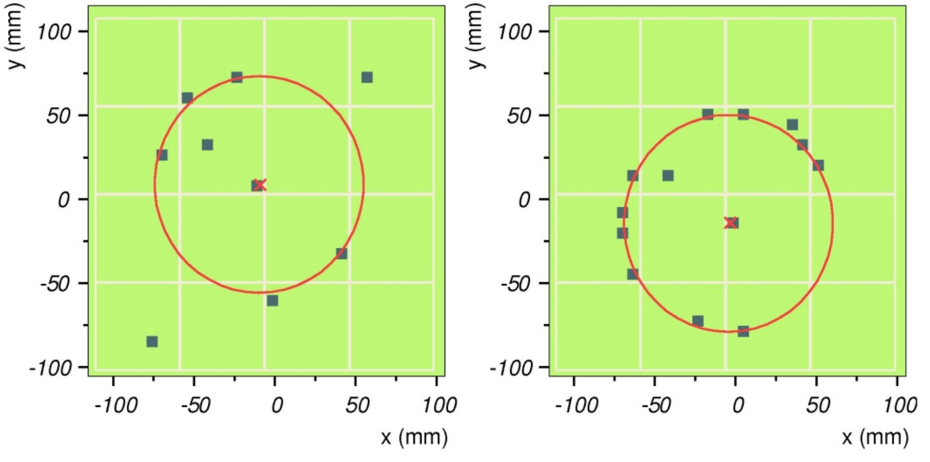

Used for the proof-of-principle test of the focusing radiator configuration

4cm aerogel single index

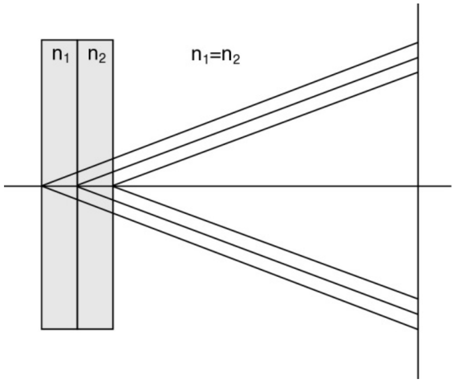

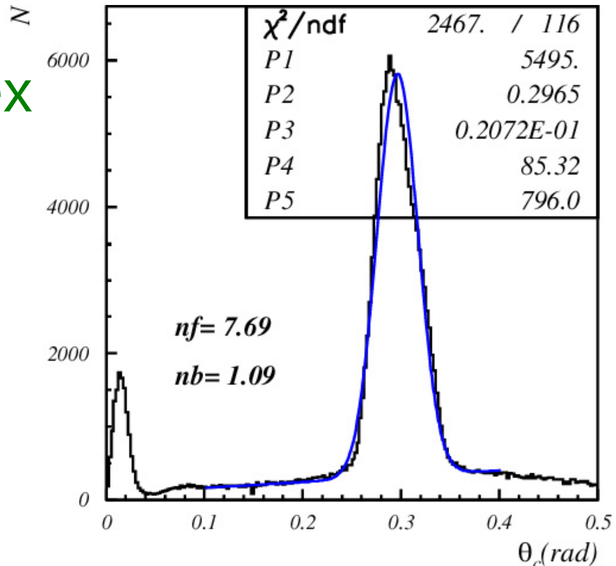

theta cerenkov

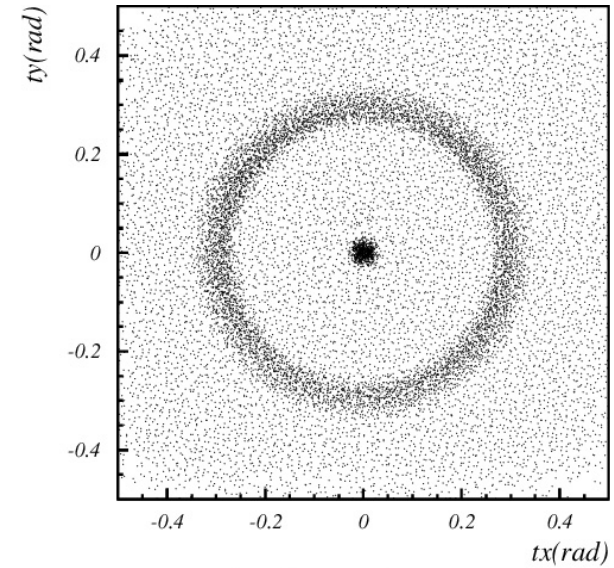

ring in cerenkov space

2+2cm aerogel

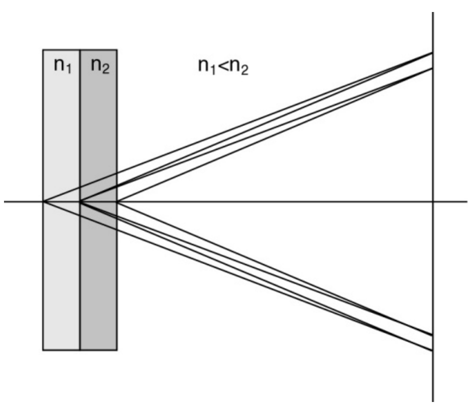

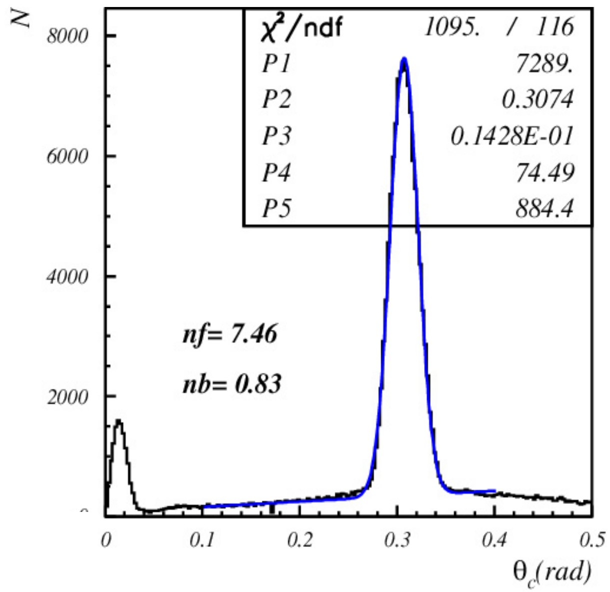

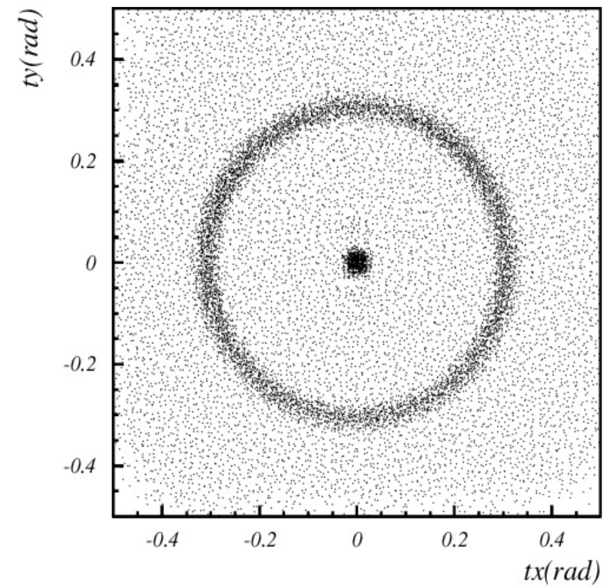

→NIM A548 (2005) 383

Micro-channel plate PMTs

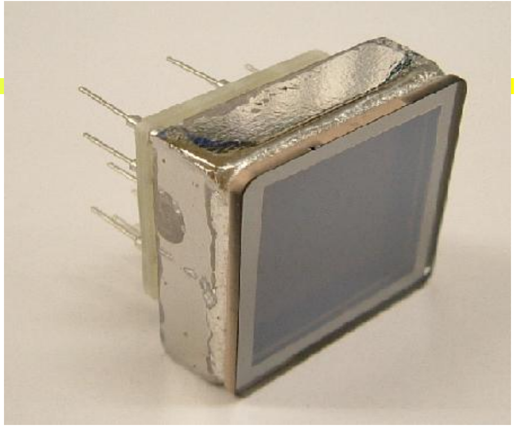

- Fast
- Immune to an axial magnetic field

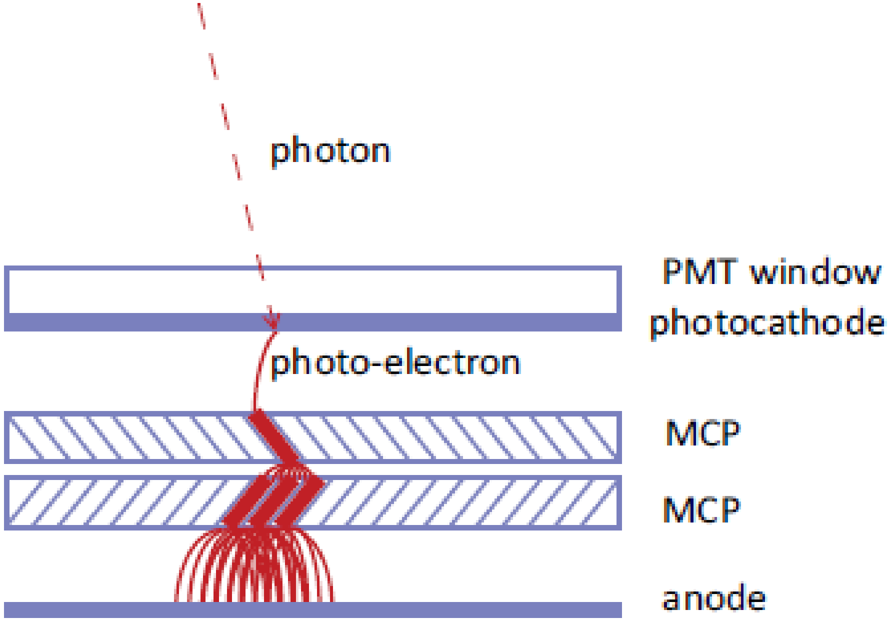

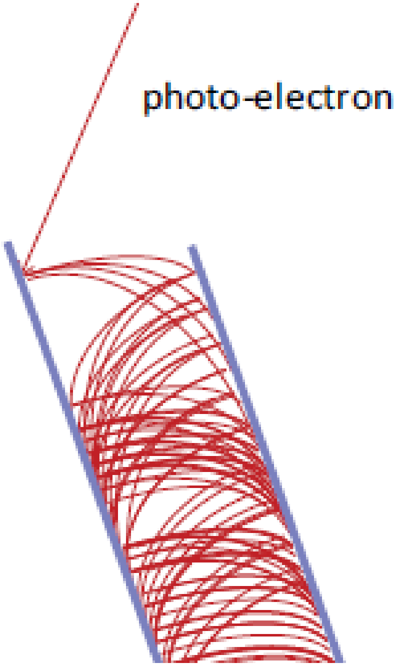

Mikrokanalne plošče

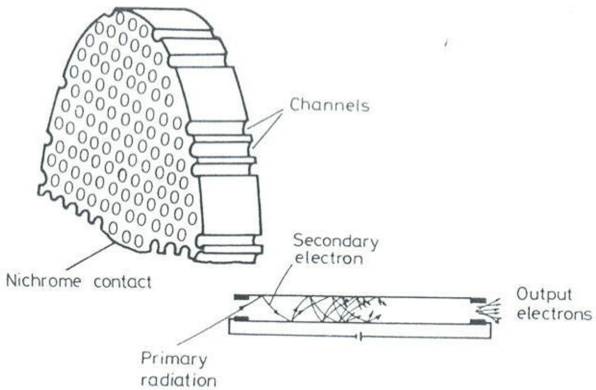

Fig. 8.6. Schematic diagram of a microchannel plate. The many channels act as continuous dynodes (from *Dhawan* [8.4]; picture © 1975 IEEE)

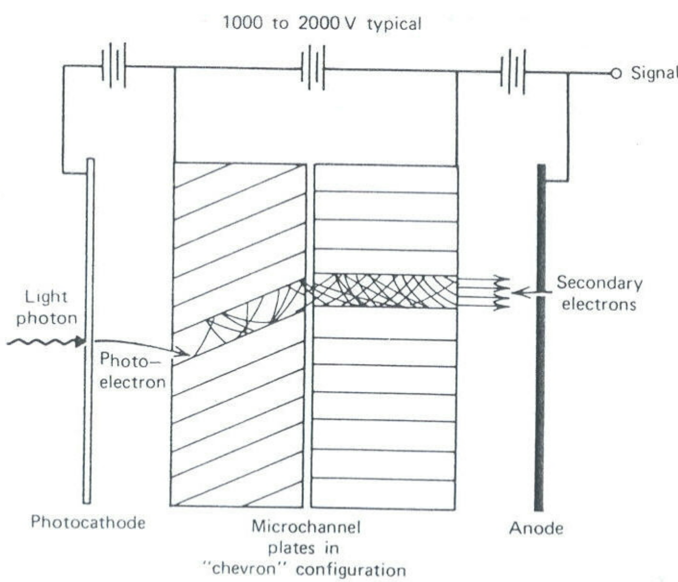

Figure 9-9 Elements of a PM tube based on microchannel plate electron multiplication.

- pore diameter 10-100 μm
- channel length $\approx$ 1mm
- multiplication G $\approx 10^5$-10^7 ("chevron")
- time resolution <100 ps
- spatial sensitivity
- 25 μm pores: up to B$\approx$0.8T
- 10 μm: up to B$\approx$1.5T

MCP PMT timing

MCP PMTs: main peak with excellent timing accompanied with a tail

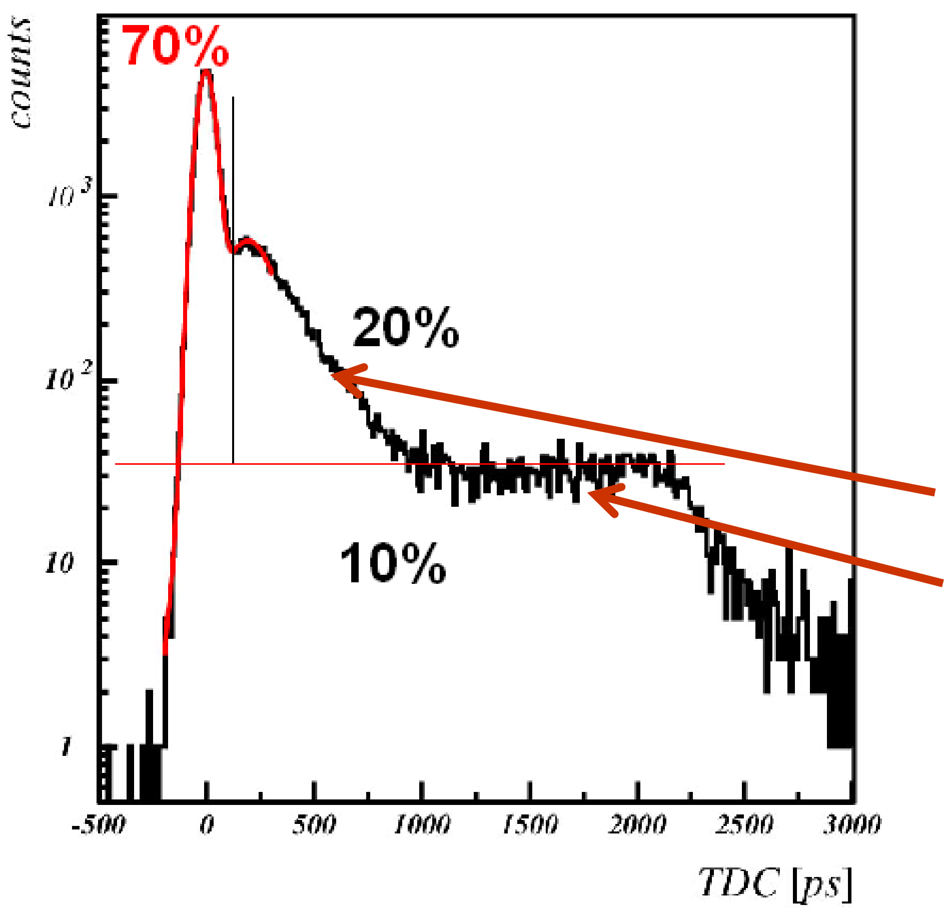

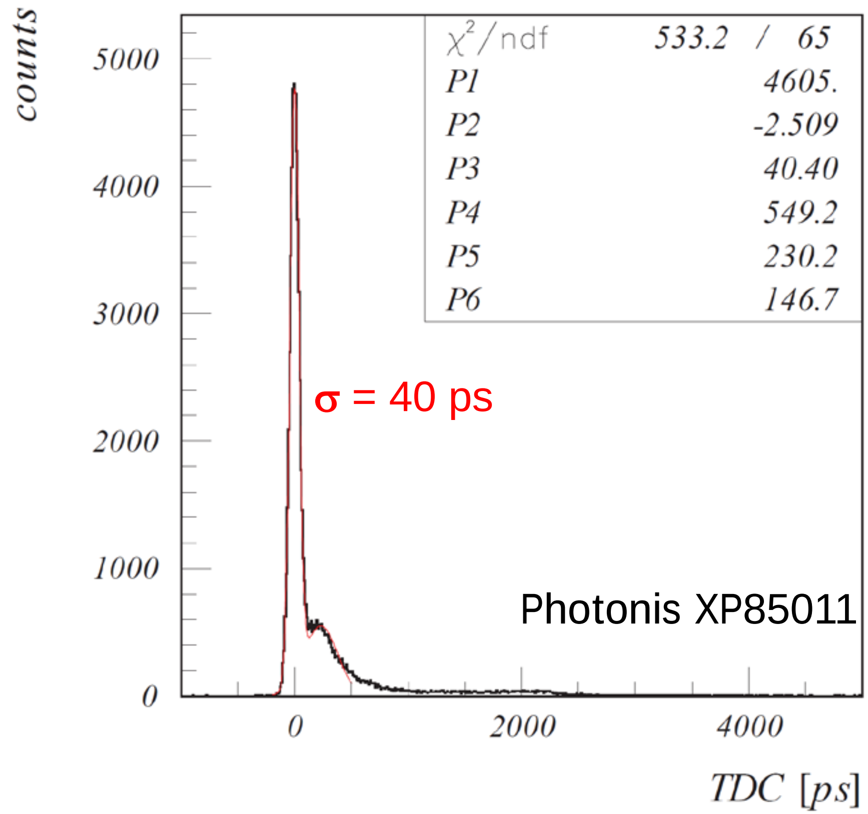

- Inelastic back-scattering
- Elastic back-scattering

→good agreement with a simple model →

→ NIMA 595 (2008) 169

→ JINST 4 (2009) P11017

Elastically backscattered photoelectrons

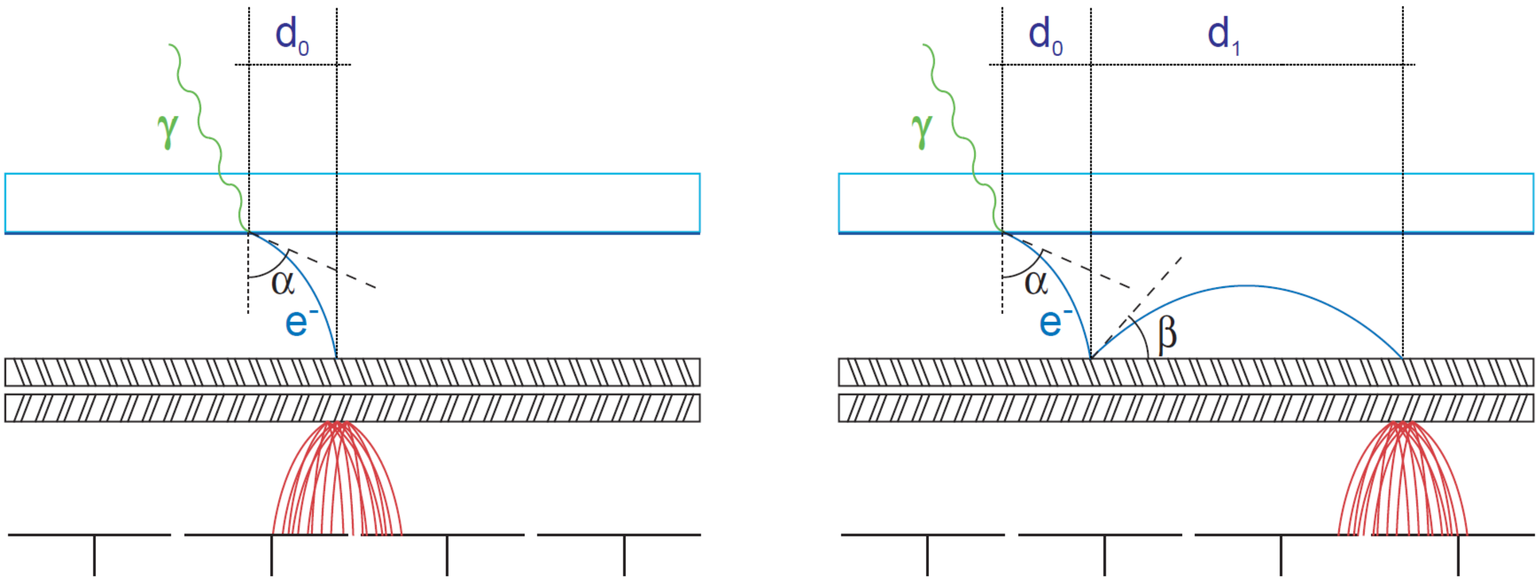

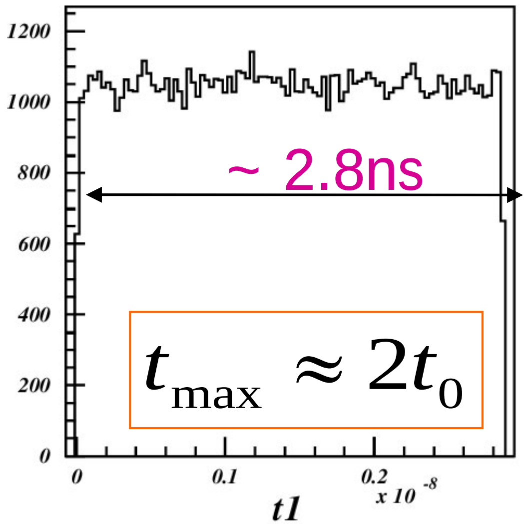

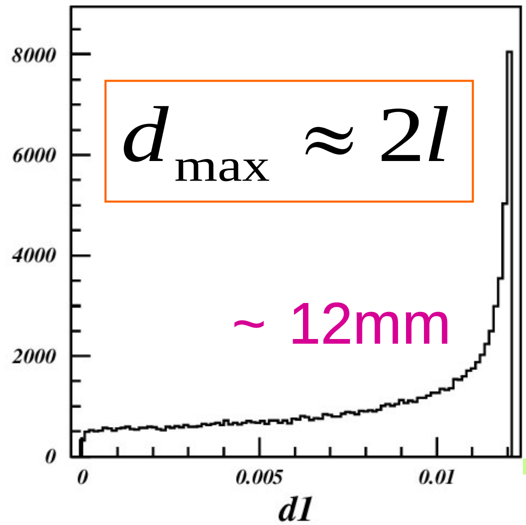

Results of a simple modeling: we assume that the photoelectron back-scattering by the angle β is uniform over the solid angle.

→ NIMA 595 (2008) 169
JINST 4 (2009) P11017

MCP PMT: processes involved in photon detection

MCP PMT parameters used: Photonis XP85011

Parameters used:

- $U = 200$ V
- $l = 6$ mm (K-MCP)
- $E_0 = 1$ eV
- $m_e = 511$ keV/c^2
- $e_0 = 1.6\ 10^{-19}$ As

$$t_{\max} \approx 2t_0$$

$$d_{\max} \approx 2l$$

Tails can be significantly reduced by:

- decreased photocathode-MCP distance and
- increased voltage difference

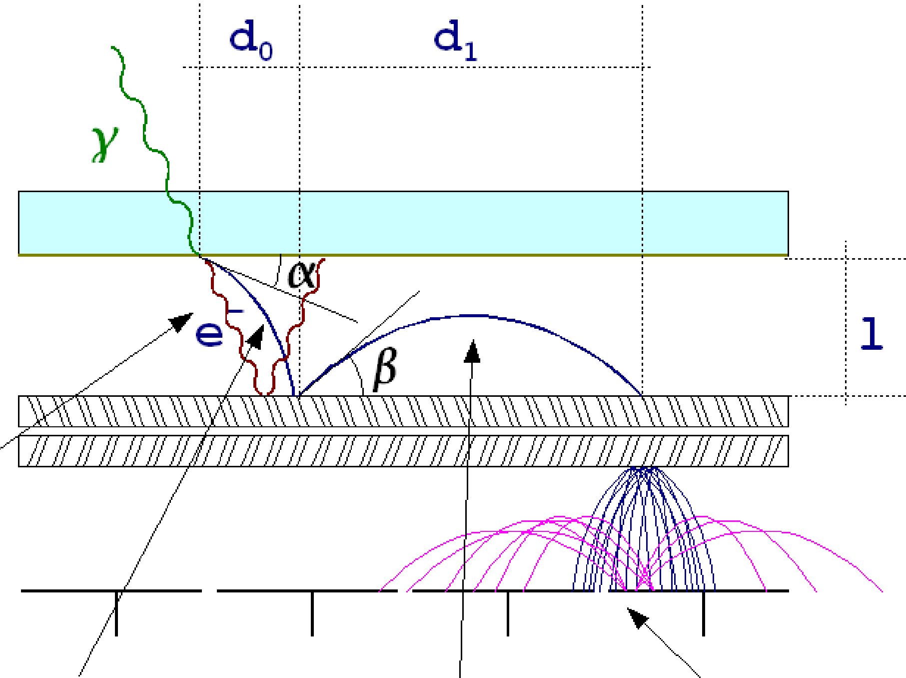

Internal-reflection

Photo-electron:

- $d_{0,max} \sim 0.8$ mm
- $t_0 \sim 1.4$ ns
- $\Delta t_0 \sim 100$ ps

Backscattering:

- $d_{1,max} \sim 12$ mm
- $t_{1,max} \sim 2.8$ ns

Charge sharing

→ NIMA 595 (2008) 169
JINST 4 (2009) P11017

MCP PMTs in magnetic field

Gain vs B field for different tilt angles

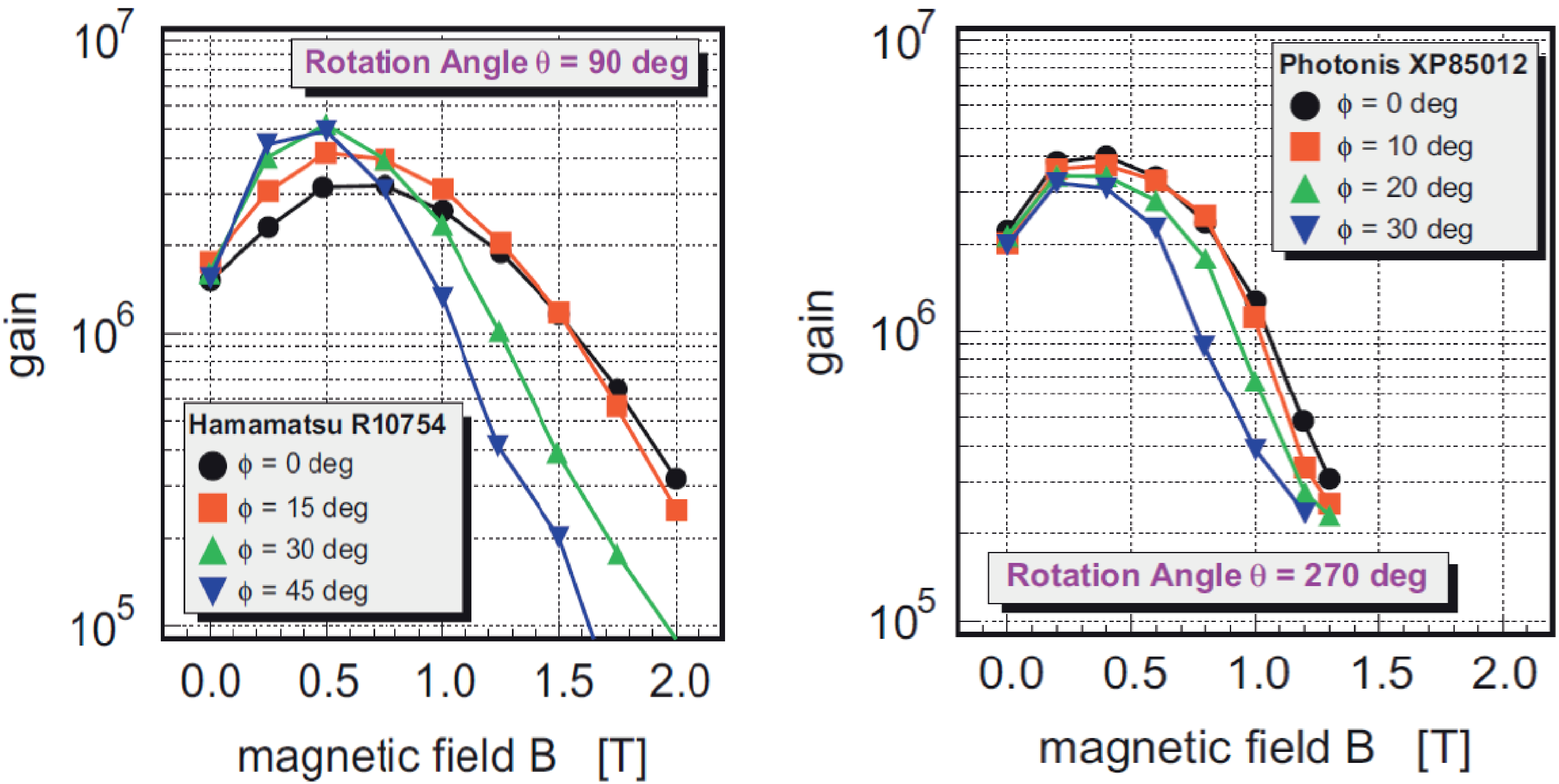

→ NIMA 639 (2011) 144

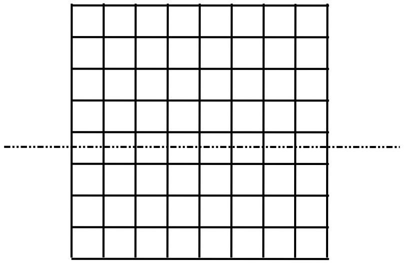

MCP PMT: improved performance in magnetic field

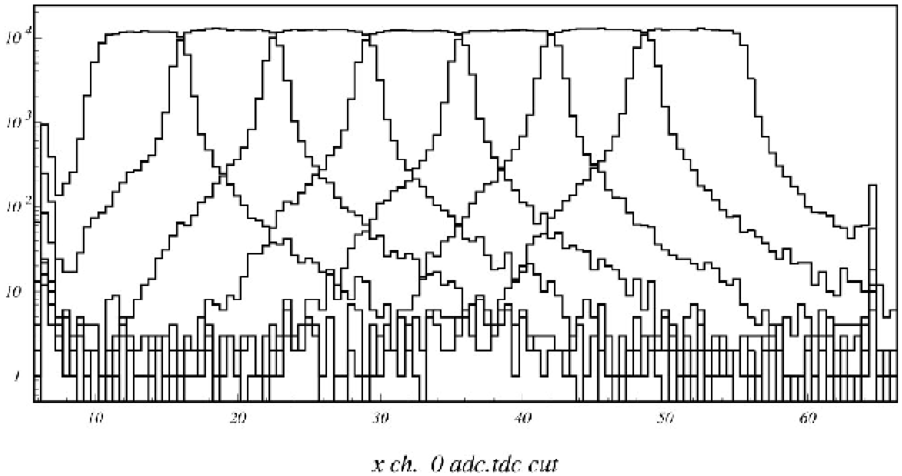

Number of detected hits on individual channels as a function of light spot position.

B = 0 T,
HV = 2400 V

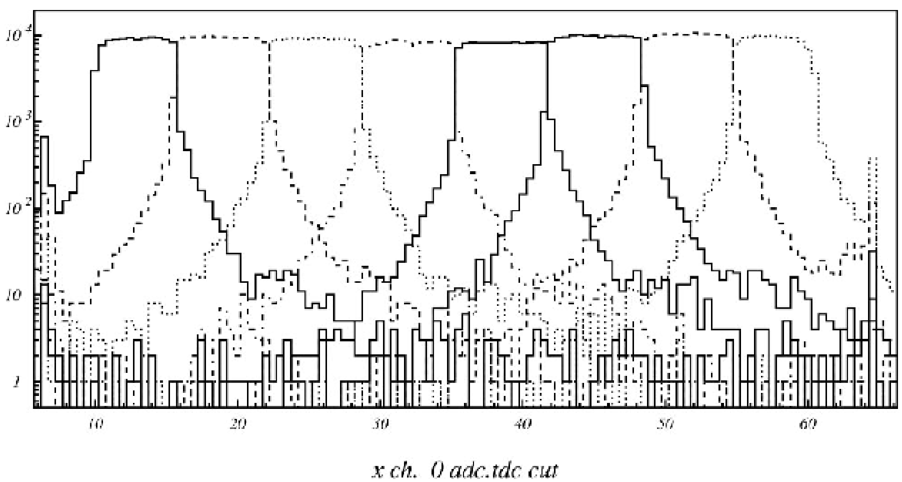

B = 1.5 T,
HV = 2500 V

Backscattered photoelectrons get ″locked″ to the B field lines

In the presence of magnetic field, charge sharing and cross talk due to long range photoelectron back-scattering are considerably reduced.

MCP PMTs ageing

MCP PMT ageing: a serious problem in most of the planned aplications.

Cures:

- Better cleaning of the MCPs, better vacuum
- Al foil between PC and first MCP
- Al foil between two MPC stages
- Atomic layer deposition (ALD)

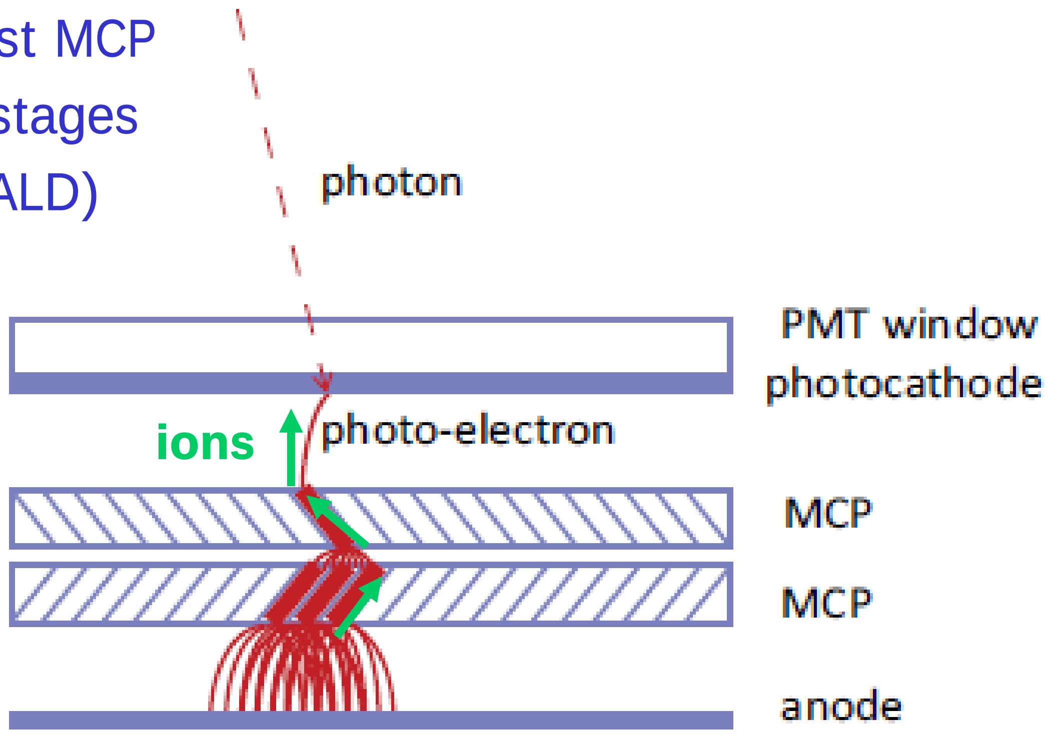

MCP PMTs ageing, cure

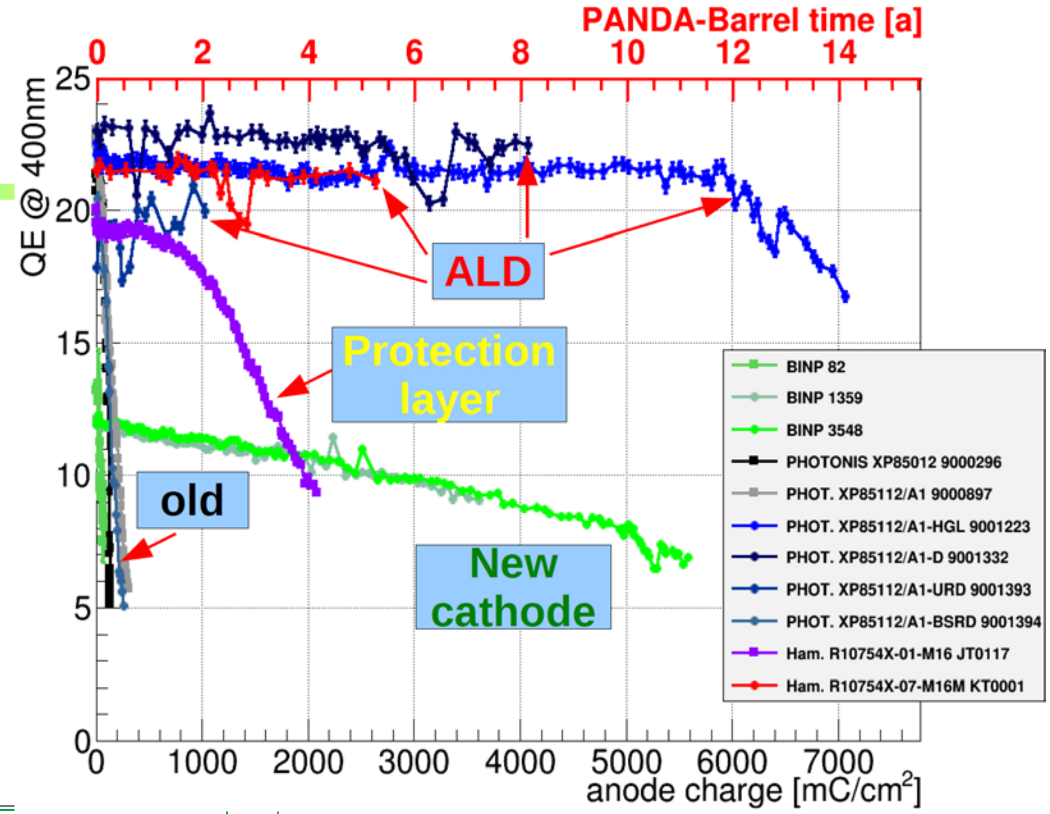

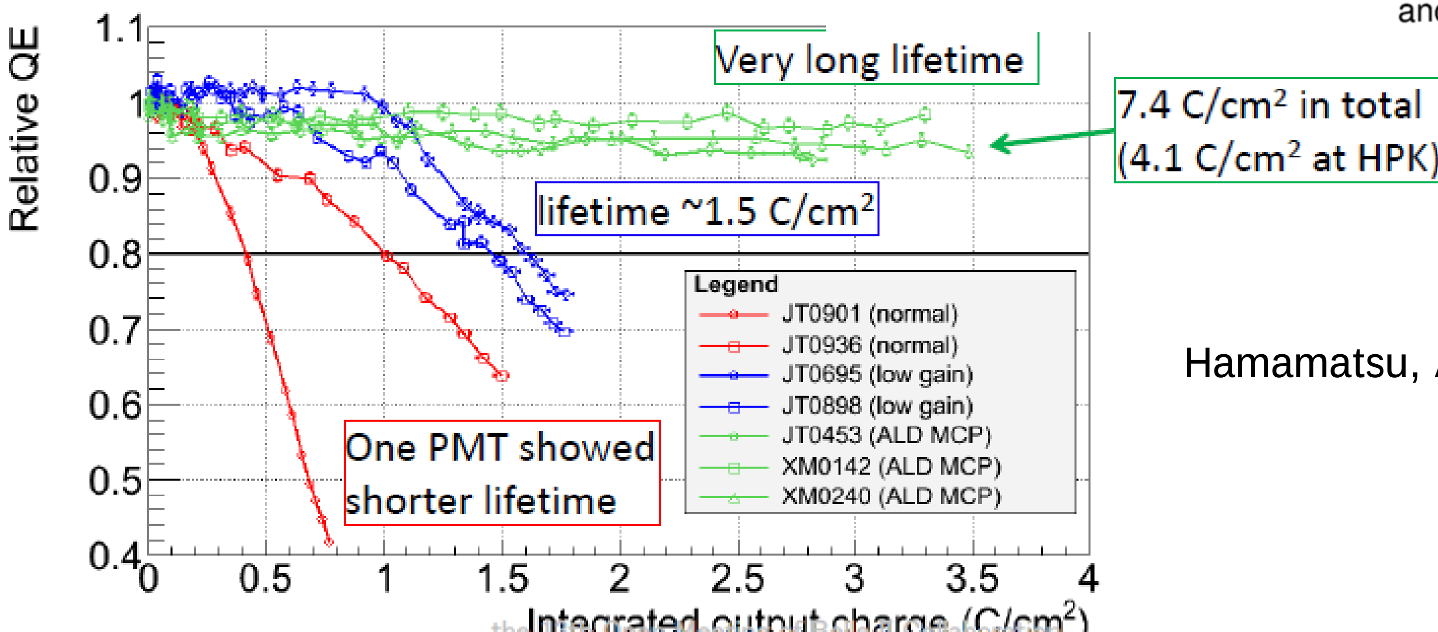

Hamamatsu, ALD deposition

Semiconductor light sensor: photodiode

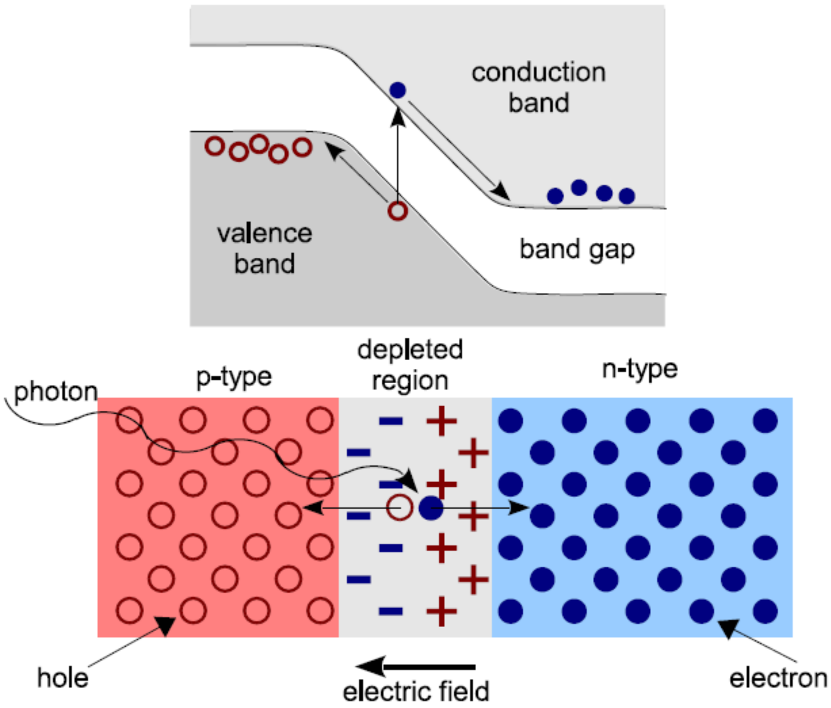

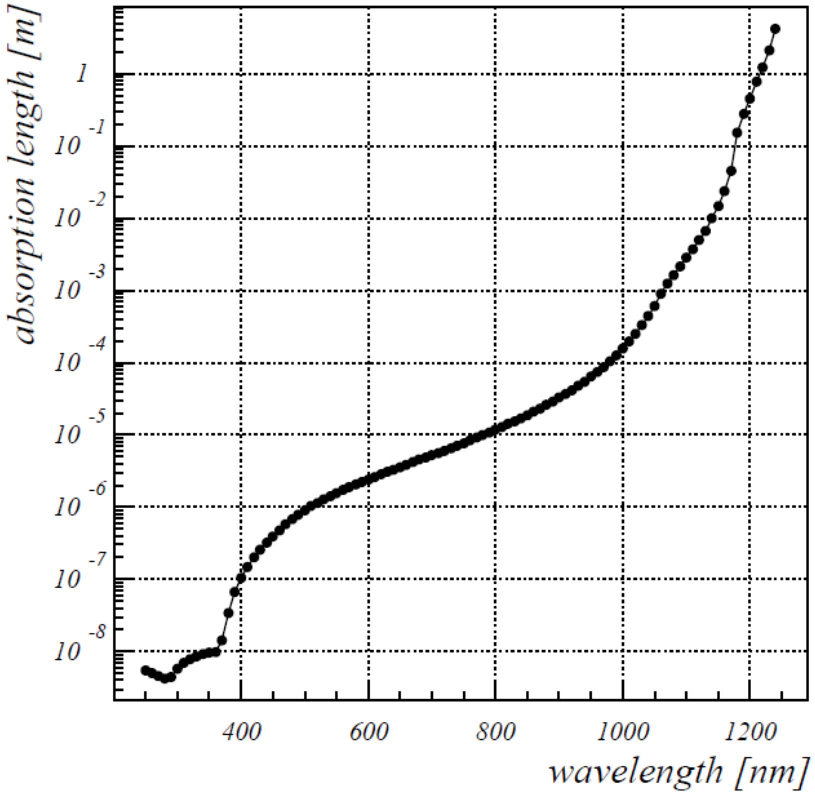

Semiconductor light sensor: CCD

- In cameras and phones - but not useful for single (or few) photons...

Semiconductor light sensors

Photodiodes (PD)

•High QE (also in the IR region),
• No multiplication
• Can be used in cases with large light yields (calorimeters)

Avalanche photodiodes APD

• high E field -> multiplication in an avalanche, $G \approx 10^2$-10^3.
• signal/noise still poor compared to a PMT
• used for calorimeters

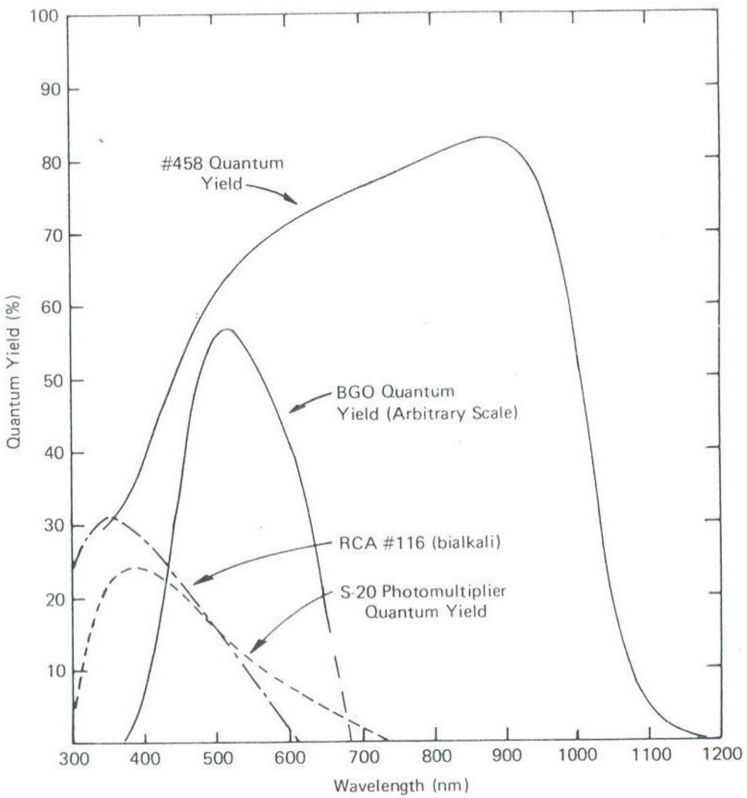

Figure 9-14 A comparison of the quantum efficiency of a silicon photodiode (labeled #458) with representative bialkali and S-20 photocathode quantum efficiencies. The emission spectrum from a BGO scintillator is shown for reference. (From Groom.[53])

Semiconductor light sensor: G-APD

G-APD: Geiger mode avalanche photo-diode, also known as SiPM – Silicon Photomultiplier

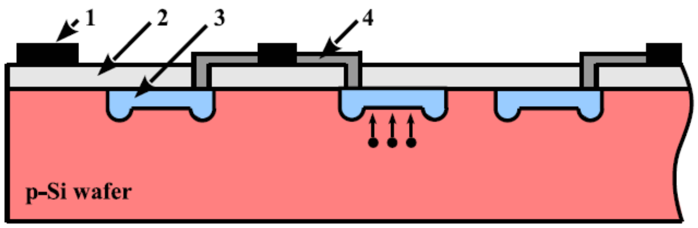

Figure 9: Schematic drawing of a cross-section of a SiPM: metal electrode (1), silicon oxide layer (2), p-n junctions/micro-cell (3) and individual quenching resistor (4) (23).

SiPM is an array of APDs operating in Geiger mode. Characteristics:

- low operation voltage ~ 10-100 V
- gain ~ 10^6
- peak PDE up to 65%(@400nm)

  PDE = QE x ε_{geiger} x ε_{geo} (up to 5x PMT!)
- ε_{geo} – dead space between the cells
- time resolution ~ 100 ps
- works in high magnetic field
- dark counts ~ few 100 kHz/mm^2
- radiation damage (p,n)

SiPMs as photon detectors

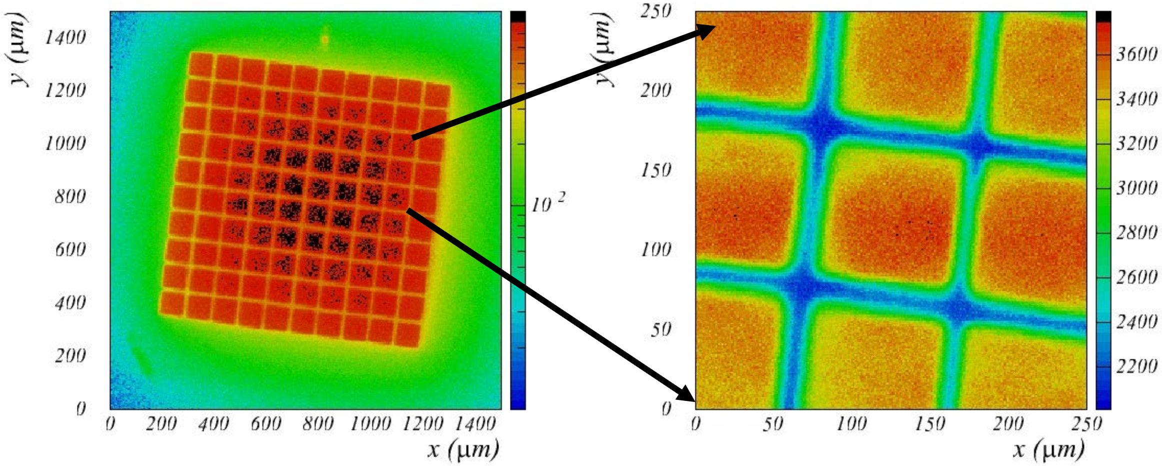

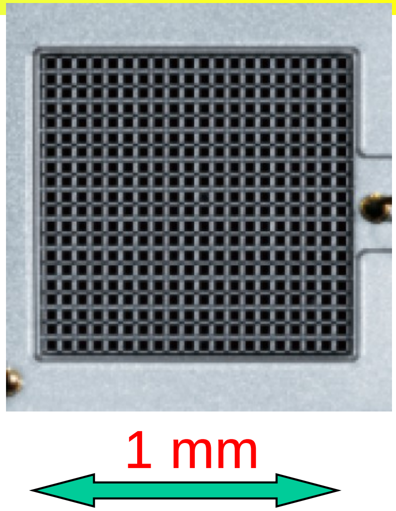

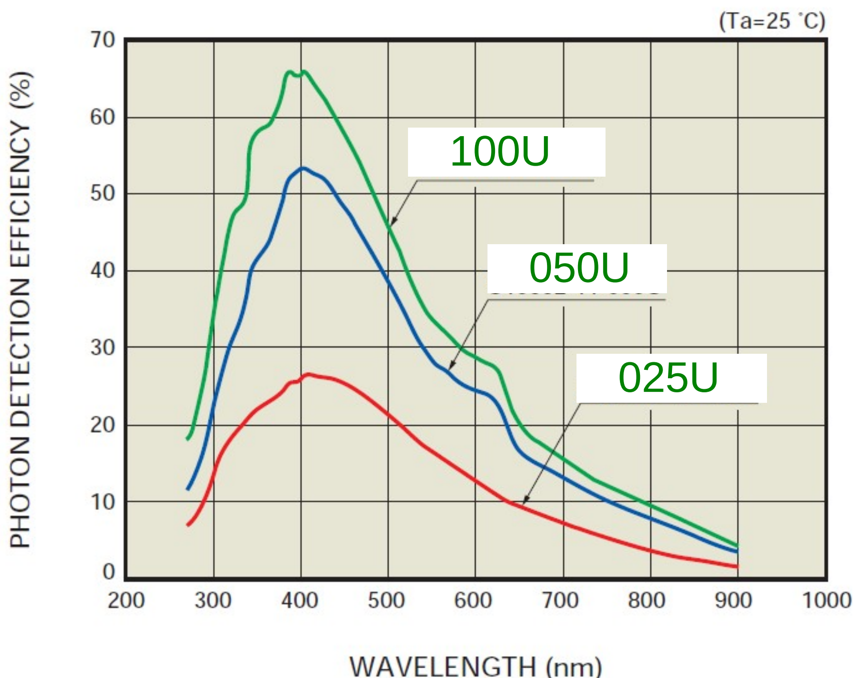

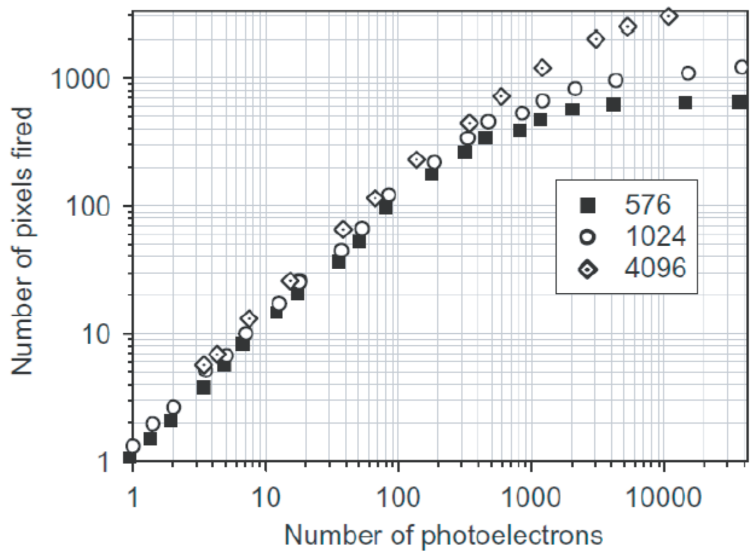

SiPM as photon detector?

Can we use SiPM (Geiger mode APD) as the photon detector in a RICH counter?

+immune to magnetic field

+high photon detection efficiency, single photon sensitivity

+easy to handle (thin, can be mounted on a PCB)

+potentially cheap (not yet…) silicon technology

+no high voltage

-very high dark count rate (100kHz – 1MHz) with <u>single photon pulse height</u>

-radiation hardness

Can such a detector work?

Improve the signal to noise ratio:

- Reduce the noise by a narrow (<10ns) time window
- Increase the number of signal hits per single sensor by using light collectors and by adjusting the pad size to the ring thickness

E.g. light collector with reflective walls

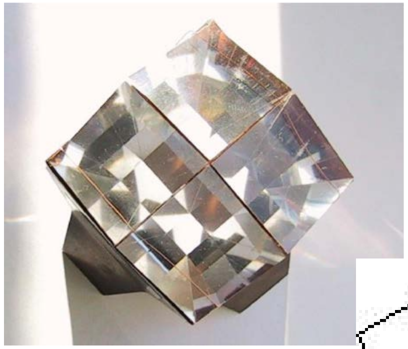

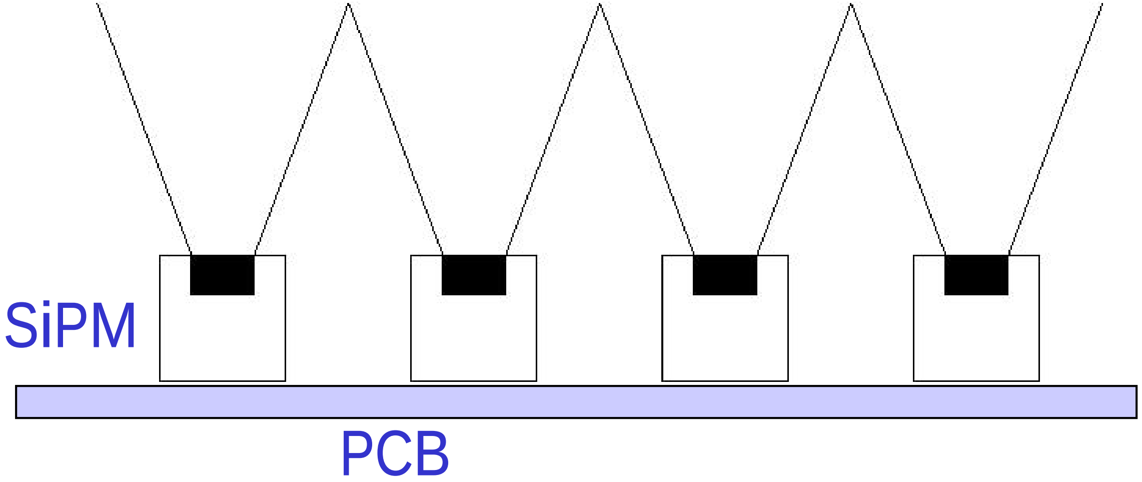

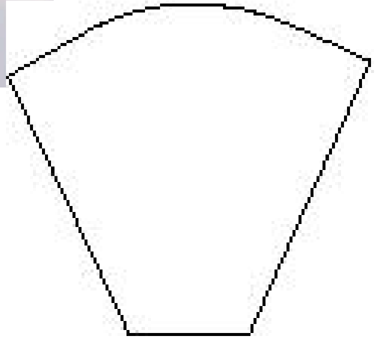

or combine a lens and mirror walls

Detector module design

SiPM array with light guides

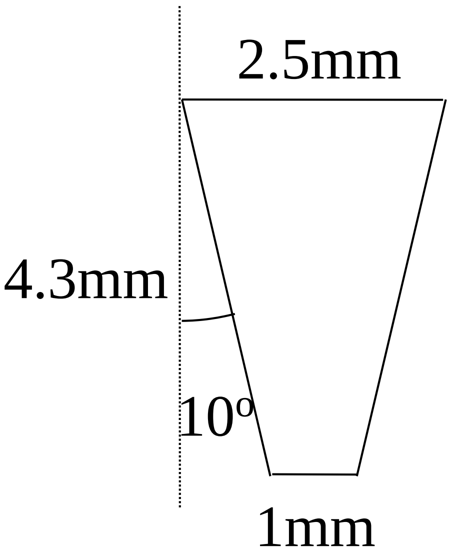

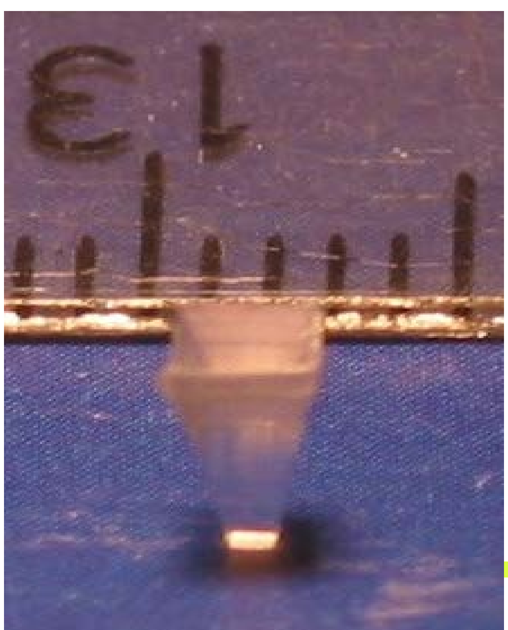

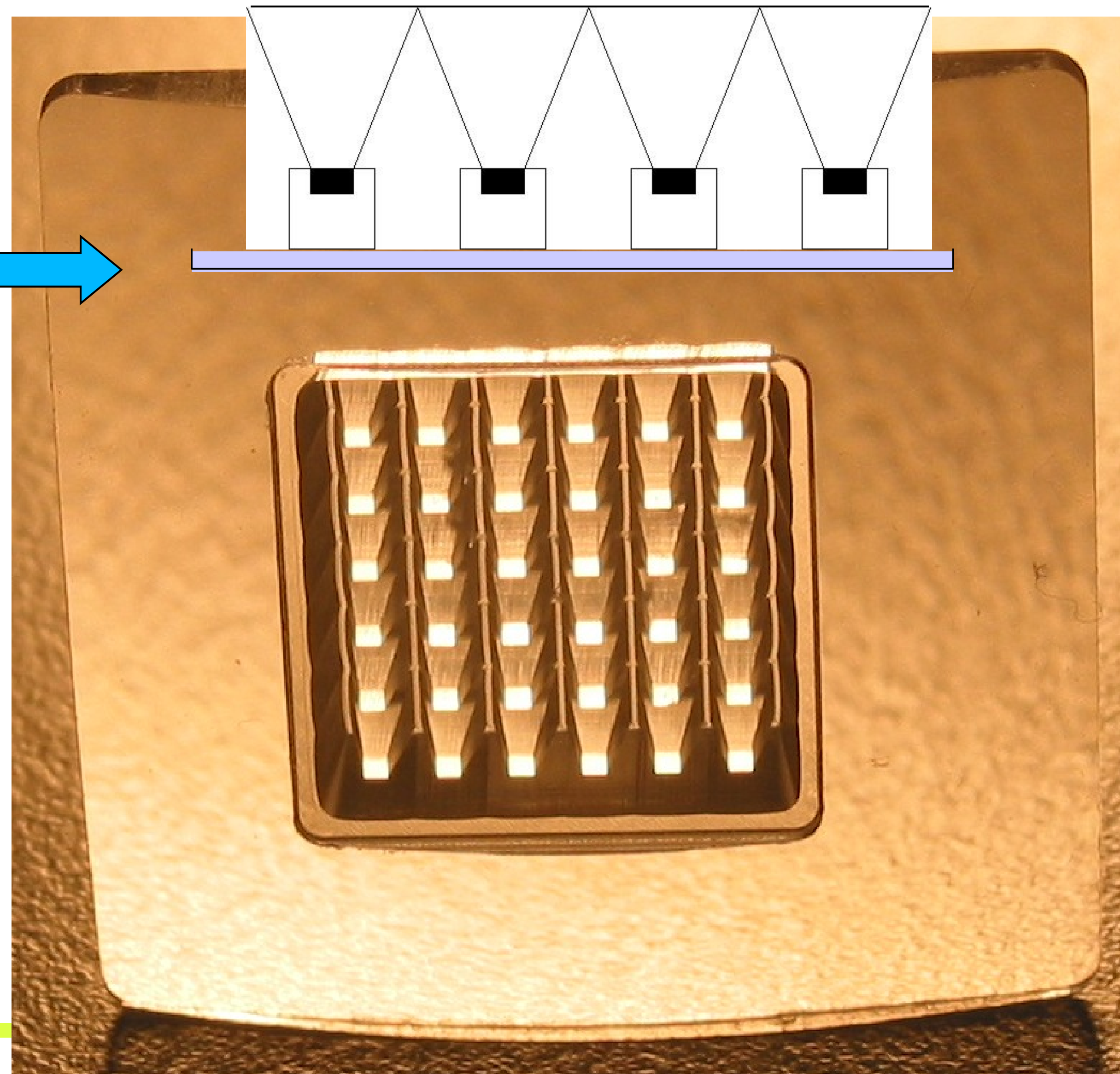

Photon detector with SiPMs and light guides

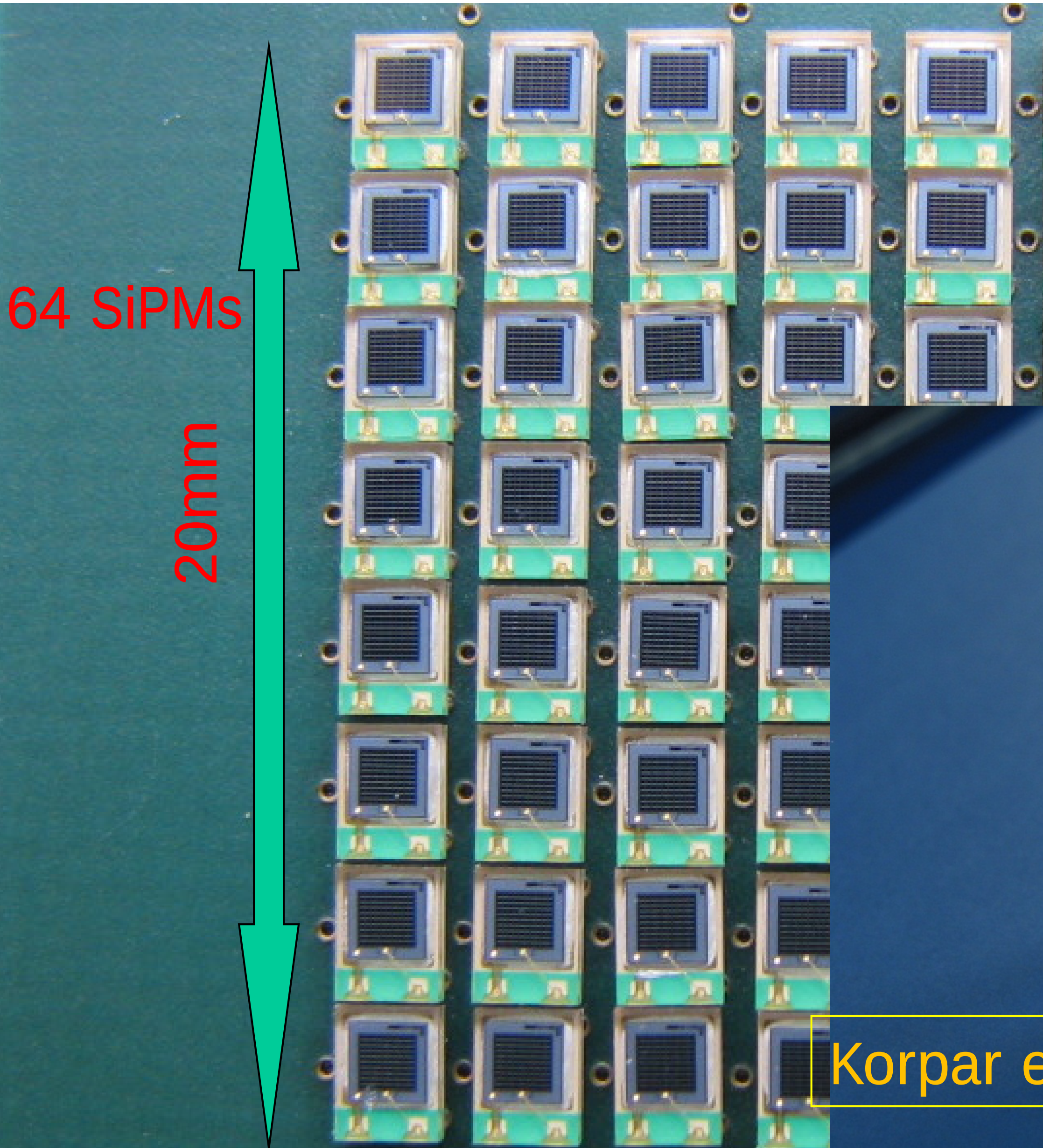

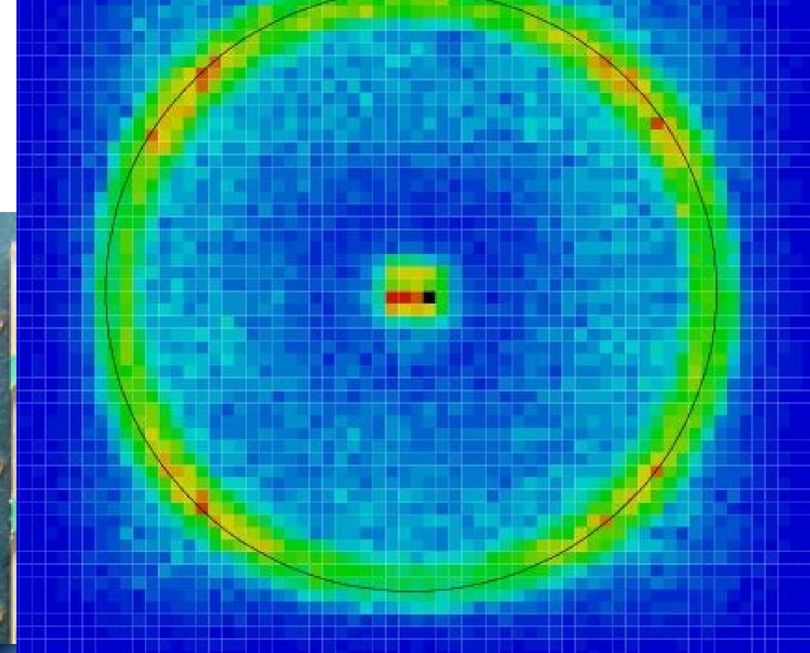

Full ring in a pion beam

Korpar et al., NIM A613 (2010) 195

A new SiPM device

Array of SiPMs: Hamamatsu MPPC S11834-3388DF

- A novel type of a multi-pixel Photon Counter (MPPC)
- 8x8 SiPM array, with 5x5 mm^2 SiPM channels
- Active area 3x3 mm^2
- Cell size: 50 μm
- Rather low dark count rate (~100 kHz/mm^2)
- Operating voltage: (70 ± 10) V

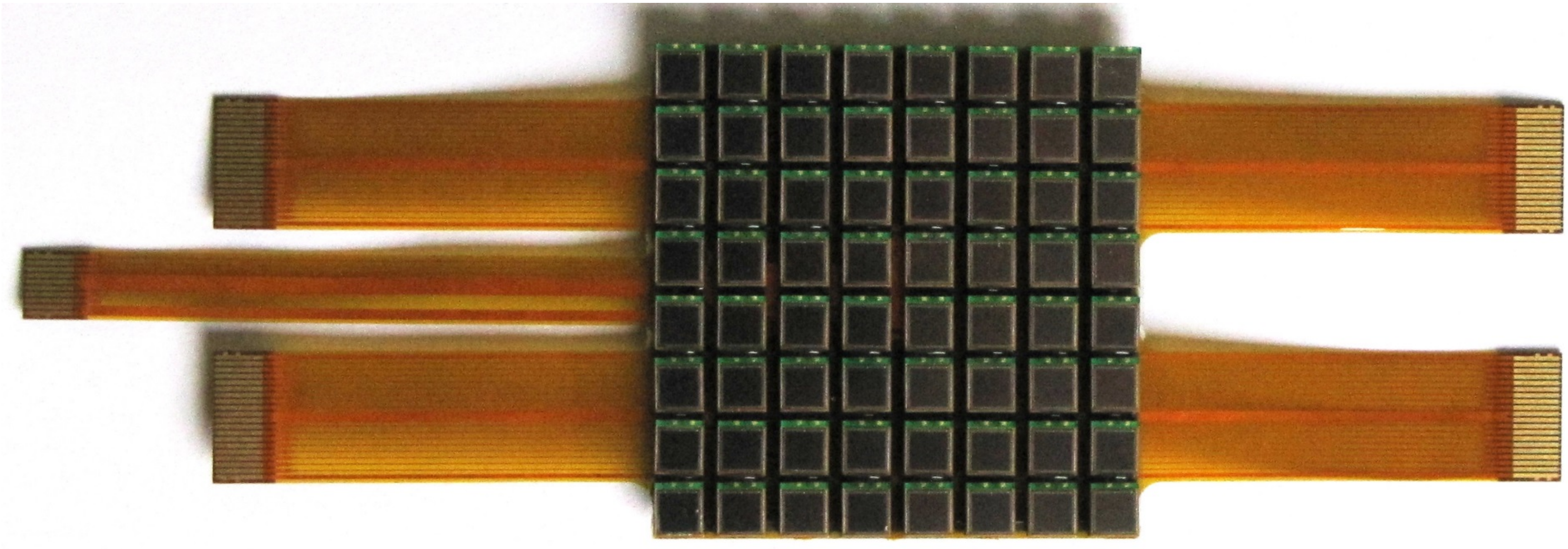

Detector module

Consists of the MPPC, light concentrator and support

Measured gain: ~3.5 x 10^5 @ 72.8 V

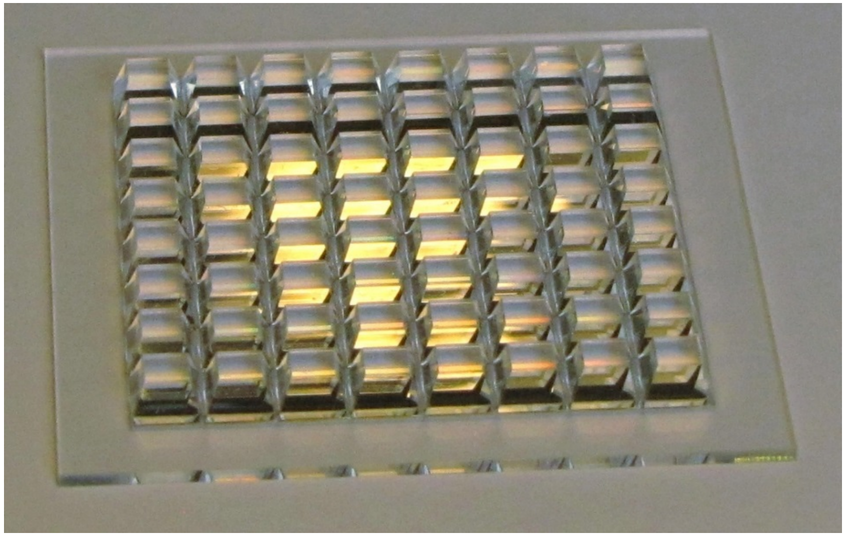

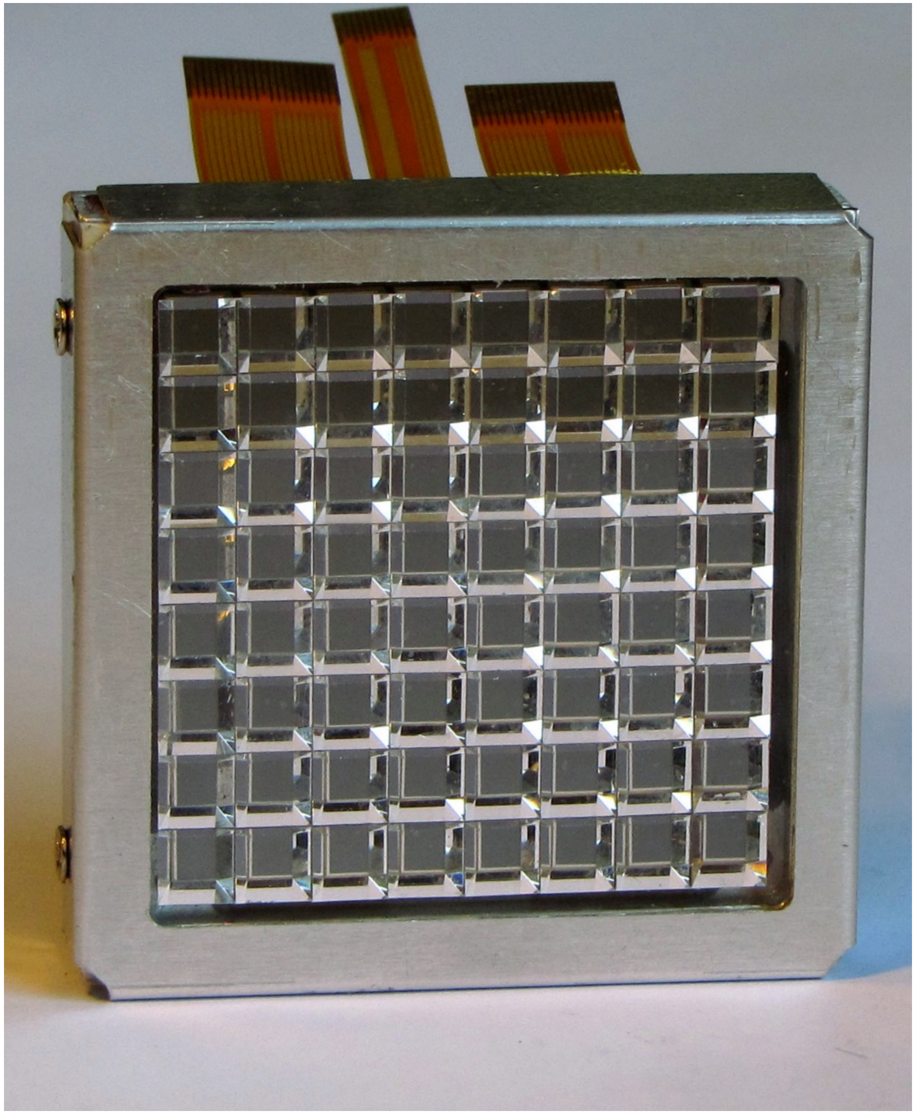

Pulse height distribution for low light levels

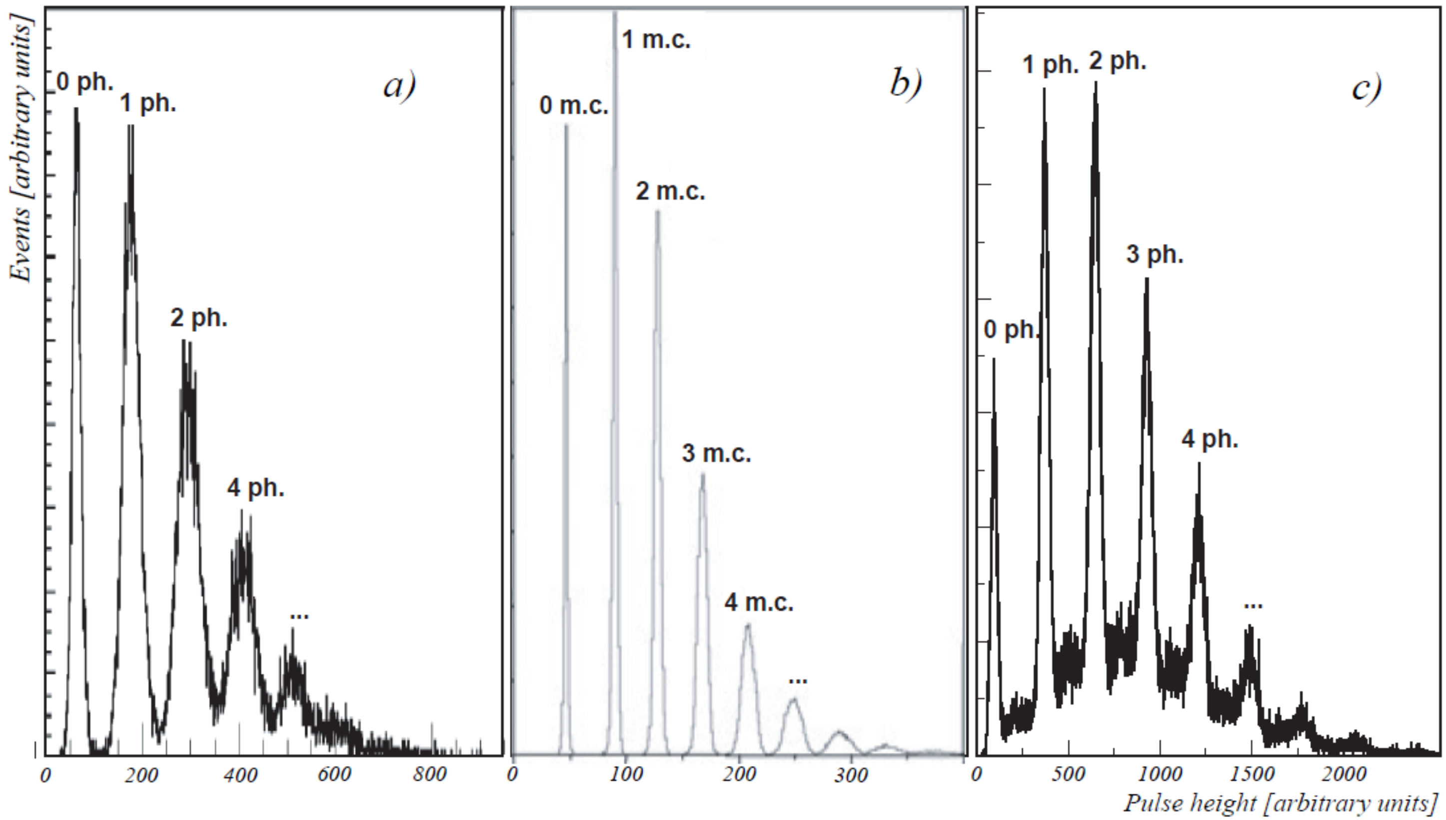

Figure 8: Pulse height spectrum of low intensity light pulses recorded with a VLPC (left, adopted from (20)), SiPM (middle, adopted from (21)) and HAPD (right)

SiPM: time resolution for single photons

Very fast analog SiPM

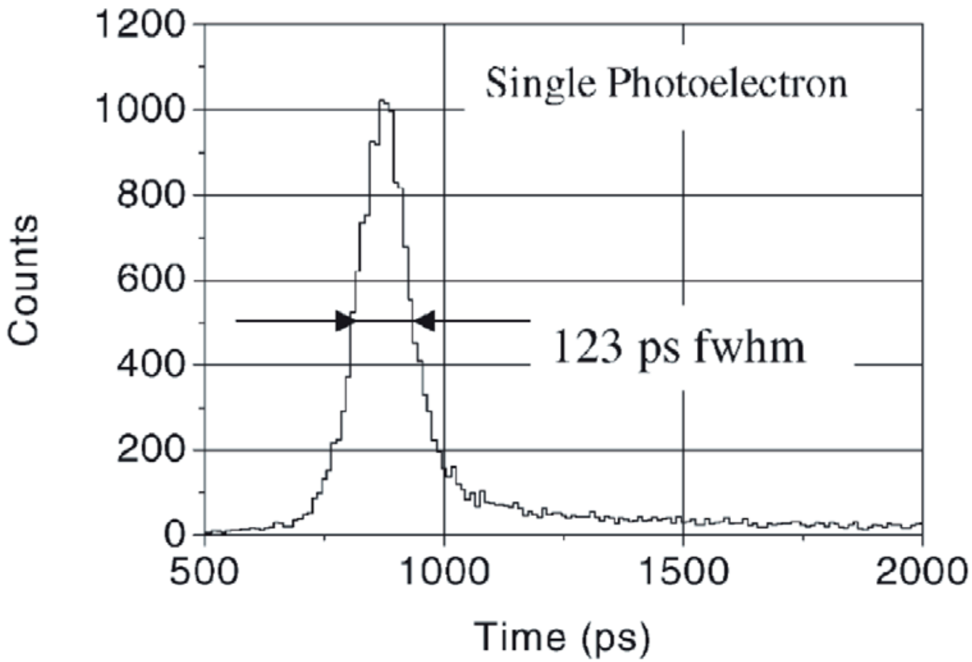

Digital SiPM

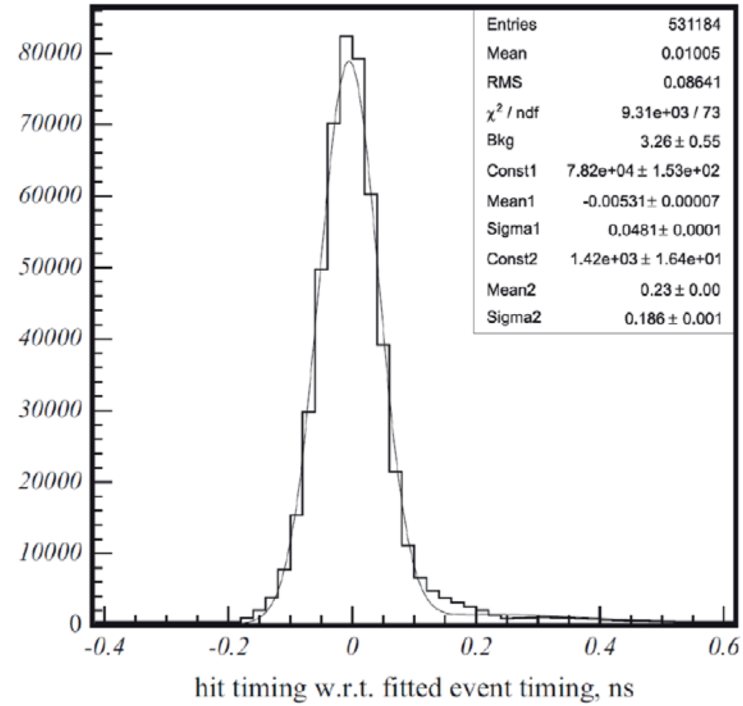

Analog SiPMs: typically 80 ps (sigma), 200 ps FWHM

Digital SiPMs: main peak 48 ps (sigma)!

New player: digital dSiPM

DPC: Front-end Digitization by Integration of SPAD & CMOS Electronics

analog SiPM

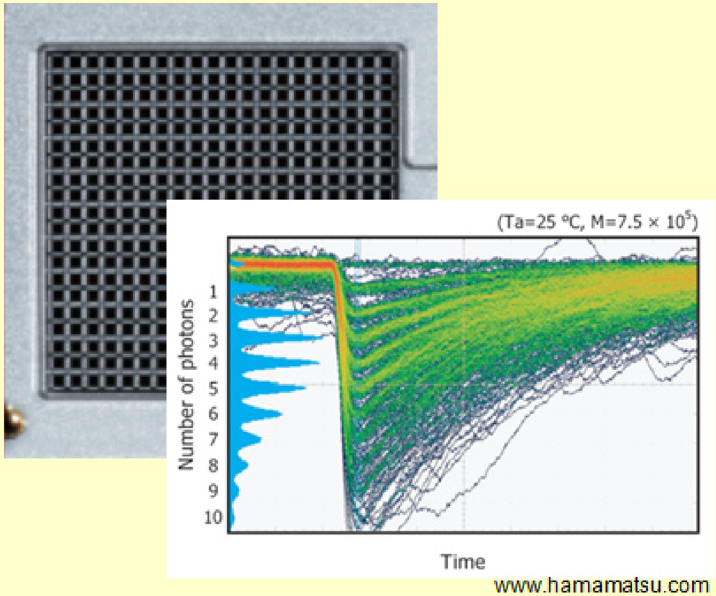

Summing all cell outputs leads to an analog output signal and limited performance

digital SiPM (dSiPM)

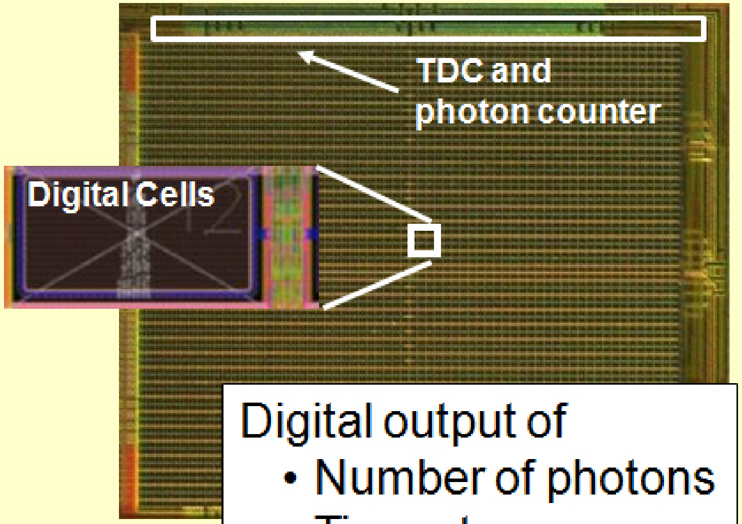

Digital output of

- Number of photons
- Time-stamp

Integrated readout electronics is the key element to superior detector performance

T. Frach, G. Prescher, C. Degenhardt, B. Zwaans, IEEE NSS/MIC (2010) pp.1722-1727
C. Degenhardt, T. Frach, B. Zwaans, R. de Gruyter, IEEE NSS/MIC (2010) pp.1954-1956

dSiPM in beam tests

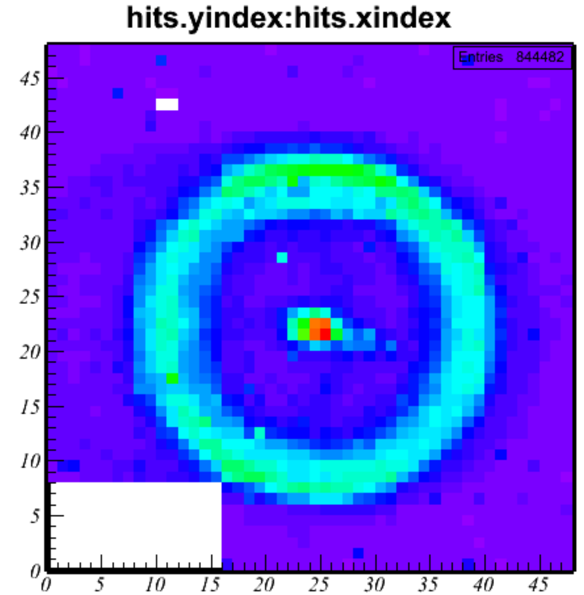

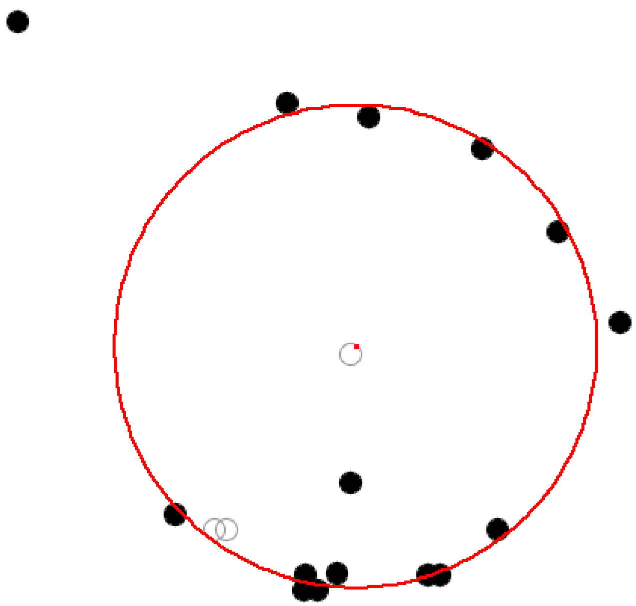

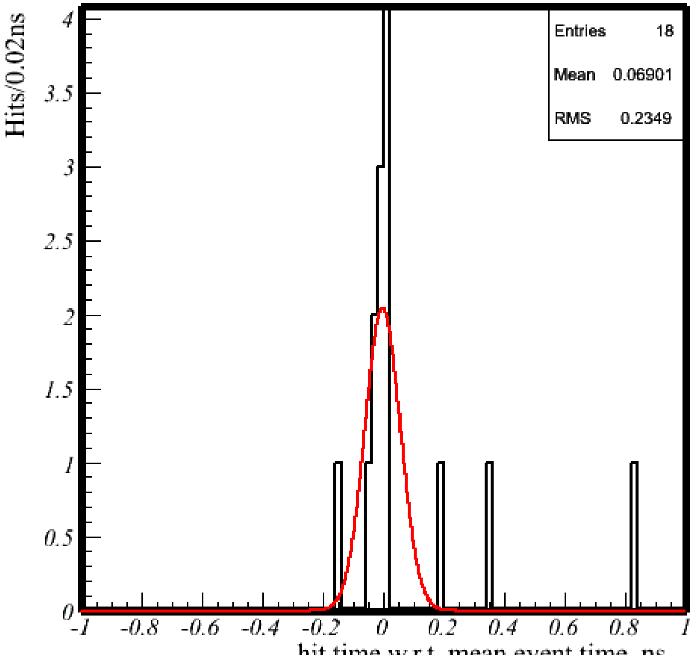

Radiation damage

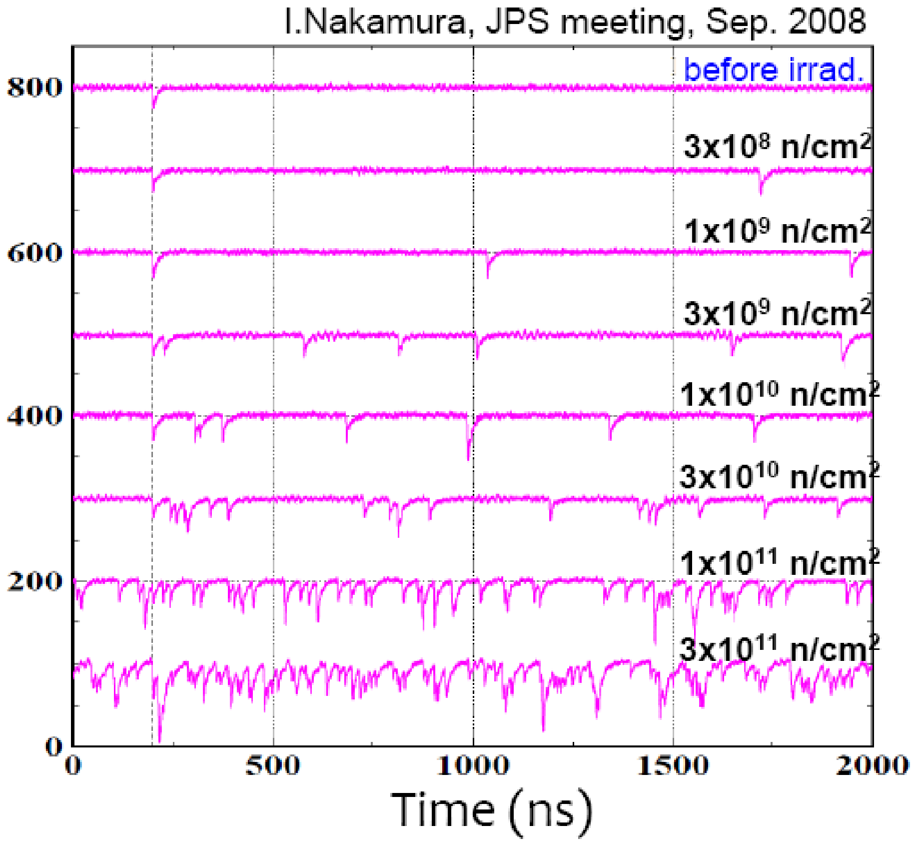

Expected fluence at 50/ab at Belle II: 2-20 10^{11} n cm^{-2}

→ Worst than the lowest line

→Very hard to use present SiPMs as single photon detectors in many applications (including Belle II) because of radiation damage by neutrons

→ Also: could only be used with a sofisticated electronics – wave-form sampling

Hybrid photodetectors

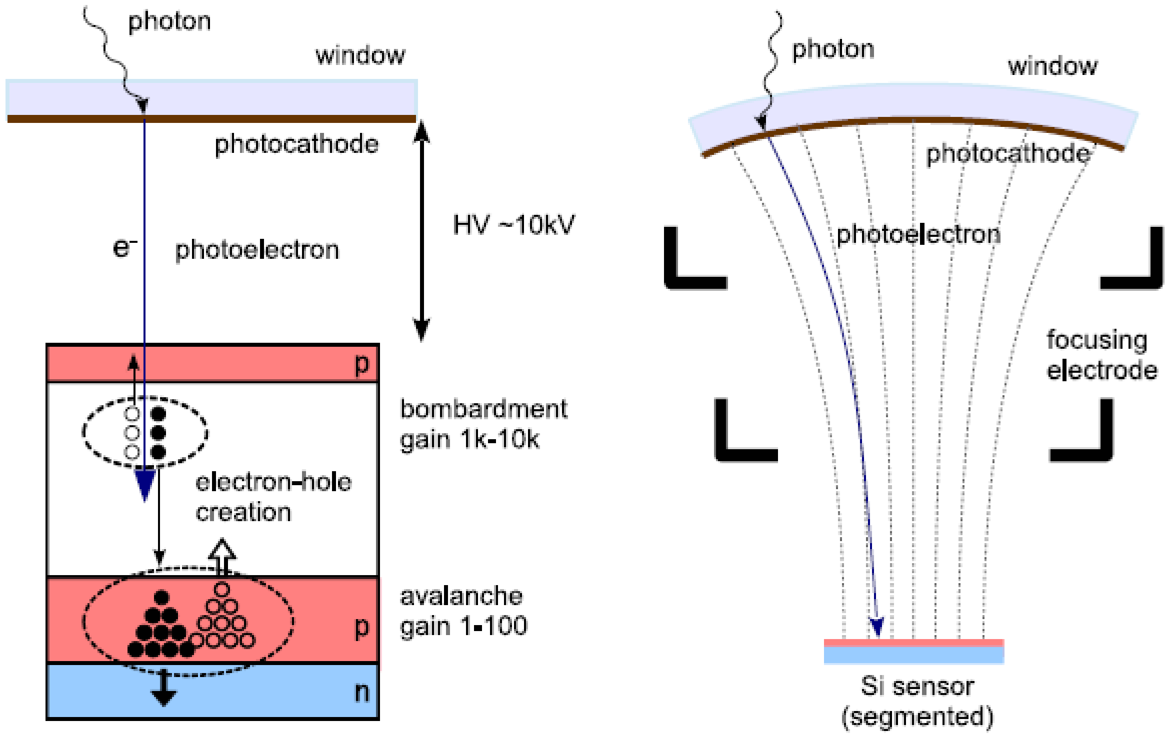

Hybrid photodetector: LHCb RICHes

Photon detector: hybrid PMT (R+D with DEP) with 5x demagnification (electrostatic focusing).

Hybrid PMT: accelerate photoelectrons in electric field (~20kV), detect it in a pixelated silicon detector.

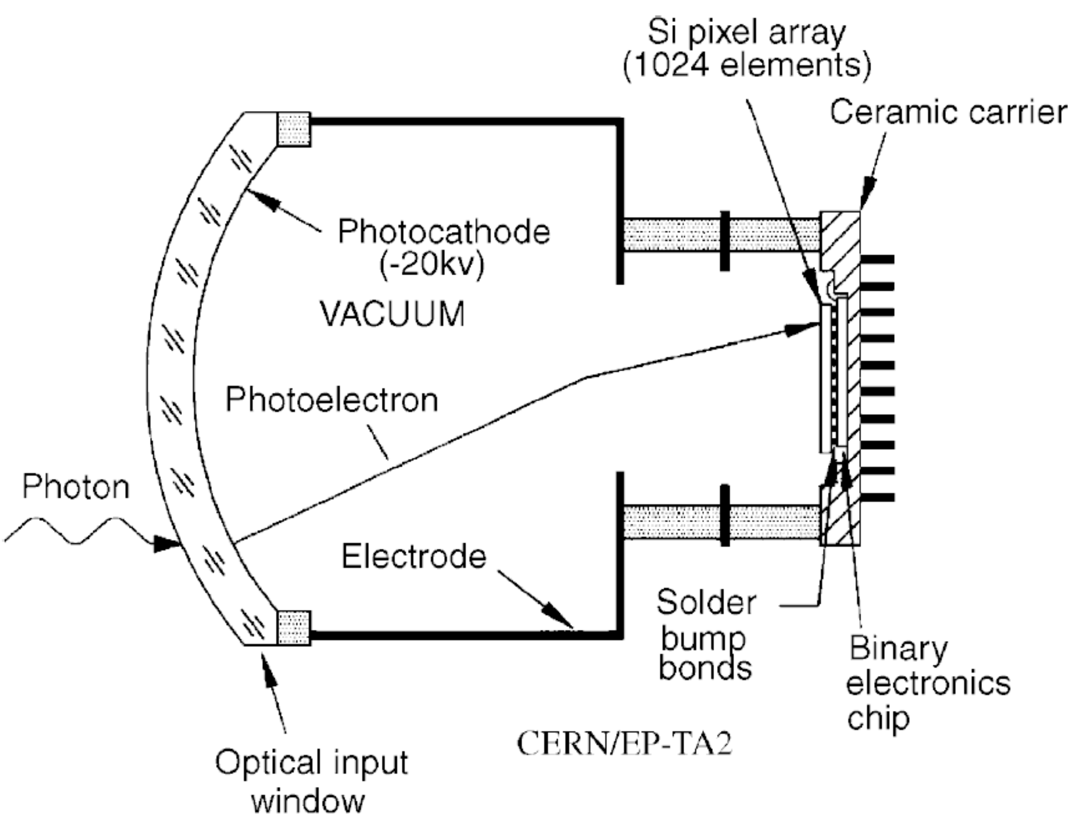

NIM A553 (2005) 333

Aerogel RICH

Need:
Operation in 1.5 T magnetic field
Pad size ~5-6mm

Photosensor: large active area HAPD of the proximity focusing type

Endcap PID: Aerogel RICH (ARICH)

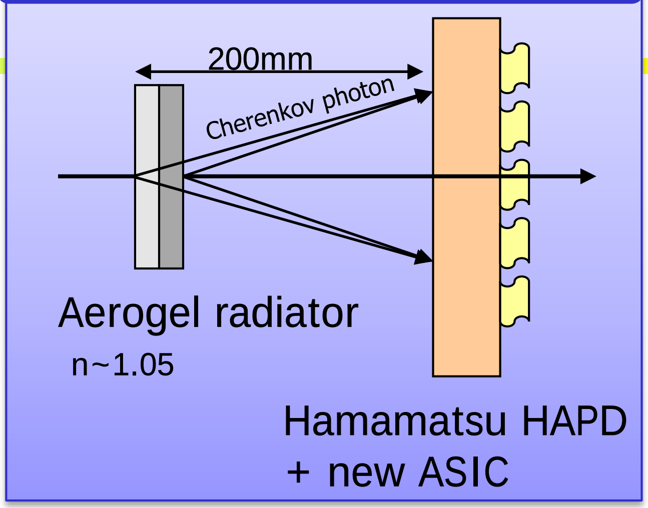

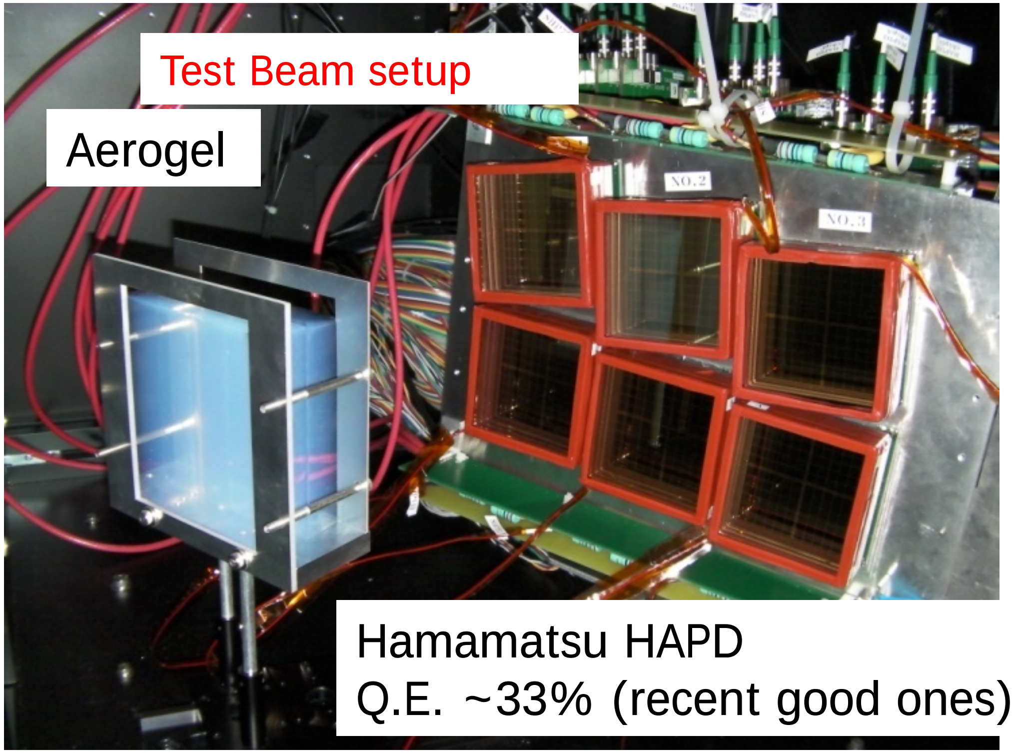

Clear Cherenkov image observed

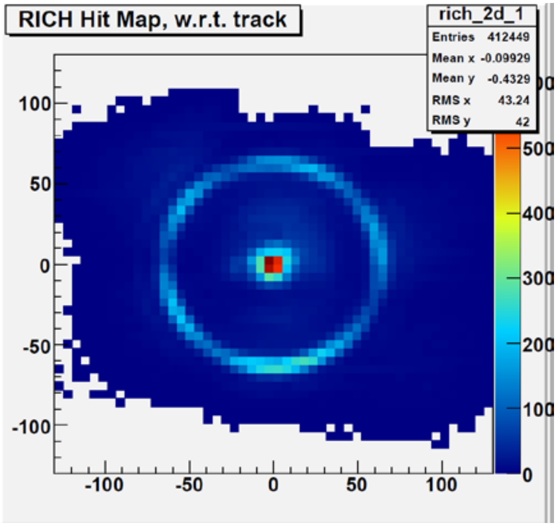

6.6 σ p/K at 4GeV/c !

→ NIM A595 (2008) 180

ARICH photon detector: HAPD

Hybrid avalanche photo-detector developed in cooperation with Hamamatsu Photonics K.K. (proximity focusing configuration):

- 12 x12 channels (~ 5 x 5 mm^2)
- size ~ 72 mm x 72 mm
- ~ 65% effective area
- total gain > 4.5x10^4 (two steps: bombardment > 1500, avalanche > 30)
- detector capacitance ~ 80pF/ch.
- super bialkali photocatode, typical peak QE ~ 28% (> 24%)
- works in mag. field (~ perpendicular to the entrance window)

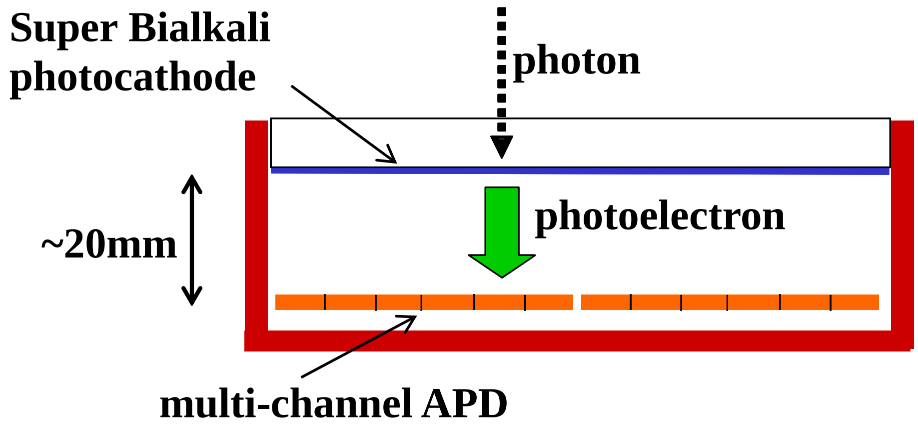

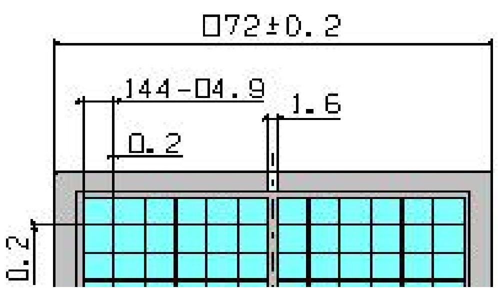

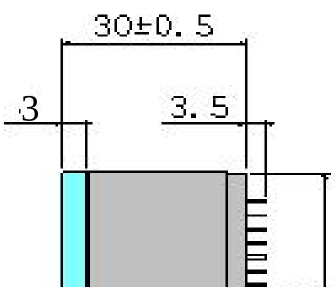

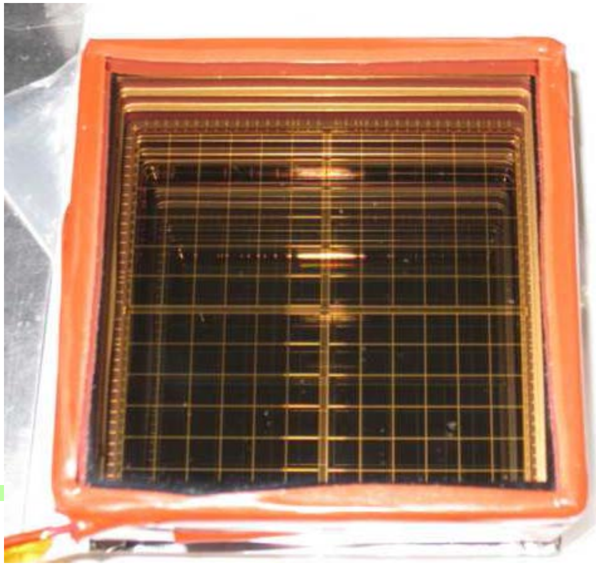

HAPD QE

- peak QE improved by Hamamatsu with super bialkali photocathode: 25% → >30%
- typically QE is somewhat lower at the edges of the HAPD

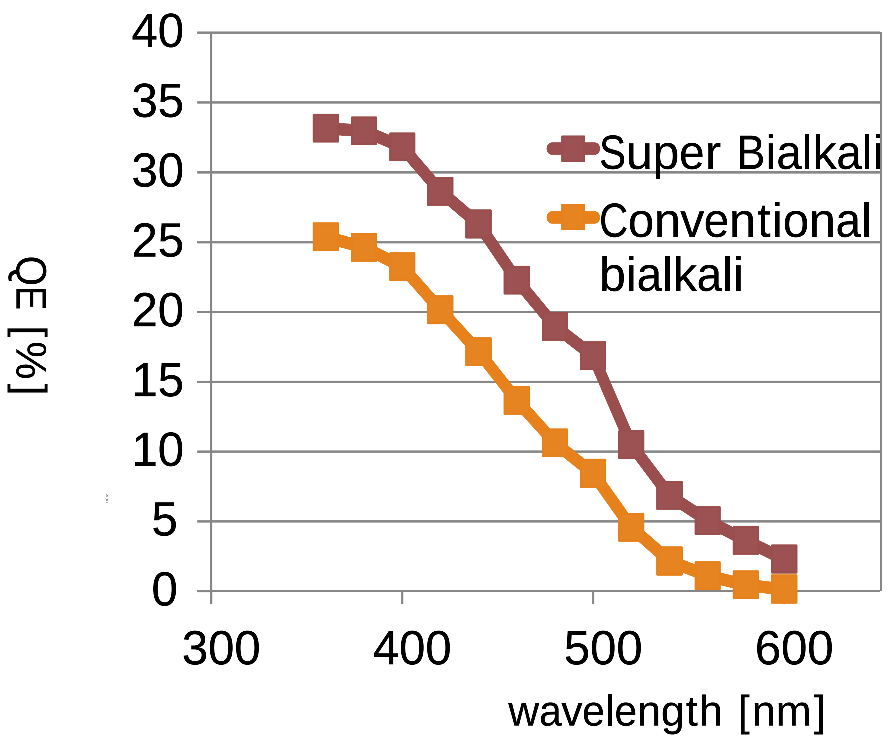

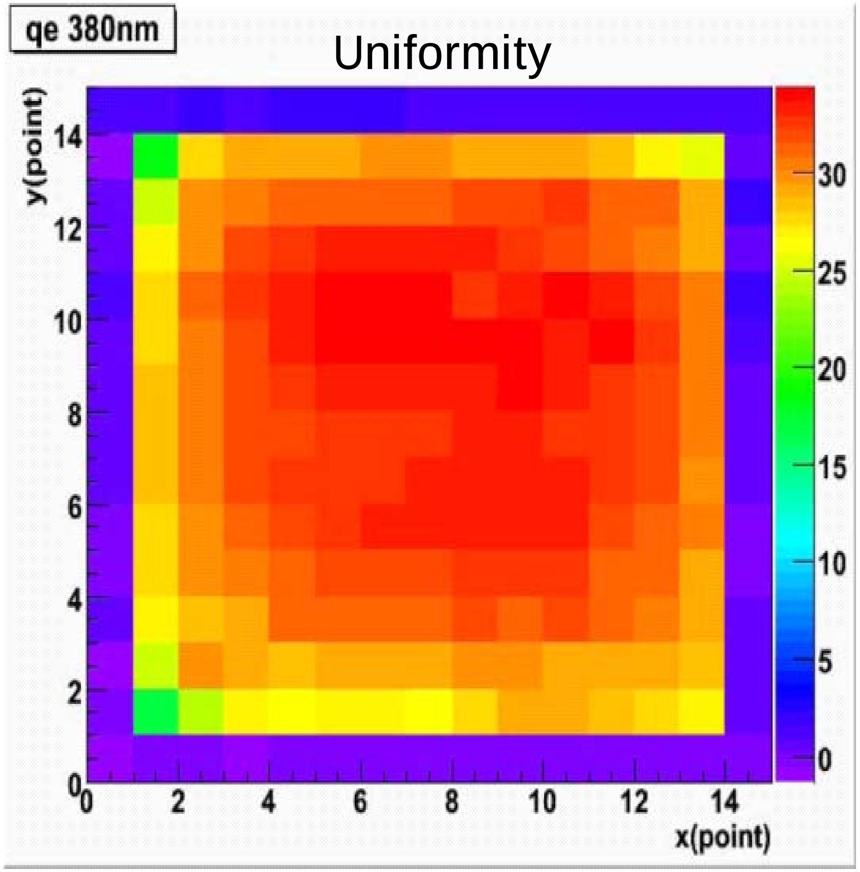

HAPD performance @ B=0T

- excellent photon counting affected only by photo-electron back-scattering → high single photon counting efficiency
- sharp transition between channels
- image distortion due to a non-uniform electric field at the edges
- back-scattering induced cross-talk
- optical cross-talk by reflection from APD surface → weak echo ring

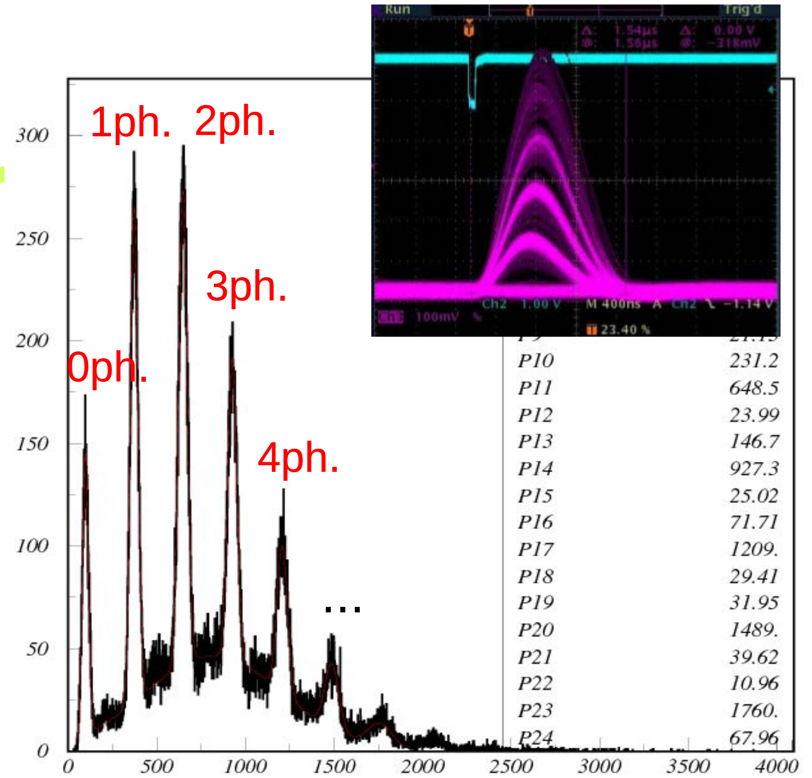

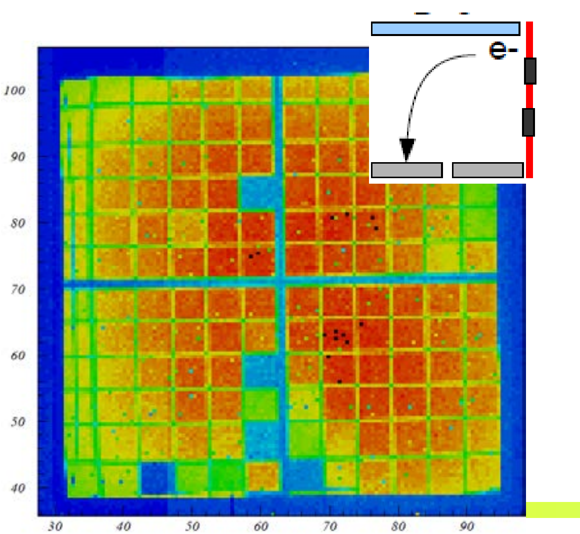

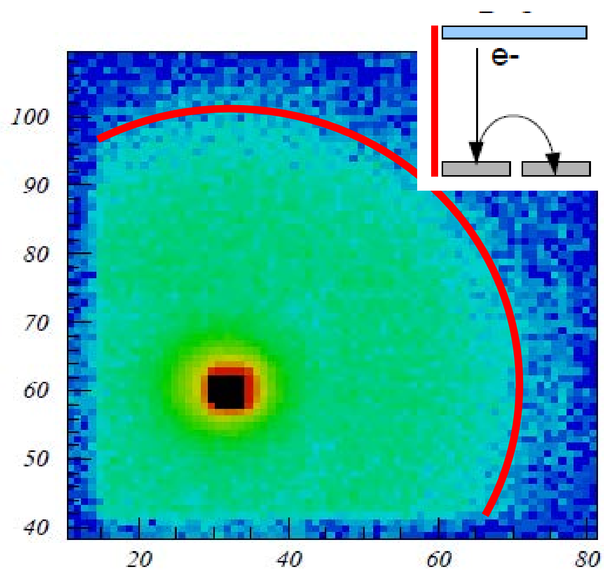

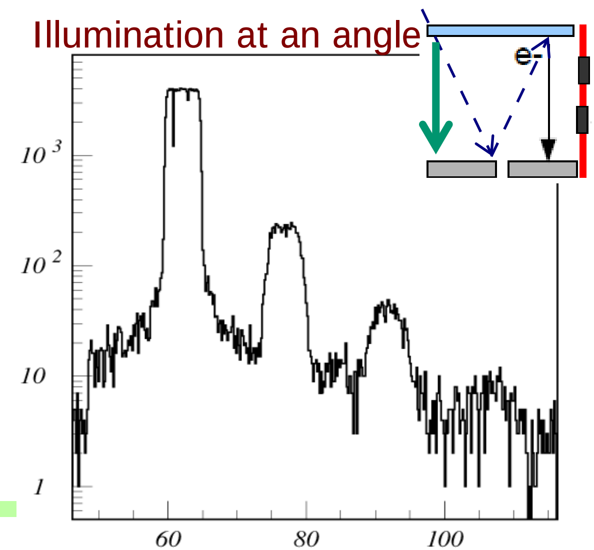

Another hybrid photo-detector: add a fast scintillator

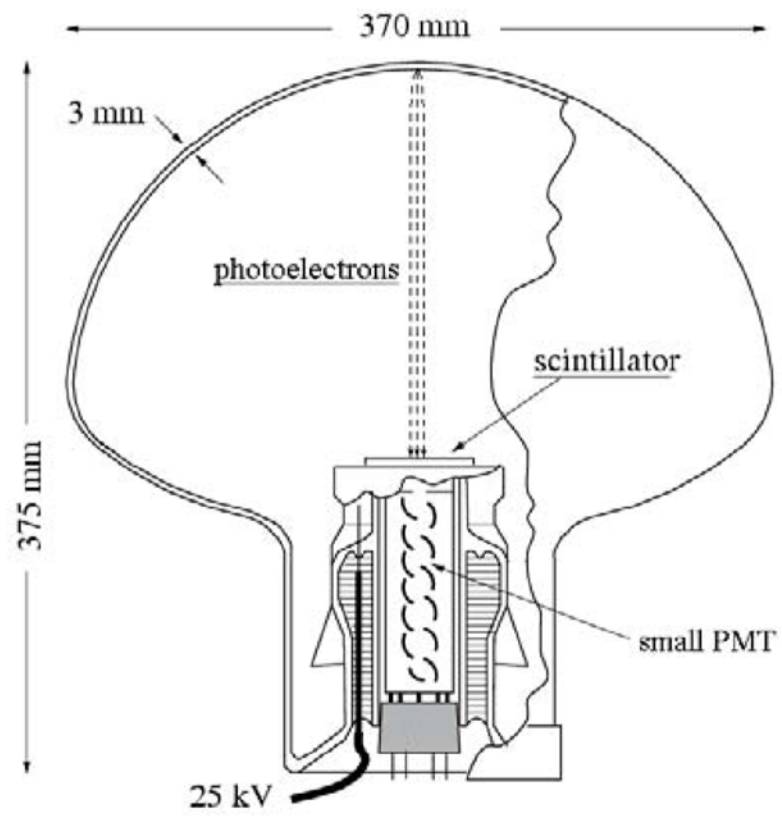

Figure 14: Hybrid photon detector with a scintillating crystal QUASAR-370 (31).

4) Gas chamber based photosensors

=MWPC + (TMAE, TEA or CsI)

gas additive to the MWPC gas

- -TEA ; E_{ion} =7.5 eV, p_n =5 tor, $\lambda \approx$ 0.6 mm pri 20^0C
- -TMAE; E_{ion}=5.4 eV, p_n==0.35tor, $\lambda \approx$ 23 mm pri 20^0C

CsI

- evaporate ≈500 nm onto the chamber cathode plane

Gas chamber based photosensors

Multiwire chamber with
cathode pad read-out:
→ short drift distances, fast detector

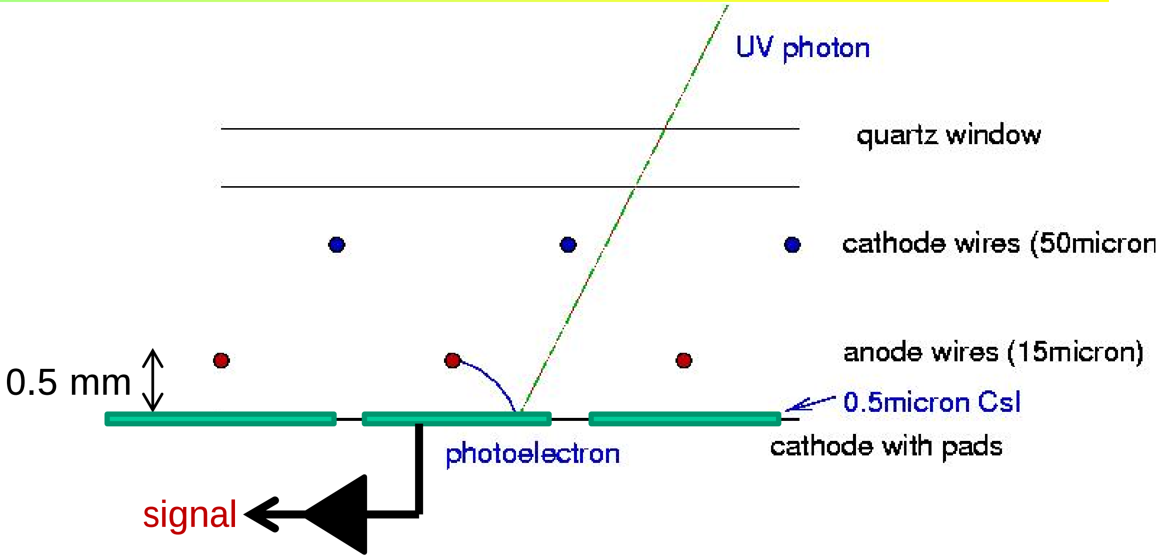

Photosensitive component:

•in the gas mixture (TEA): CLEOIII RICH

•or a layer on one of the cathodes (CsI on the printed circuit cathode with pads) →

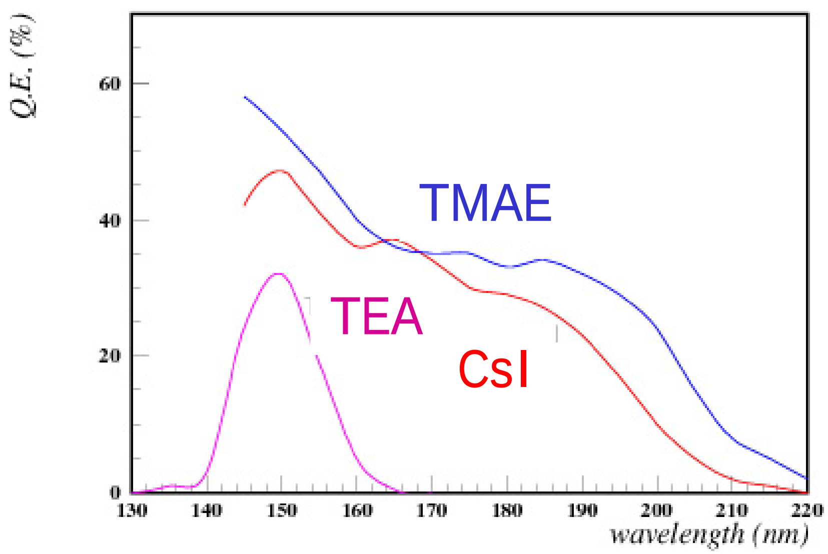

Works in high magnetic field!

CsI based RICH counters: HADES, COMPASS, ALICE

HADES and COMPASS RICH: gas radiator + CsI photocathode – long term experience in operation

ALICE:

- liquid radiator
- proximity focusing

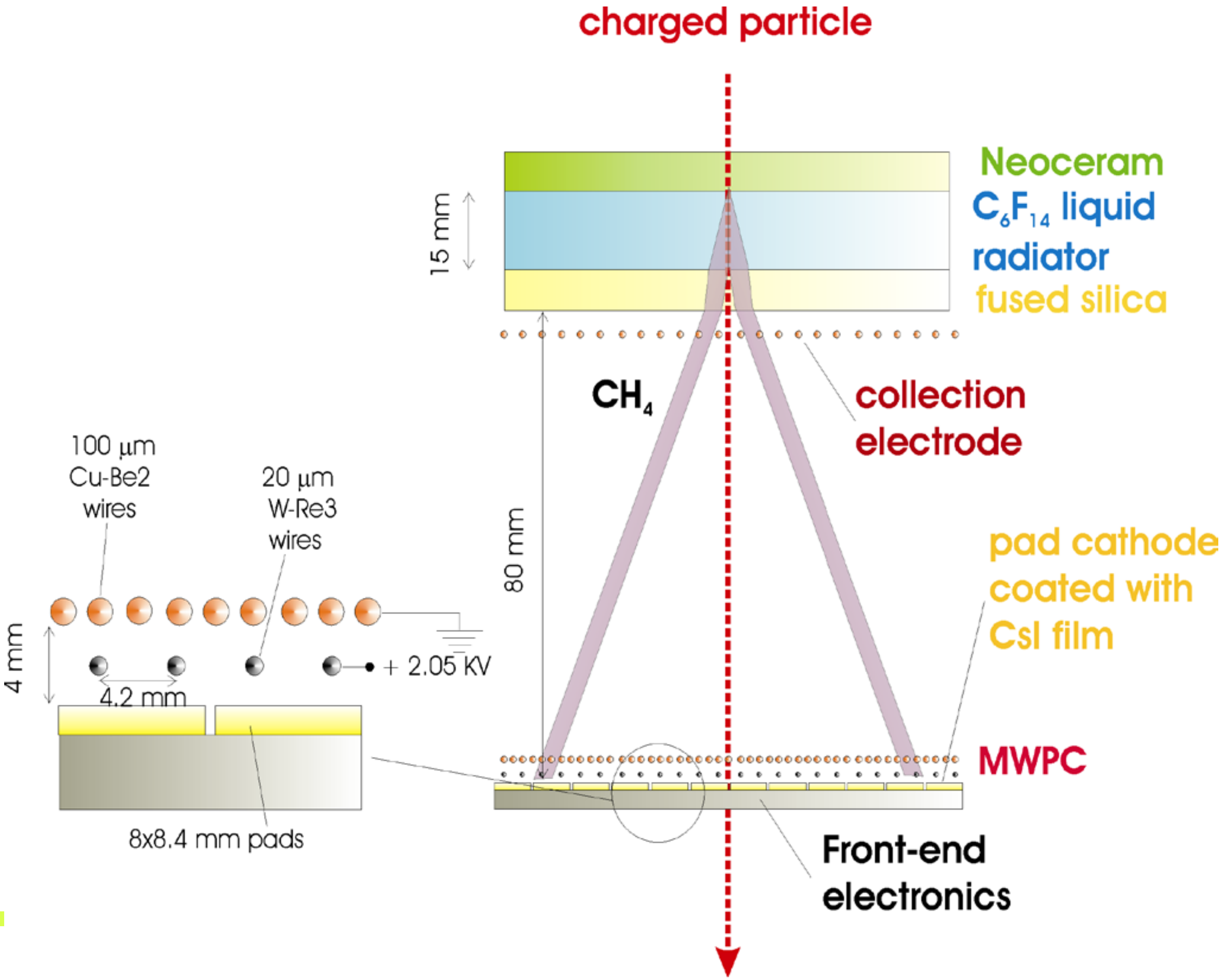

CERN CsI deposition plant

Photocathode produced with a well defined, several step procedure, with CsI vaccum deposition and subsequent heat conditioning

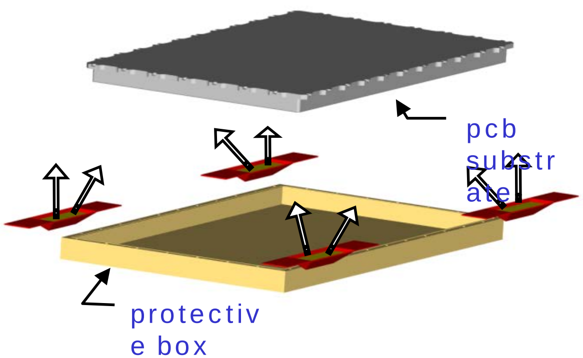

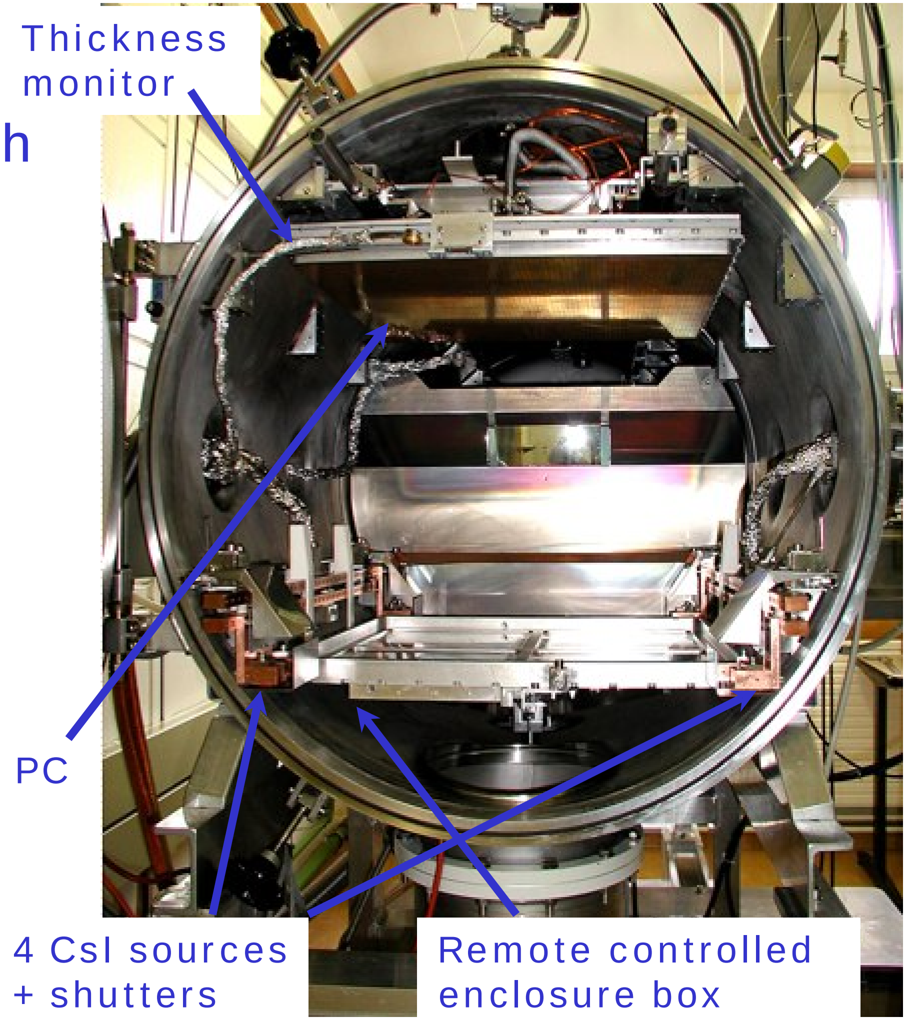

Examples of applications

HERA-B RICH

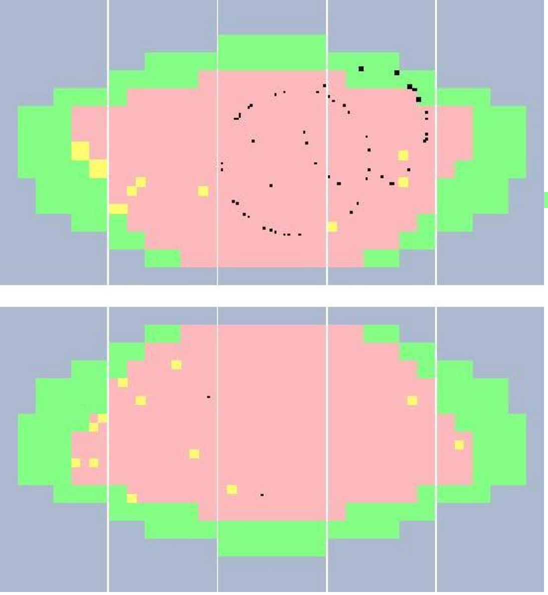

← Little noise, ~30 photons per ring

Typical event →

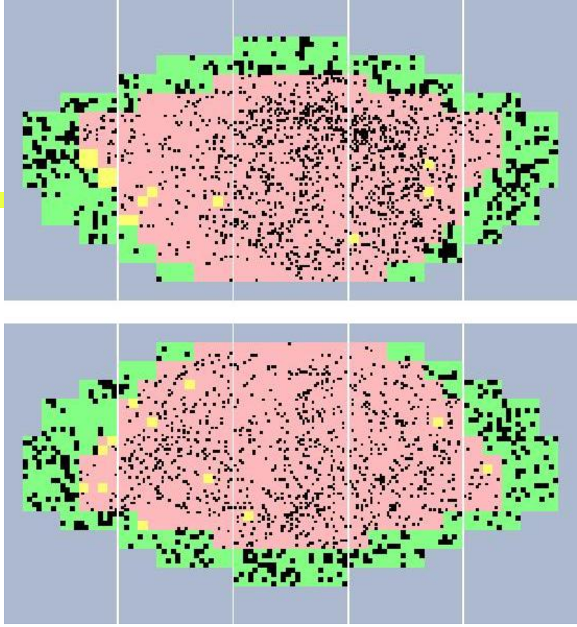

Very good performance:

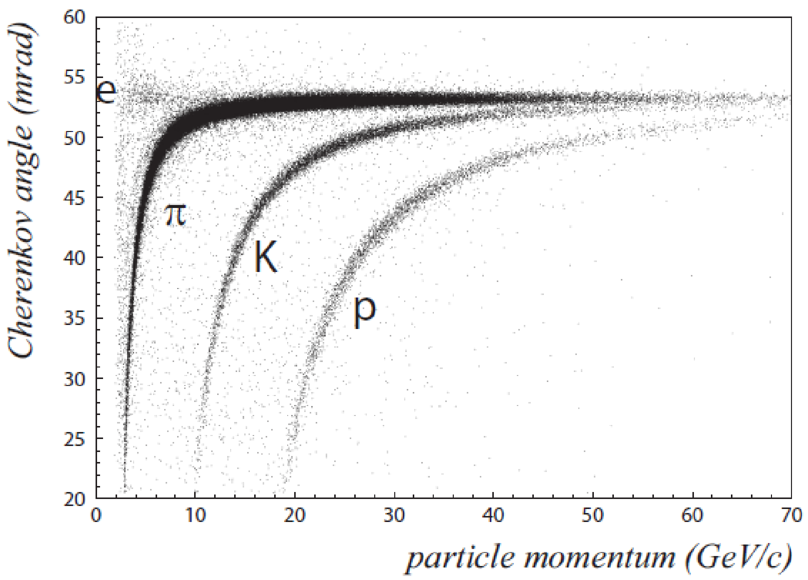

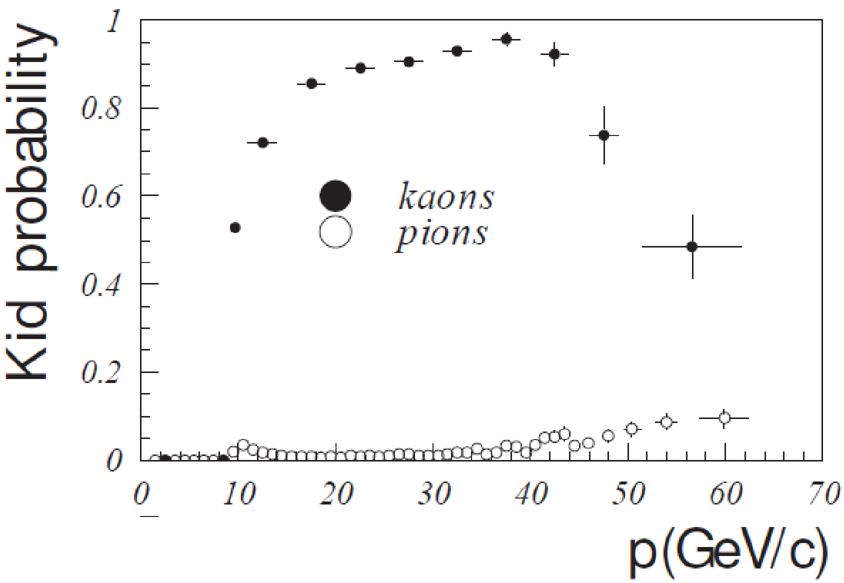

Kaon efficiency and pion fake probability

Belle II Cherenkov detectors

Barrel PID: Time of Propagation Counter (TOP)

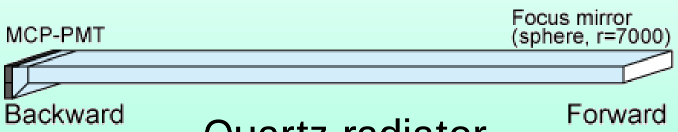

Quartz radiator

Focusing mirror

Small expansion block

Hamamatsu MCP-PMT (measure t, x and y)

Endcap PID: Aerogel RICH (ARICH)

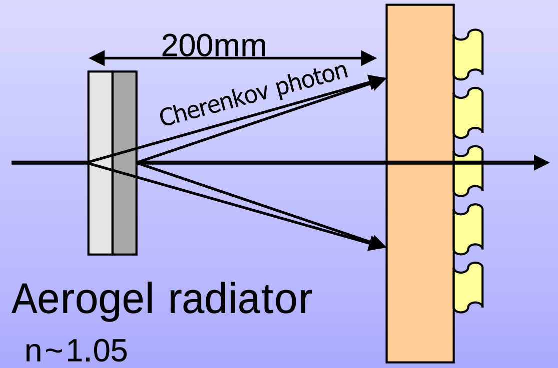

Aerogel radiator

n~1.05

Hamamatsu HAPD

+ new ASIC

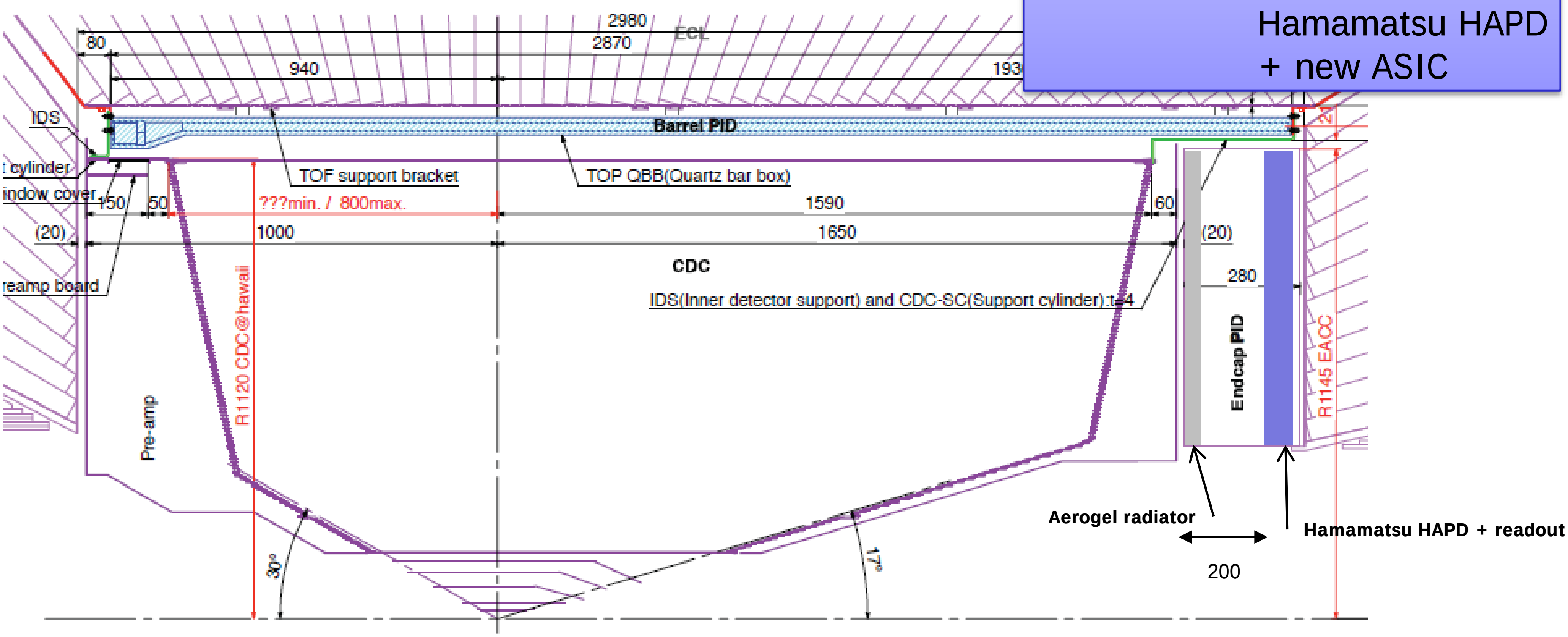

Time-Of-Propagation (TOP) counter

- Quartz radiator
  - With mirror and expansion block
- Mechanics, Quartz Bar Box (QBB)
- MCP-PMT + Readout electronics
  - 32 PMTs x 16ch = 512ch

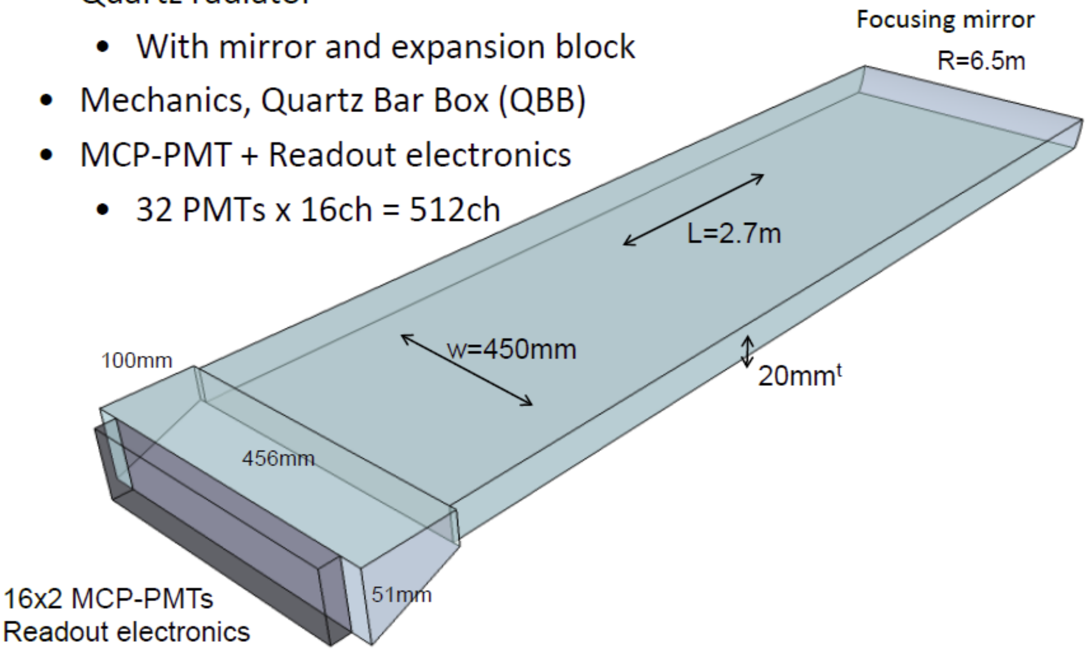

Hamamatsu
SL10 MCP-PMT

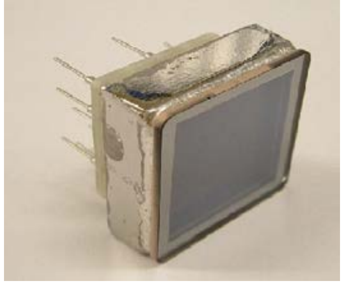

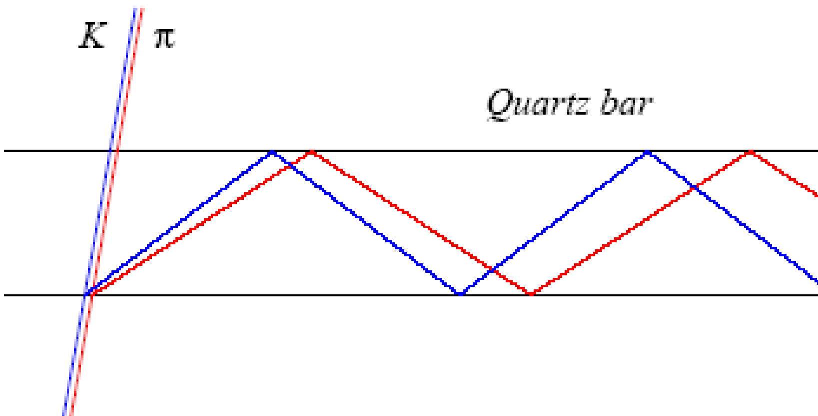

Instead of a 2D image in two coordinates ('ring') measure:

– One (or two coordinates) with a few mm precision

– Time-of-arrival

→ Excellent time resolution < 100ps (incl. read-out) required for single photons in 1.5T B field

TOP counter: principle of operation

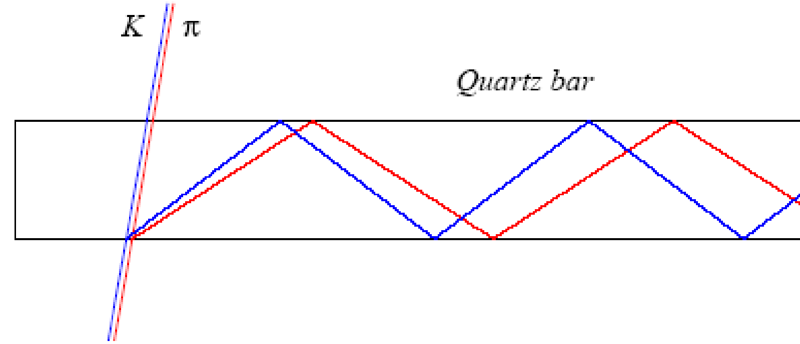

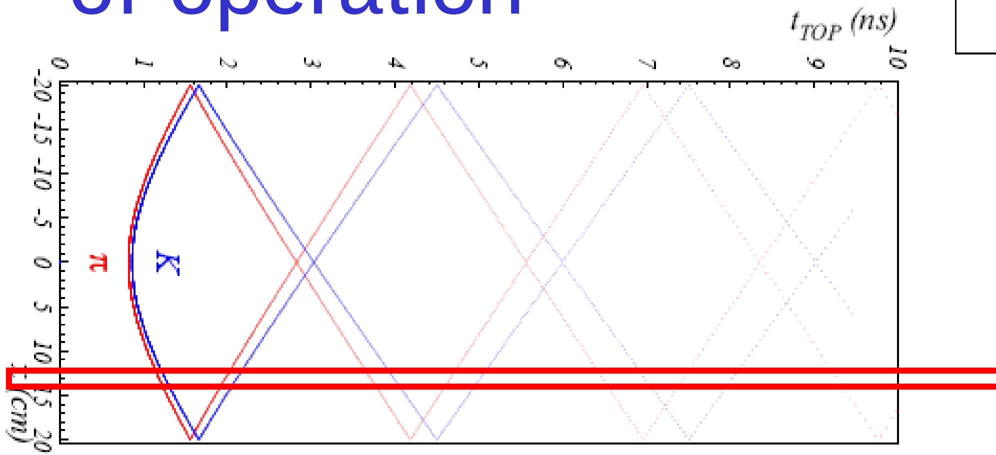

Pattern in the coordinate-time space ('ring') of a pion and a kaon hitting a quartz bar

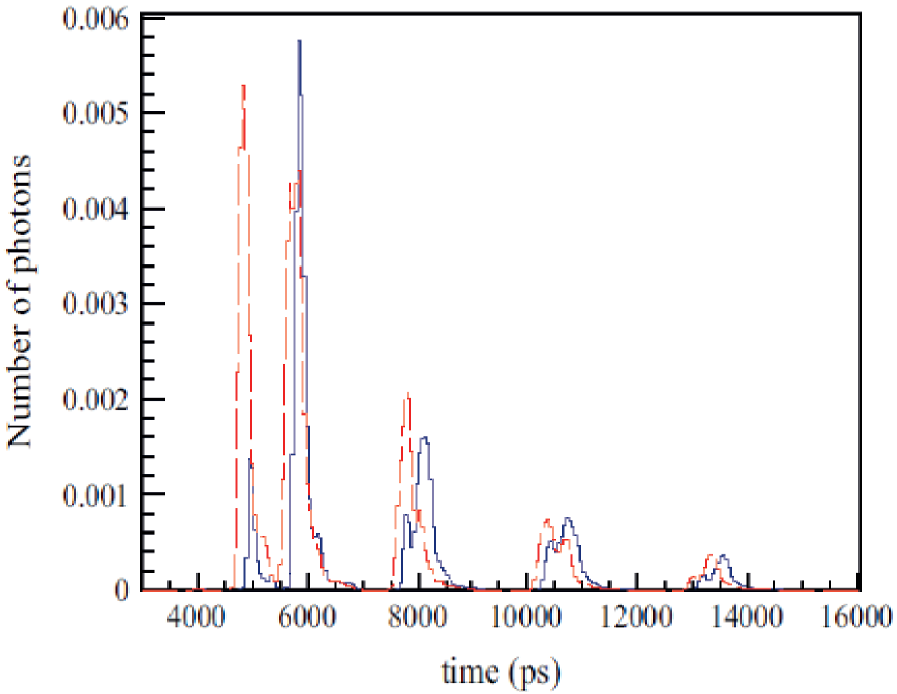

Time distribution of signals recorded by one of the PMT channels: different for π and K (~shifted in time)

Fast photon detection

New generation of Cherenkov counters: precise time information needed to further improve performance:

- Reduce chromatic abberation in a RICH detector (measure group velocity): Focusing DIRC
- Combine TOF and RICH techniques: TOP (Time-of-propagation counter), TORCH
- Dedicated TOF

New possibilities in medical imaging: TOFPET with Cherenkov light

→ Need photo sensors with excellent timing

DIRC counters for PANDA (FAIR, GSI)

Two DIRC-like counters are under preparation for the PANDA experiment

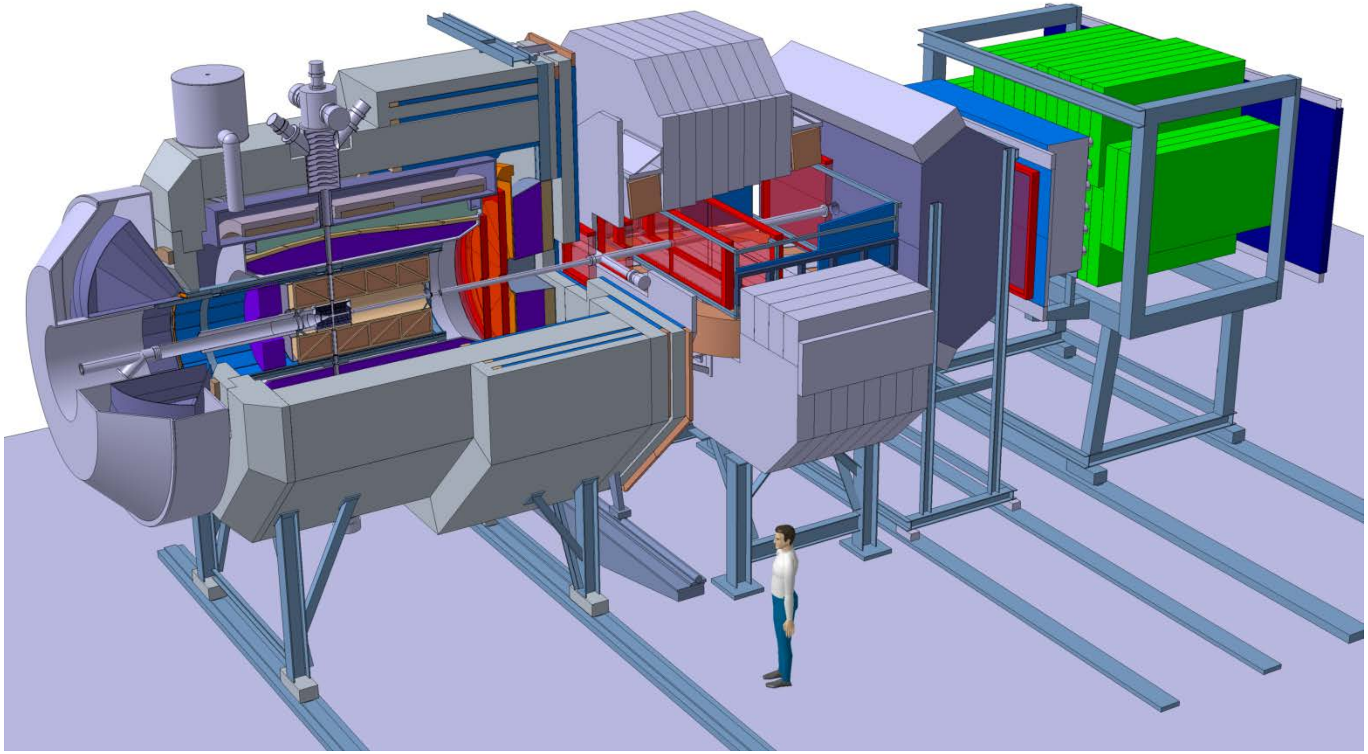

PANDA barrel DIRC

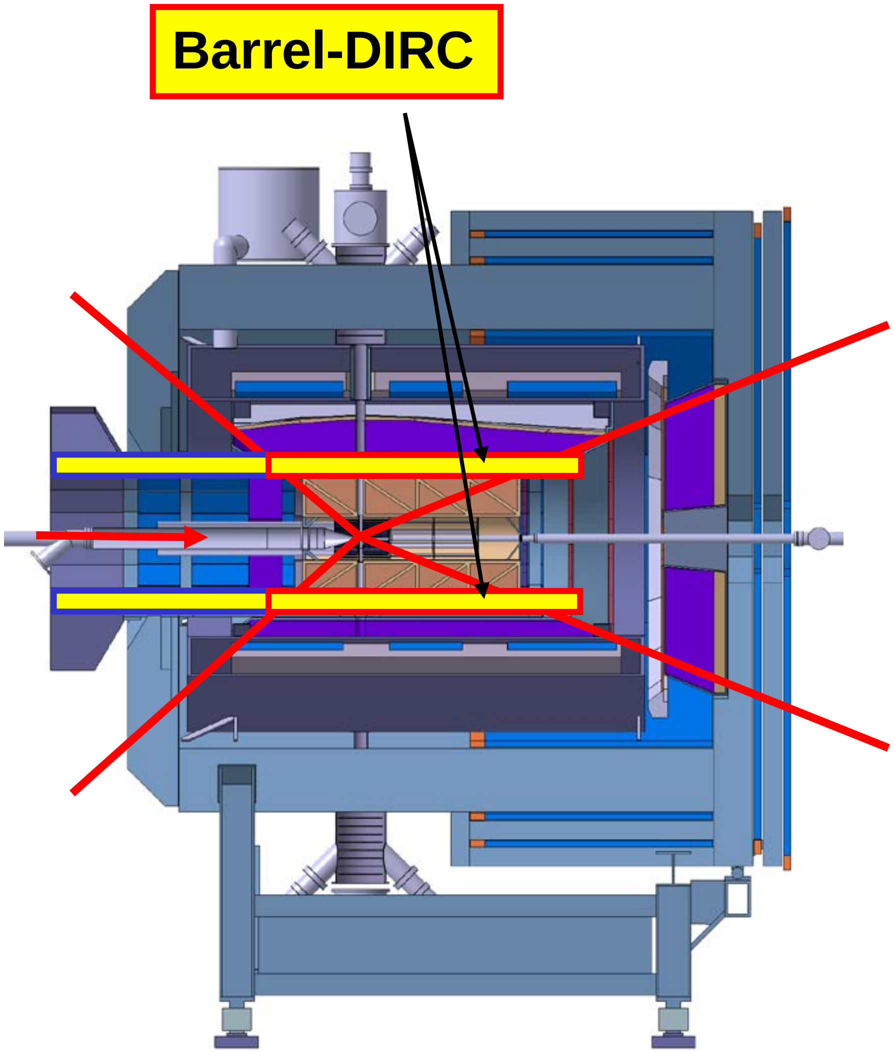

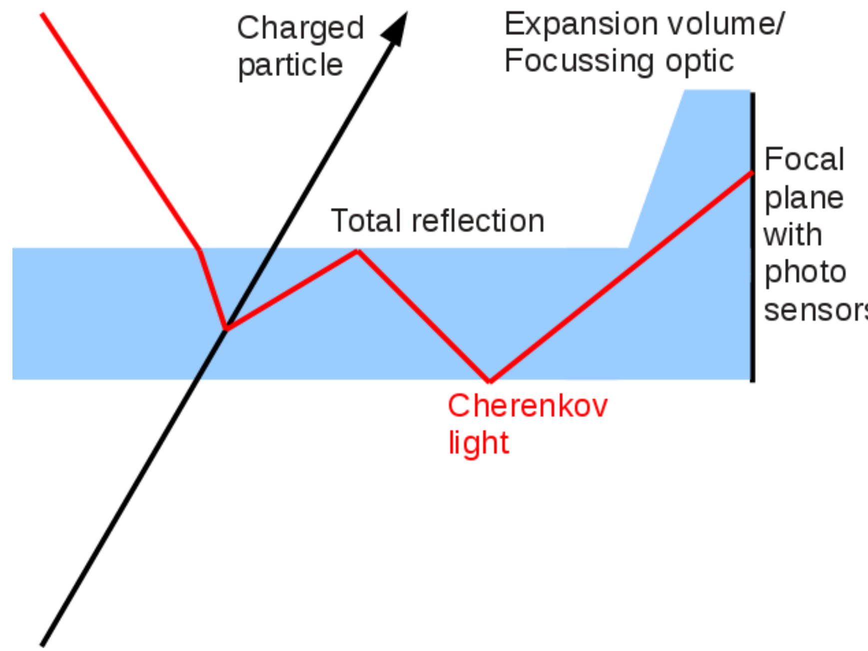

PANDA endcap DIRC

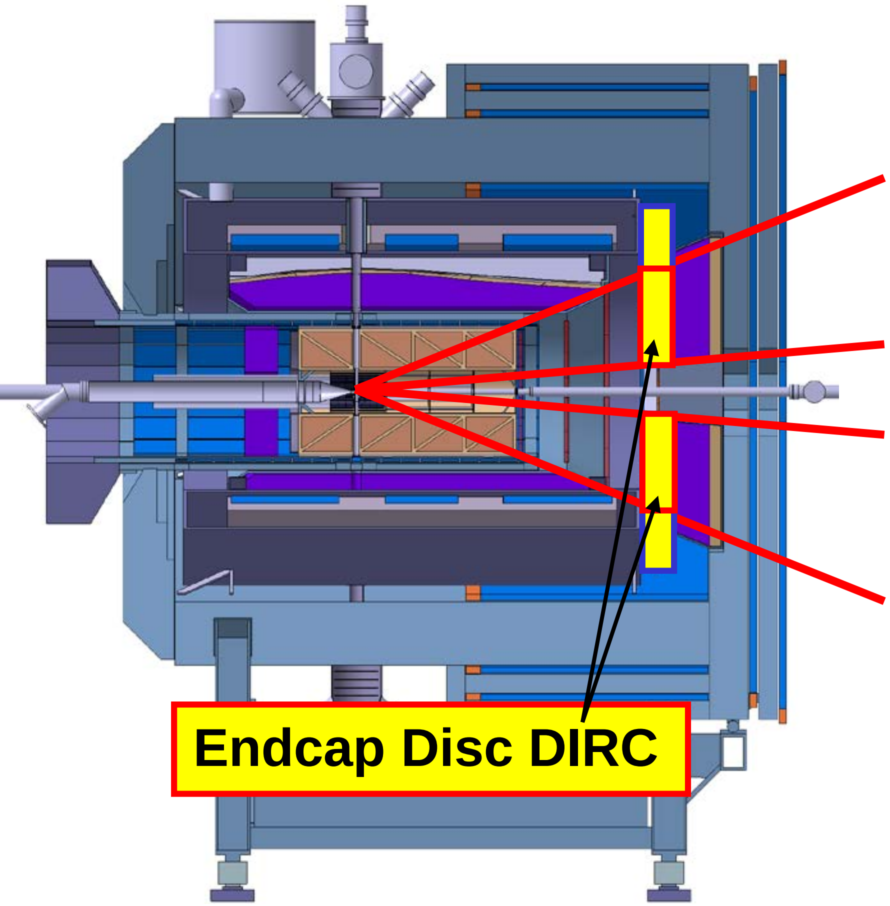

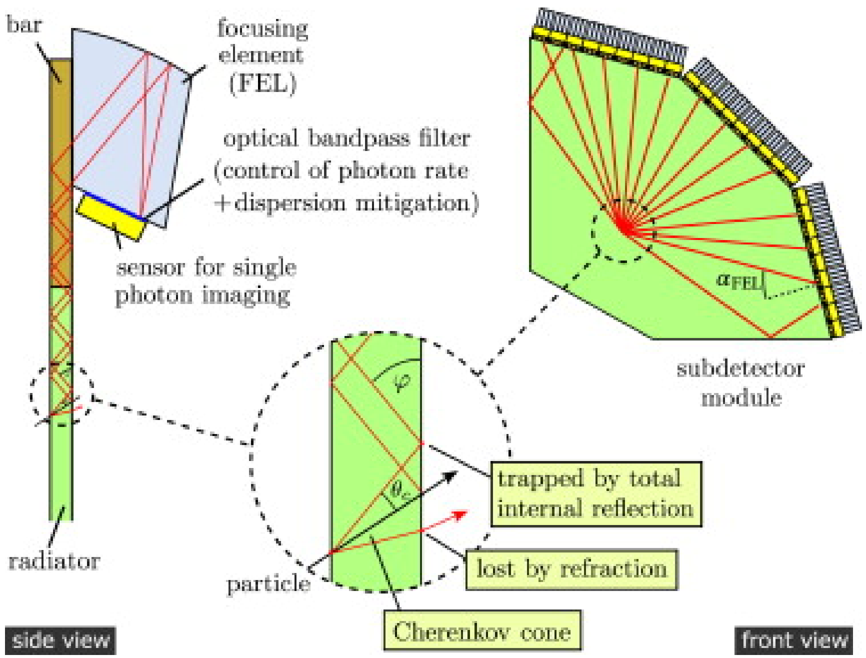

LHCb PID upgrade: TORCH

A special type of Time-of-Propagation counter for the LHCb upgrade

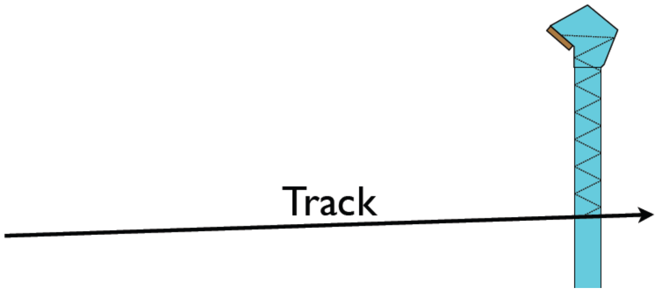

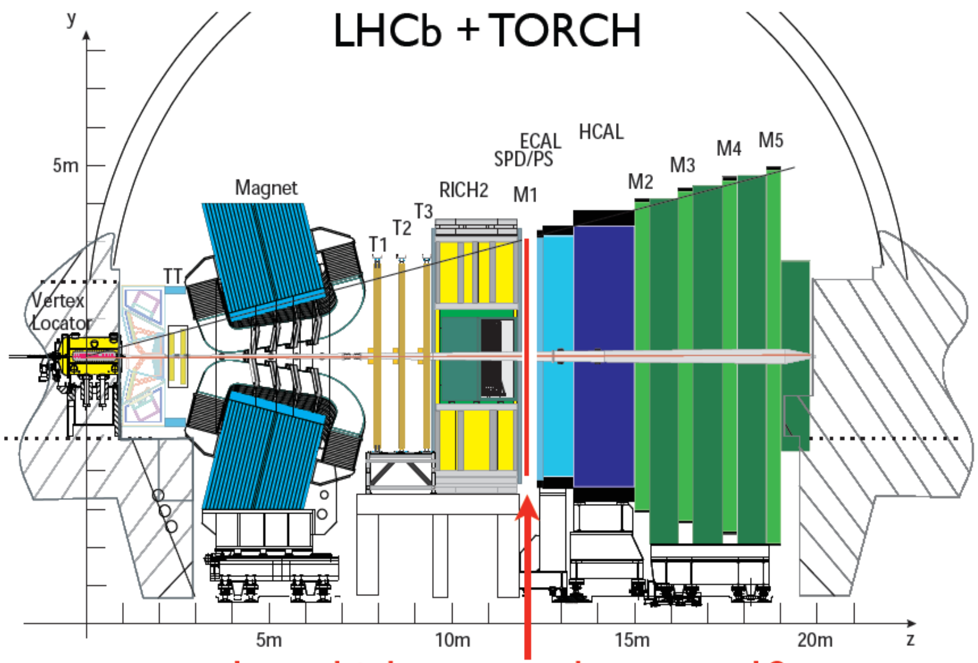

1cm-thick quartz plate at z=12m

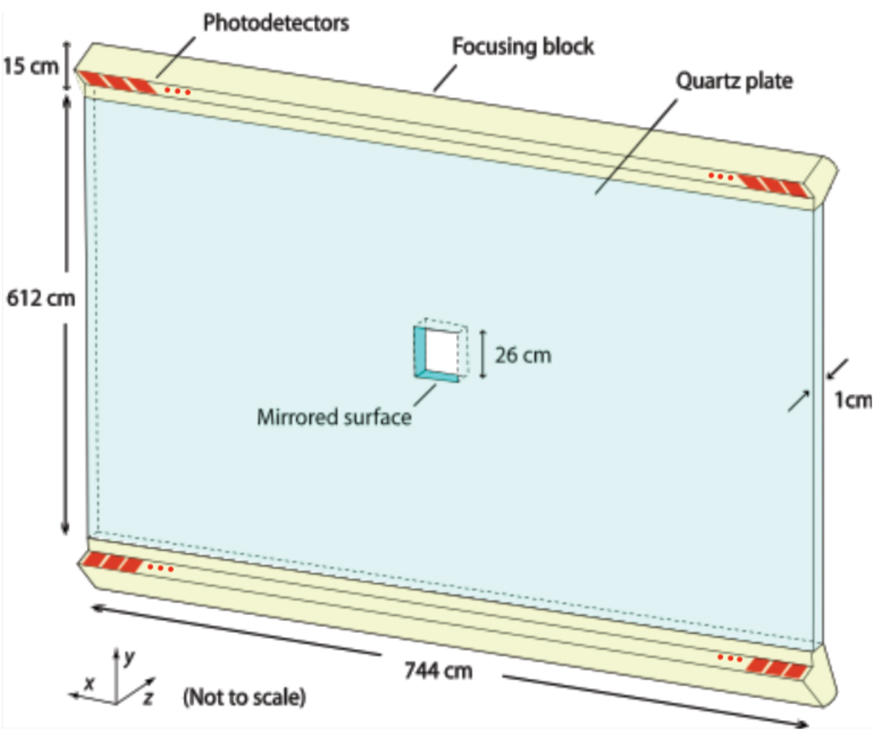

Sides are instrumented too (not shown)

New possibilities in medical imaging: TOFPET with Cherenkov light

Time-of-Flight difference of annihilation gammas is used to improve the contrast of images obtained with PET:

- localization of source position on the line of response
- reduction of coincidence background
- improvement of S/N

Novel photon detectors – MCP-PMT and SiPM – have excellent timing resolution → TOF resolution limited by the scintillation process

Cherenkov light is promptly produced by a charged particle traveling through the medium with velocity higher than the speed of light c_0/n.

Disadvantage of Cherenkov light is a small number of Cherenkov photons produced per interaction → detection of single photons!

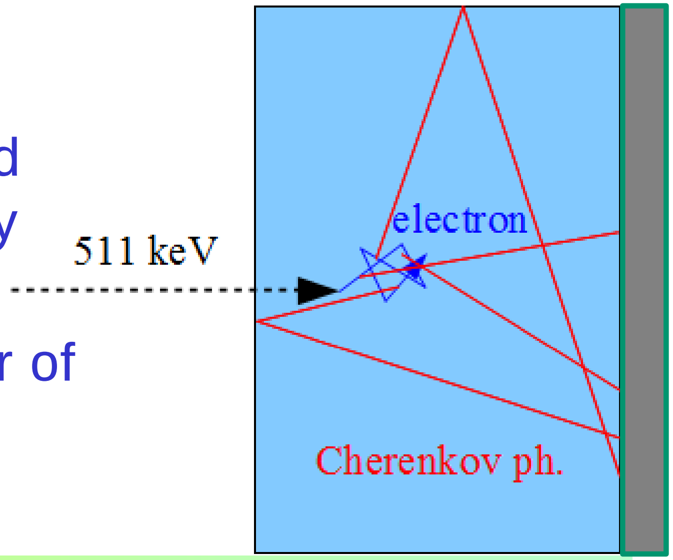

TOF-PET with Cherenkov light

Two detectors in a back-to-back configuration with 25x25x15 mm^3 crystals coupled to MCP-PMT with optical grease.

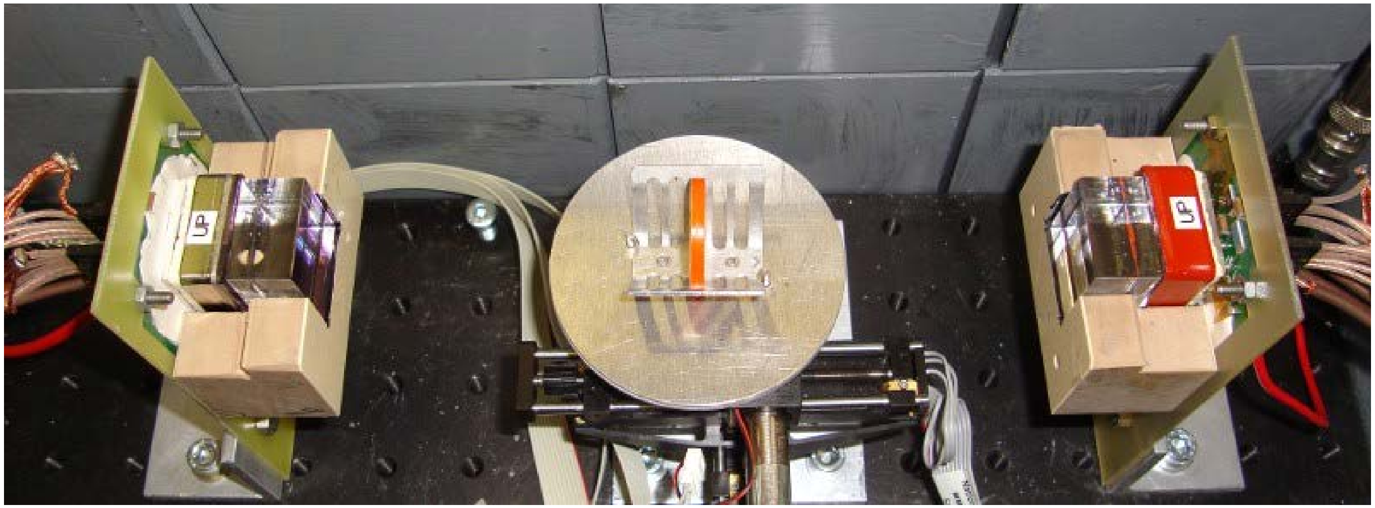

5 mm long crystal:

→ FWHM ~ 70 ps

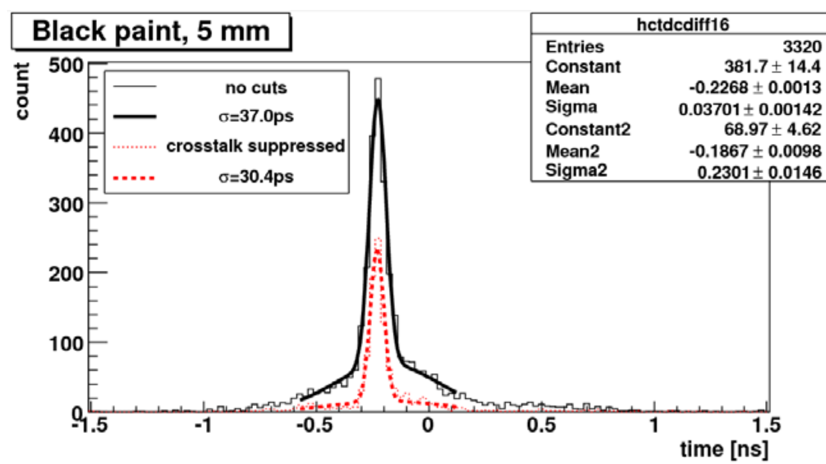

→ NIM A654(2011)532–538

→ Talk by P. Križan - tomorrow

Summary

- Low light level detection is at the hearth of many detectors in particle and nuclear physics
- New methods require very fast timing in radiation harsh environments
- A number of new detectors has been developed recently to cope with these requirements
- A very active field!

Back-up slides

ALD for MCP PMTs: born in Chicago area.
ALD can turn a borosilicate glass substrate into an MCP

Borosilicate Substrate Atomic Layer Deposited Microchannel Plates

Micro-capillary arrays (Incom) with 10µm, 20 µm or 40µm pores (8° bias) – borosilicate glass. l/d typically 60:1, but can be much larger. Open area ratios from 60% to 83%. Fabricated with using hollow tubes (no etching). Separate resistive and secondary emissive layers are applied (ANL, Arradiance) using atomic layer deposition to allow these to function as MCPs. ALD secondary emissive layers can also be applied to “standard” MCPs to improve yield.

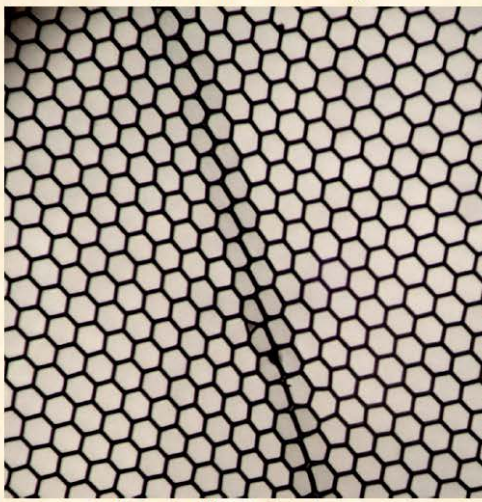

40µm pore borosilicate micro-capillary MCP with 83% open area.

Pore distortions at multifiber boundaries, otherwise very uniform.

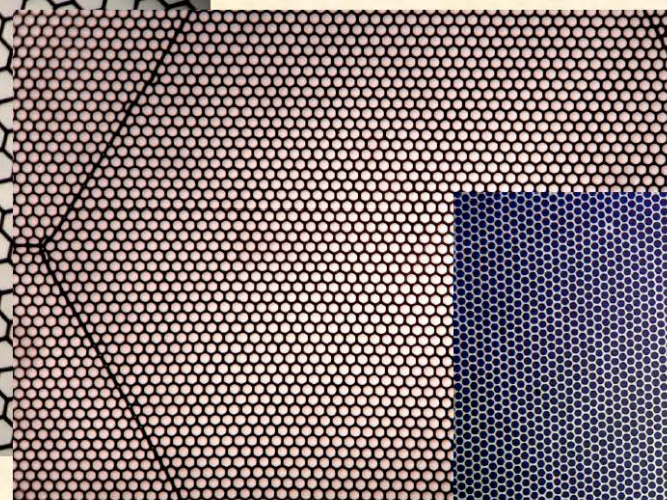

Photo of a 20 µm pore, 65% open area borosilicate micro-capillary ALD MCP (20cm).

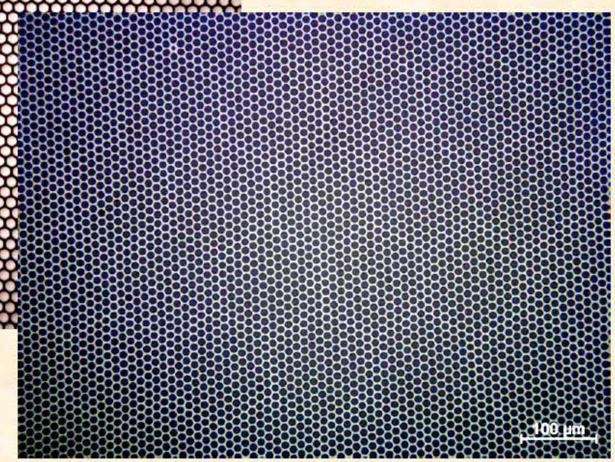

Photo of a 10 µm pore, 60% open area borosilicate micro-capillary ALD MCP.

LAPPD – Large Area Picosecond Photon Detector

MCP by Atomic Layer Deposition (ALD)

University of Chicago

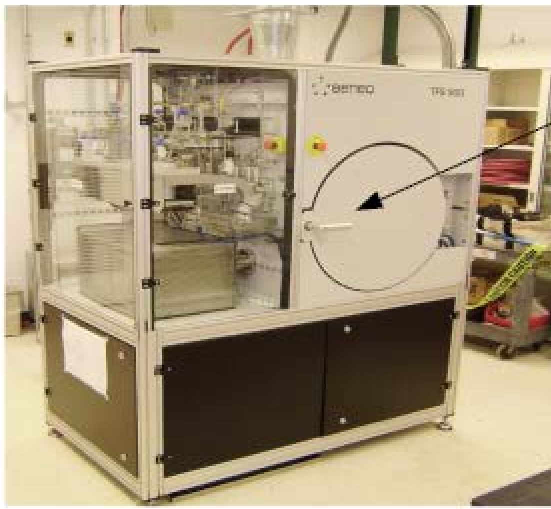

Beneq reactor for ALD

@Argonne National Laboratory

A.Mane, J.Elam

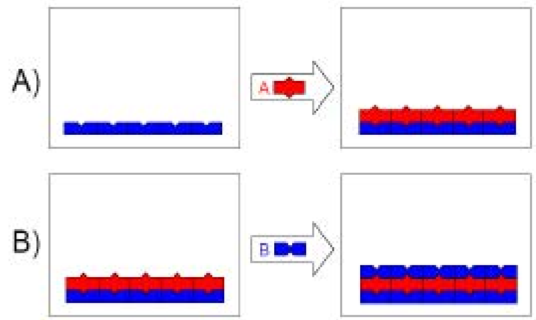

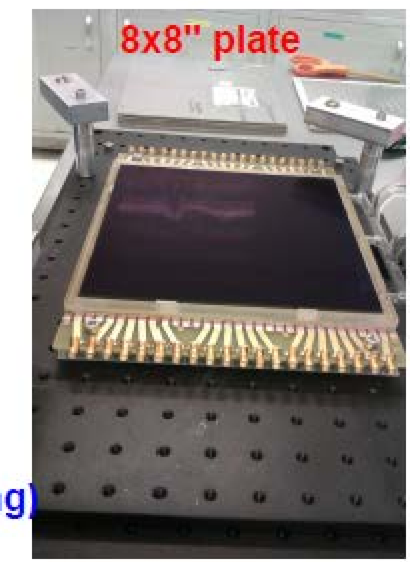

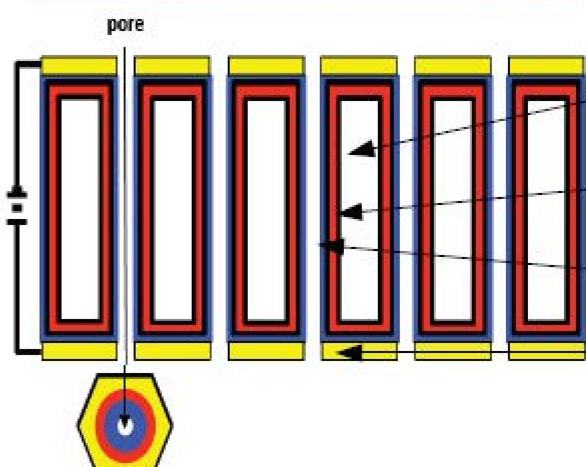

Porous glass

Resistive coating ~100nm (ALD)

Emissive coating ~ 20nm (ALD)

Conductive coating
(thermal evaporation or sputtering)

Key Issues for ALD Borosilicate MCPs

Current MCP devices have specific limitations due to the nature of the structure and processing of conventional MCPs. Atomic layer deposited (ALD) MCPs made on borosilicate substrates provide a unique way to improve on current devices or make new device types.

Borosilicate substrate:- Strong & clean compared with standard MCP glass

- Large areas can be made — large detectors for security applications
- Larger open area ratios – higher photon /electron/ion detection efficiency
- Low/no radioactive content — lower background for security applications
- Low outgassing — longer device lifetimes, shorter process/fab times
- High temperatures — deposit materials & cathodes not otherwise possible

Atomic layer deposition:- Decoupled from substrate, many materials possible

- Resistance tailored to suit — can make a wider range than standard MCPs allowing high local counting rates
- High secondary emissive layer — better pulse height at low gain, better gain
- Stable secondary emissive layer — faster gain burn-in, or none needed – very long lifetime & durability – compatibility with alkali cathodes

20cm ALD-MCP & Sealed Tube Development

LAPPD collaboration development of 20cm ALD MCPs and sealed tube with bialkali cathode and stripline anode for 2D imaging and <10ps timing.

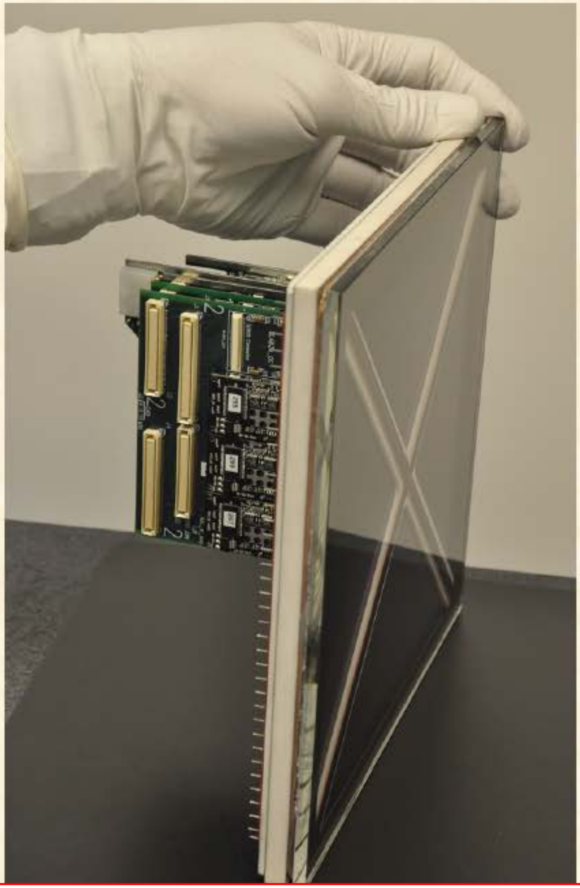

Also see Incom poster.

First tube did not seal, making new tubes this summer

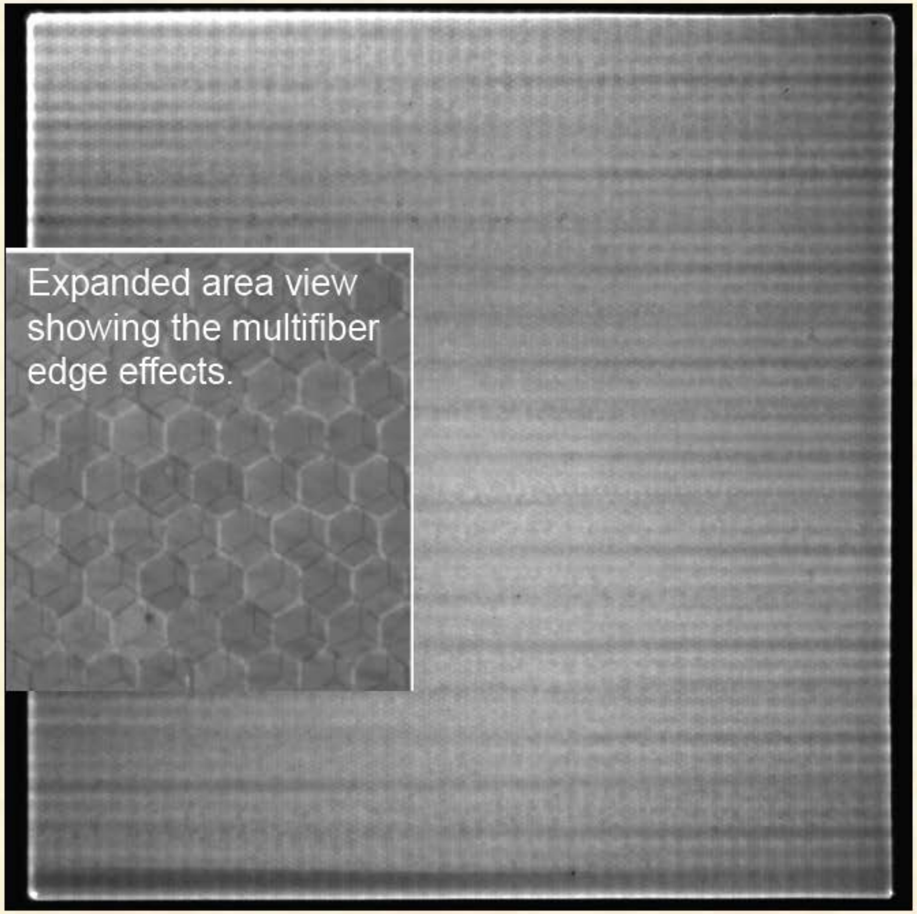

20cm, 20µm pore, Al_2O_3 SEY, MCP pair image with 185nm non-uniform UV illumination. Cross delay line photon counting anode. Image striping is due to the anode period/charge cloud size modulation.

→ Extremely important development, many talks in this workshop

Ring image, background contributions (B=0T)

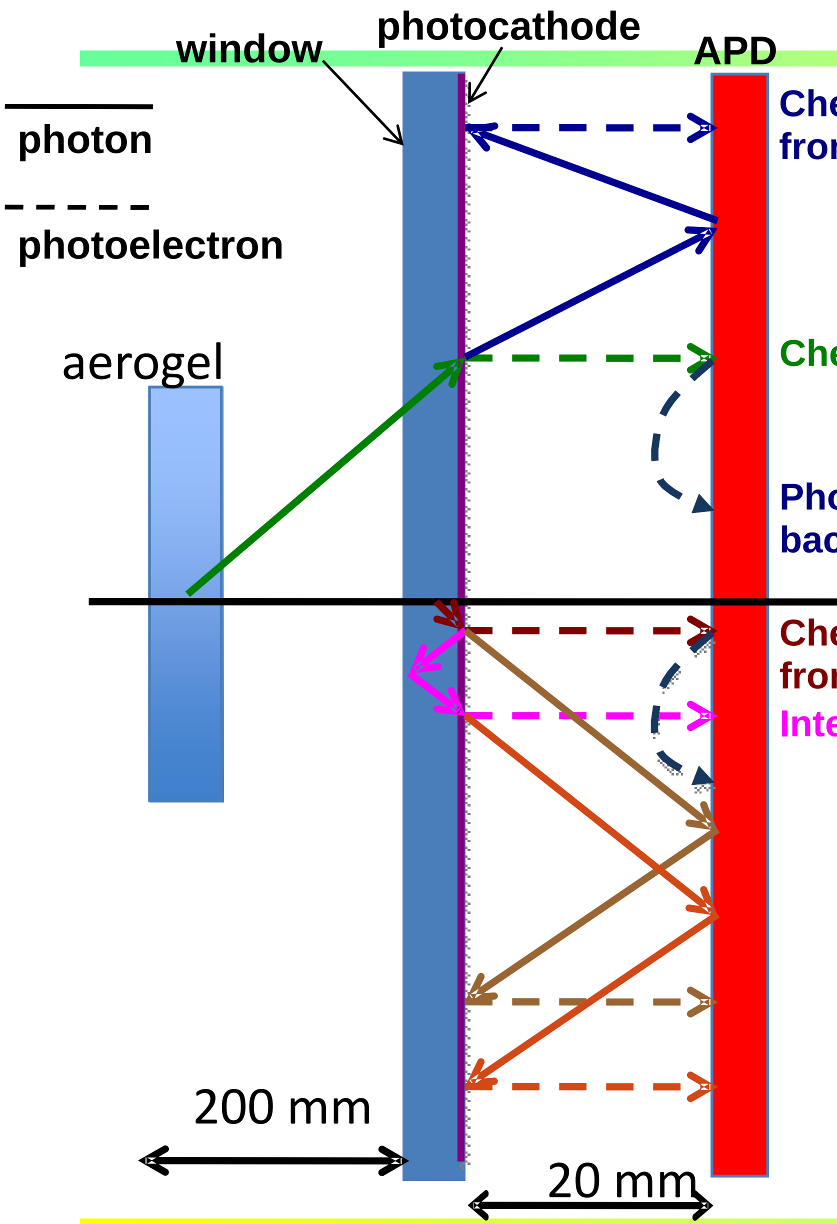

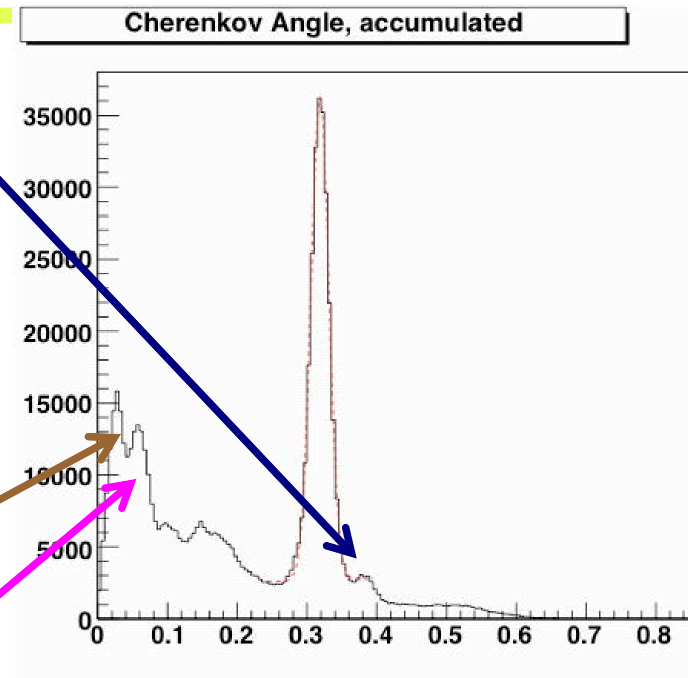

Ways to improve:

- The amount of window light can be reduced by a thinner window
- Effects of photoelectron backscattering disappears in magnetic field
- Reflected light: higher QE, more absorption In the first pass
- Anti-reflective coating?

HAPD: operation in 1.5 T

Tests in 1.5 T magnetic field show improved HAPD performance:

- no photoelectron back-scattering cross-talk
- increase of detection efficiency – photoelectron energy deposited at one place
- effect of non-uniformity of electric field disappears

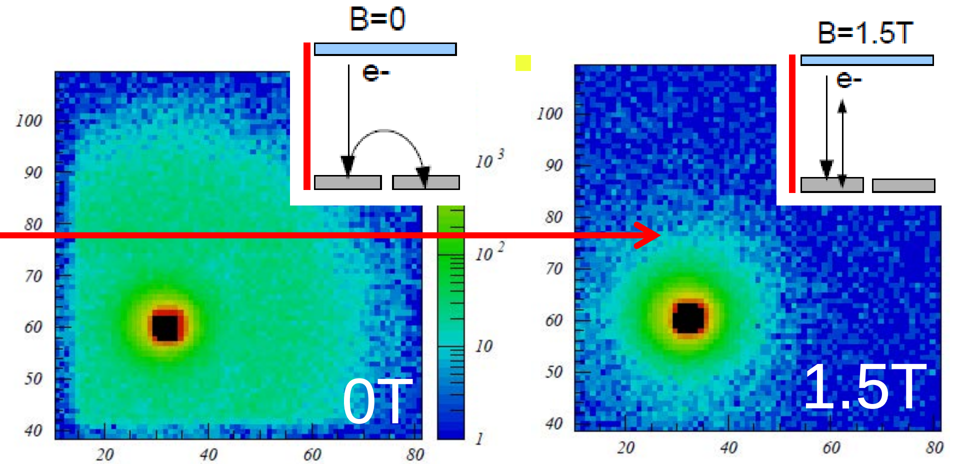

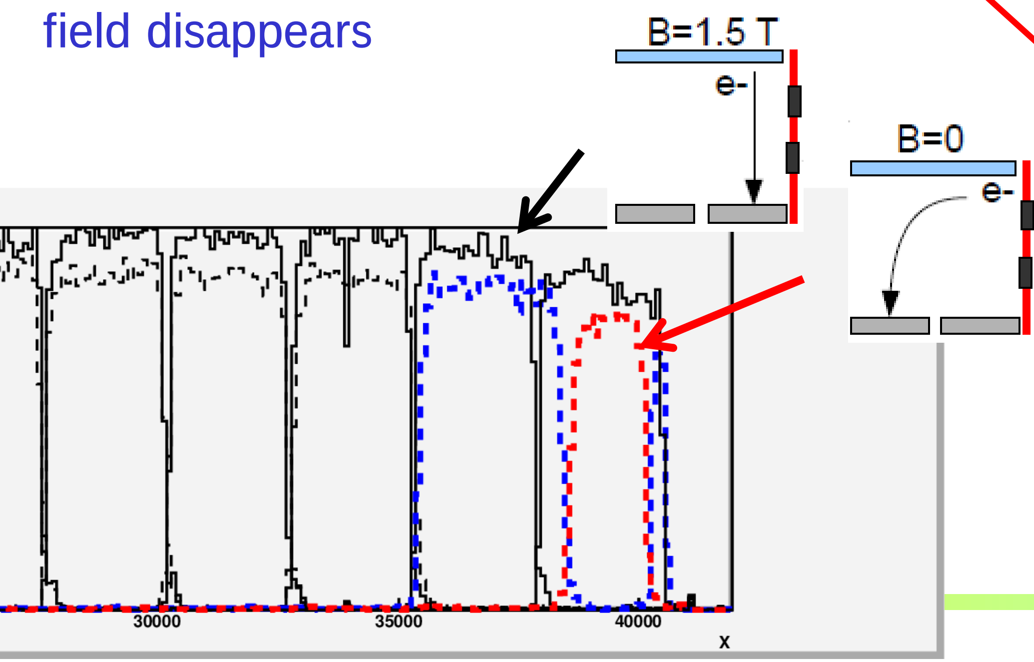

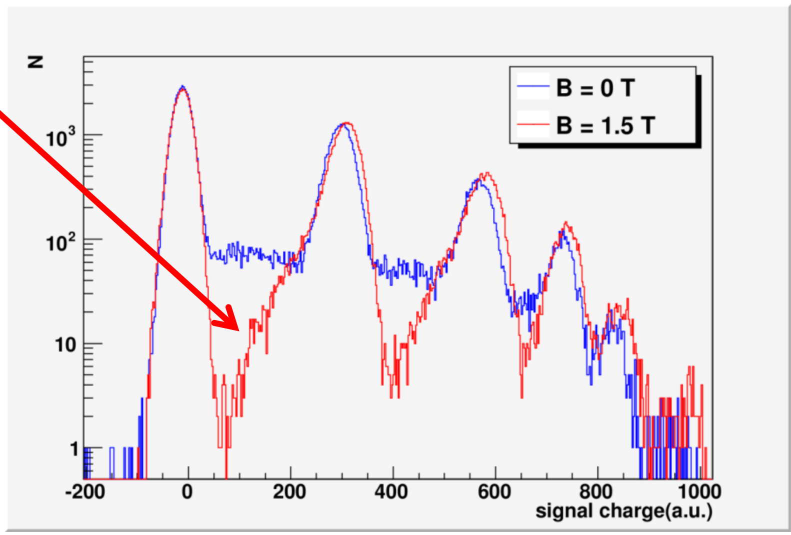

Test in magnetic field 1.5 T

- distortion of electric field lines at HAPD edge produces irregular shapes of areas covered by each channel
- in magnetic field photoelectrons circulate along the magnetic field lines and distortion disappears

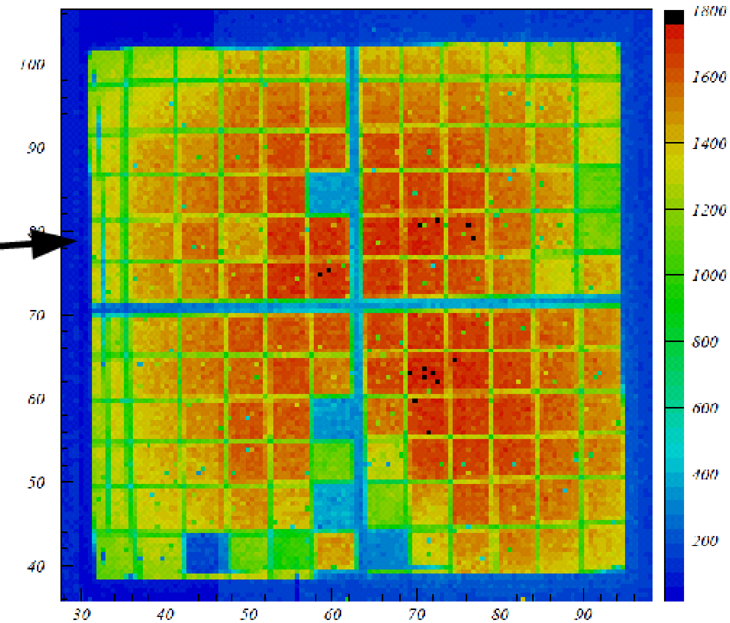

magnetic field 1.5 T

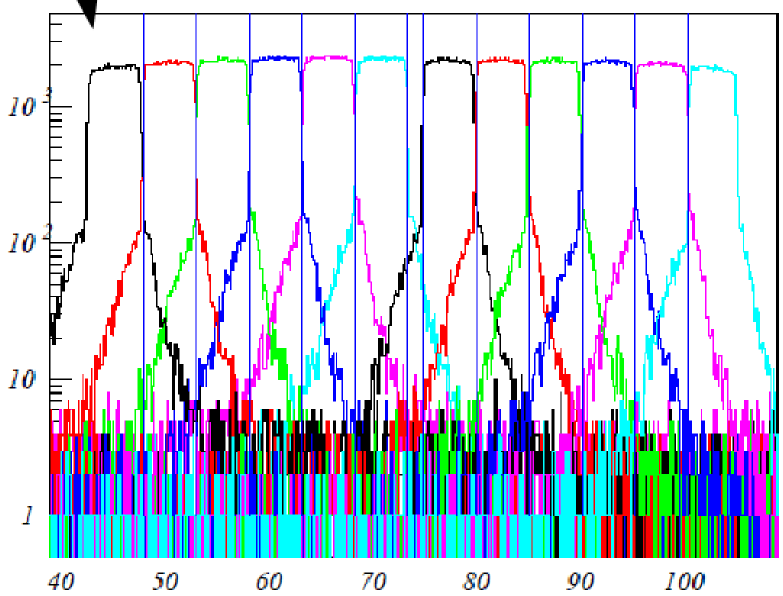

no magnetic field

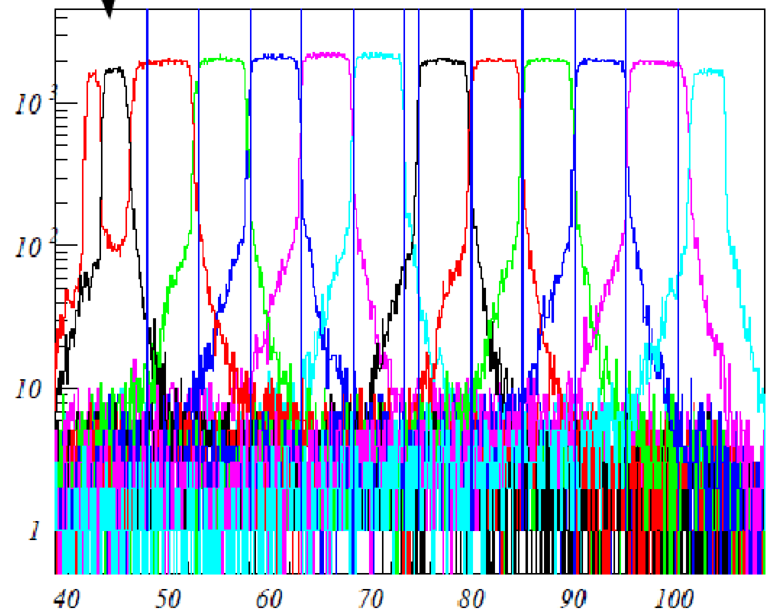

Photo-electron backscattering, light reflection from the APD etc

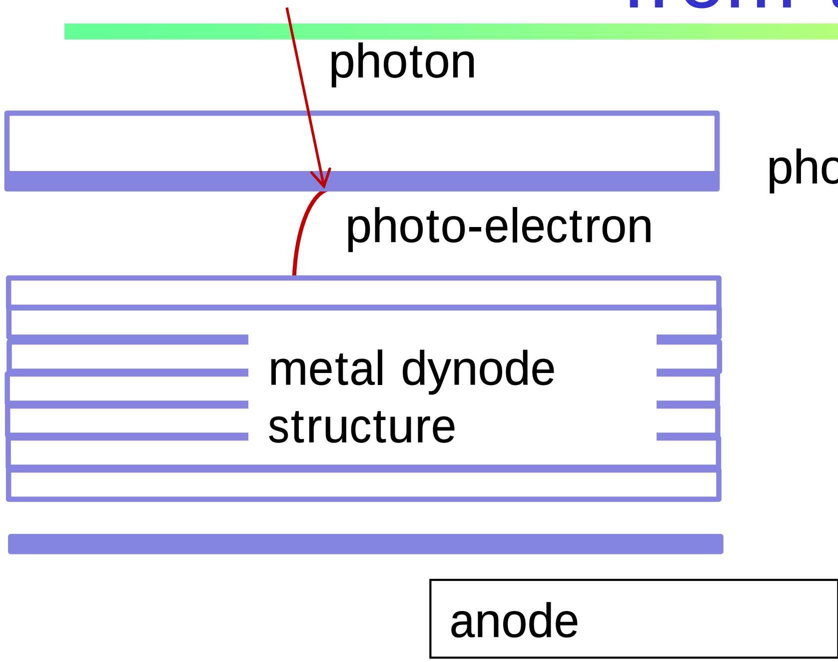

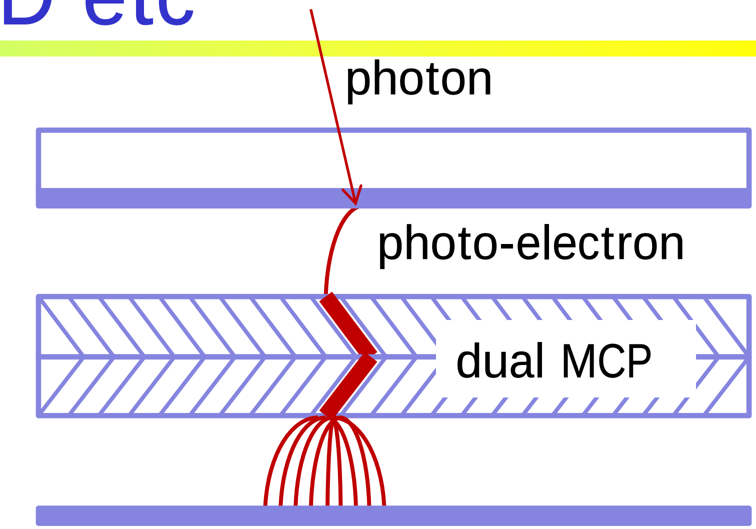

Similar geometries in the photo-electron step
→ A lot of similarities between prox. focusing HAPD, MCP PMTs and MA-PMTs